

https://dspace.org/

An analysis of the relationship between maximum cortical bone thickness and maximum curvature in the metatarsals of Pan and Homo

McClymont, Juliet

2013-04-30
http://hdl.handle.net/10539/12698

Downloaded from a DSpace repository. https://dspace.org/

An analysis of the relationship between maximum cortical bone thickness and maximum curvature in the metatarsals of *Pan* and *Homo*.

Juliet McClymont

A Dissertation submitted to the Faculty of Science, University of the Witwatersrand, Johannesburg, in fulfilment of the requirements for the degree of Master of Science

Signed on 14 November 2012 in Johannesburg

Declaration

I declare that this thesis is my own unaided work. It is being submitted for the degree of Master of Science at the University of the Witwatersrand, Johannesburg. It has not been submitted before for any degree or examination in any other university.

_____

(Signature of candidate)

Date: 14 November 2012

In: Johannesburg

Dedication

For Science

Abstract

Hominoids practice a diverse array of locomotor behavior, from obligate terrestrial bipedalism to arboreal suspensory behavior, which is reflected in the variable morphology found in their foot bones. That hominin foot bones reflect locomotor behavior is also clear, but the forms of locomotor behaviors to be inferred are less clear. Pressure plate studies indicate that the center of pressure tends to move medially in the human foot during the last half of stance phase of bipedal gaits, while it tends to remain relatively more lateral in the bonobo and chimpanzee foot during the last half of stance phase.

Here is presented a comparison of metatarsals of *Homo sapiens[n=22]* and two species of *Pan* (*Pan paniscus [n=15] Pan troglodytes schweinfurthii [n=22]*in order to explore the relationship between *Homo* and *Pan* metatarsal morphology and foot function. Specifically, this dissertation addresses whether cortical thickness is associated with the position of maximum change in geometry on the plantar surface in metatarsals.

Acknowledgements

To Dr. Bernhard Zipfel for full moral, academic, financial support and guidance, and for providing valuable insights from a clinical perspective of foot evolution. To Dr. Kristian Carlson, for great insight, new perspectives, patience and guidance along the way. To Dr. Tea Jashashvili, for allowing me to analyse your data set, teaching me Avizo and Tenglish, and for supporting and guiding my ideas throughout the project. This dissertation would not have been possible without you.

To Dr. Dominic Stratford, your support has been extraordinary, your guidance and scientific insights, remarkable. Thank you for your patience and calmness during this time. To Prof. Robin Crompton and Dr. Karl Bates, for your comments, brilliant insights, endless knowledge and full support, thank you both. To Dr. Ken Stratford, you have so many insights into the weird and wonderful world of science, but your statistical knowledge is outstanding. My greatest thanks to you and Dominic for seeing me through the most difficult part of this dissertation. To Prof. Bruce Rubridge, for financially supporting the final three months, I could not have finished without you helping so generously. To Luis Torres Cruz, thank you for inviting me into your world of beams, moments and levers.

Finally, this dissertation is dedicated to my parents. They taught me to question, and to lust for learning, and have supported me through every choice I've made in life. This small piece of science would not be, if not for them. Thank you both, with all my heart.

Contents

Declaration i

Dedication ii

Abstract iii

Acknowledgements iv

Contents v

List of Figures x

List of Tables xiv

Chapter 1 Introduction 1

1.1. Aims 1

1.2. Background 1

1.2.1. The mechanics of bending and the mechanical role of curvature

1.2.2. Bone functional adaptation

1.2.3. Cortical bone thickness

1.2.4. Bipedal locomotion and footfall patters in the *Homo* foot

1.2.5. The mechanical function of the metatarsals in *Homo*

1.2.6. Quadrupedal locomotion and footfall patterns in the *Pan* foot

1.2.7. The mechanical function of the metatarsals in *Pan*

1.2.8. Interspecific variation in footfall patterns between primates

1.3. Predictions and hypotheses 20

Chapter 2 Materials and Methods 22

2.1. Materials 22

2.2. Methods 22

2.2.1. Introduction

2.2.2. Sampling method

2.2.3. Segmentation method

2.2.4. Orientation and resampling method

2.2.5. Method for calculating cross sectional properties

- Measuring cortical bone thickness
- Measuring diaphyseal curvature for maximum point of geometry change

2.2.6. Analytical method

- Descriptive analysis

- Normalisation of the locations in maximum geometry change
- Statistical method

Chapter 3 Results 44

3.1. Intraspecific cortical bone thickness 44

3.1.1. *Pan paniscus*

3.1.2. *Homo sapiens*

3.1.3. *Pan troglodytes schweinfurthii*

3.2. Interspecific cortical bone thickness 53

3.2.1. Interspecific comparison of maximum plantar thickness locations

3.2.2. Interspecific comparison of maximum dorsal thickness locations

3.2.3. Interspecific comparison of maximum medial thickness locations

3.2.4. Interspecific comparison of maximum lateral thickness locations

3.2.5. Interspecific comparison of all cortices thickness locations across species

3.3. Positions of maximum change in geometry 62

3.3.1. *Pan paniscus*

3.3.2. *Homo sapiens*

3.3.3. *Pan troglodytes schweinfurthii*

3.4. Interspecific comparison of maximum change in geometry 65

3.4.1. *Pan paniscus*

3.4.2. *Homo sapiens*

3.4.3. *Pan troglodytes schweinfurthii*

3.5. Summary of results 73

3.5.1. Main intraspecific results

3.5.2. Main interspecific results

Chapter 4 Discussion, Conclusions and Evaluations 76

4.1. Discussion 76

4.1.1. Intraspecific comparisons of the positions of maximum thicknesses

4.1.2. Interspecific comparisons of the position of maximum thicknesses

4.1.3. Interspecific comparisons of the relationships between positions of maximum geometry change

4.1.4. Interspecific comparisons of the relationships between the positions of maximum thickness and maximum geometry change

4.2. Conclusions 88

4.3. Evaluation 91

References **93**

Appendix A: Variability tables, all species, all specimens, all metatarsals showing minimum, maximum, mean and standard deviations

Appendix B: Intraobserver error values table

Appendix C: *P*-value SPSS outputs

List of Figures

Figure 1.1 Long bones modelled as beams and viewed with the applied forces and strain distribution in compression, bending, twisting, shearing.

Figure 1.2 Schematic of the human foot during the three stages of stance phase; heel strike, mid-stance and toe off.

Figure 1.3 Schematic showing a typical peak pressure map for normal straight-legged bipedal walking.

Figure 1.4 A schematic of the relationship between the internal forces of the plantar aponeurosis and the metatarsal heads.

Figure 1.5 Examples of the plantar pressure distribution in bonobos (*P. paniscus*) during terrestrial locomotion.

Figure 2.1 The 6 different stages of rotation of the rendered metatarsal surface in Avizo 6.3 to define the principal axes of each bone and apply distal and proximal landmarks.

Figure 2.2 Representation of the technique employed by which cross sections are defined and analysed from a scanned metatarsal diaphysis.

Figure 2.3 Three examples of the 5^{th} cross section of metatarsal 2 taken from A) *Homo sapiens* (A13), B) *Pan paniscus* (20882) and C) *Pan troglodytes schweinfurthii* (15235).

Figure 2.4 Depiction of the method by which 21 cross sections were taken showing the cross- sectional positions along the diaphysis and the

landmarks defining the longitudinal axis and a view through the medullary cavity.

Figure 2.5 Example of the sixth cross section from left metatarsal 2, *P. t. schweinfurthii* representing the principal and the anatomical axes (i.e., mediolateral and dorsoplantar), and indicates the points at which thickness measurements were taken.

Figure 2.6 Example of the sixth cross section representing the the maximum vertical distance between the longitudinal axis and the plantar surface; i.e. the proxy location of geometry change; 0.99mm.

Figure 2.7 Frequency distribution of cross sections (CS) at which maximum geometry change occurs along the diaphysis of metatarsal 1 in *P. t. schweinfurthii*.

Figure 2.8 Location of the median cross section for maximum geometry change in all metatarsals in *P. t. schweinfurthii*

Figure 2.9 Example of non-normalised raw values from 17 cross sections from 6 specimens of metatarsal 2, in *P. t. schweinfurthii.* The values defining the curves indicate the location of maximum change in geometry

Figure 2.10 Example of normalised values from 17 cross sections from 6 specimens of metatarsal 2, in *P. t. schweinfurthii* representing values that define the location of maximum change in geometry

Figure 3.1 Cross sections (CS) containing ROI locations (median values) of maximal cortical thickness in metatarsal diaphyses (M1-5) of *P. paniscus*.

Figure 3.2 Cross sections (CS) containing ROI locations (median values) of maximal cortical thickness in metatarsal diaphyses (M1-5) of *H. sapiens*.

Figure 3.3 Cross sections (CS) containing ROI locations (median values) of maximal cortical thickness in metatarsal diaphyses (M1-5) of *P. t. schweinfurthii*.

Figure 3.4 Cross sections (CS) containing ROI locations (median values) of maximum cortical thickness on the plantar surface in metatarsal diaphyses (M1-5) of *P. paniscus (P.p), H. sapiens (H.s) and P. t. schweinfurthii (P.t.s)*.

Figure 3.5 Cross sections (CS) containing ROI locations (median values) of maximal cortical thickness on the dorsal surface in metatarsal diaphyses (M1-5) of *P. paniscus (P.p), H. sapiens (H.s) and P. t. schweinfurthii (P.t.s)*.

Figure 3.6 Cross sections (CS) containing ROI locations (median values) of maximum cortical thickness on the medial surface in metatarsal diaphyses (M1-5) of *P. paniscus (P.p), H. sapiens (H.s) and P. t. schweinfurthii (P.t.s)*.

Figure 3.7 Cross sections (CS) containing ROI locations (median values) of maximal cortical thickness on the lateral surface in metatarsal diaphyses (M1-5) of *P. paniscus (P.p), H. sapiens (H.s) and P. t. schweinfurthii (P.t.s)*.

Figure 3.8 Illustration of interspecific relationships in maximum thicknesses in all four cortices

Figure 3.9 Group comparisons of cross sections (CS) containing ROI locations (median values) of maximum change in geometry on the plantar surface in metatarsals (M1-5).

Figure 3.10 Cross sections (CS) containing ROI locations (median values) of maximum change in geometry compared to all anatomical cortices in metatarsal (M1-5) of *P. paniscus.*

Figure 3.11 Cross sections (CS) containing ROI locations (median values) of maximum change in geometry compared to all anatomical cortices compared to all cortices in metatarsals 1-5 of *Homo sapiens.*

Figure 3.12 Cross sections (CS) containing ROI locations (median values) of maximum change in geometry compared to all anatomical cortices compared to all cortices in metatarsals (M1-5) of *P. t. schweinfurthii*.

List of Tables

Table 2.1 Total number of specimens per species and the total number of measurements taken per metatarsal, per cross section.

Table 2.2 Cross section positions at which maximum geometry change occurs in metatarsal 1 of each specimen in *P. t. schweinfurthii*.

Table 3.1 *P*-values for Wilcoxon pairwise comparisons between positions of maximum thickness at all cortices in *P. paniscus*.

Table 3.2 *P*-values for Wilcoxon pairwise comparisons between positions of maximum thickness at all cortices in *H. sapiens.*

Table 3.3 *P*-values for Wilcoxon pairwise comparisons between positions of maximum thickness at all cortices in *P. t. schweinfurthii*.

Table 3.4 *P*-values for Kruskal-Wallis tests of positions of maximum thickness at plantar cortices between all species.

Table 3.5 *P*-values for Kruskal-Wallis tests between positions of maximum thickness at dorsal cortices between all species.

Table 3.6 *P*-values for Kruskal-Wallis between positions of maximum thickness at medial cortices between all species.

Table 3.7 *P*-values for Kruskal-Wallis between positions of maximum thickness at lateral cortices between all species.

Table 3.8 *P*-values for Kruskal-Wallis tests between positions of maximum geometry change in all species across metatarsals.

Table 3.9 *P*-values for Kruskal-Wallis between positions of maximum geometry change in *P. paniscus and P. t. schweinfurthii* across metatarsals.

Table 3.10 *P*-values for Wilcoxon pairwise comparisons of maximum thickness and maximum geometry change locations in *P. paniscus* across metatarsals.

Table 3.11 *P*-values for Wilcoxon pairwise comparisons of maximum thickness and maximum geometry change locations in *H. sapiens* across metatarsals

Table 3.12 Pairwise comparisons of maximum thickness and maximum geometry change in *P. t. schweinfurthii* across metatarsals.

1. CHAPTER 1 – Introduction

1.1. Aims

The aim of this study is to document the diaphyseal position of the most thickly distributed cortical bone in the metatarsals of two species of *Pan* and *Homo sapiens.* The overarching questions concern whether the position of maximum thickness, determined by a predefined cross section, coincides with the theoretical location of a stress concentration – a major point of geometry change (here, defined as the greatest depth of the plantar surface from the longitudinal axis). The relationship will be assessed in the metatarsal diaphyses of *Homo sapiens* and *Pan* (i.e., *Pan troglodytes schweinfurthii* and *Pan paniscus*). If a relationship exists, this could signal bone functional adaptation for the modulation of bending stresses within individual metatarsals. Patterns across the metatarsus will be explored to see if configurations may reflect the documented transfer of the centre of pressure during stance phase in *Homo* and *Pan* (Wunderlich 1999; Arndt *et al.* 2002; Vereecke *et al.* 2003).

1.2. Background

1.2.1. The mechanics of bending and the mechanical role of curvature

Mammalian long bones are functionally adapted to withstand bending loads (Currey 2003; Sverdlova and Witzel 2010) with typical long bones such as the femur being primarily loaded in compression. In metatarsals, the diaphysis is buttressed at the proximal end by the tarsometatarsal joint structure and loaded at

the distal end during locomotion. The diaphysis is curved in the dorsoventral aspect (ventrally concave) and is loaded primarily in the axis of bending, allowing the bone to be 'open' to the substrate with which it is orientated. This curved shape facilitates an uneven distribution of force along the cortex, which requires an unequal distribution of bone material to support the structural integrity of the diaphysis against failure (Lanyon 1980; Currey 1984). Typically, the dorsal aspect of the cortex is in tension (stretched) and the plantar aspect of the cortex is in compression (compressed). Cortical bone is stronger in compression than in tension (Cowin 1983; Martens 1985; Reilly and Burnstein 1975; Savvidis and Sabrey 1996; Currey 2003; Scerdlova and Witzel 2010). Long bone diaphyses can be modelled as hollow beams, which in engineering theory suggests they are optimised as light-weight structures that can withstand bending (and torsion) (e.g., like in a shaft of bamboo) (Gambhir 2009; Sverdlova and Witzel 2010). Minimizing material is also helpful for reducing the cost of transport, particularly in distal parts of the limbs (Carrano 2001). Ultimately, when force is transferred along a curved bone (e.g., a metatarsal), a bending moment is produced proportional to the displacement of the diaphysis and directed perpendicular to the longitudinal axis of the bone (Frost 1964; Swartz 1990; Gambhir 2009).

Studies regarding the development of curvature, how curvature influences the distribution of strain across a shaft and the function of curvature in general are popular in the theoretical (Frost 1964, 1973; Lanyon and Baggott 1976; Lanyon and Bourne 1979; Lanyon *et al.* 1979; Lanyon 1980, 1987; Biewener 1988; Biewener *et al*, 1983; Bertram and Biewener 1988; Swartz 1990, Les *et al.* 1997) and experimental literature (Jouffroy and Lessertisseur 1960; Oxnard 1963; Tuttle

1969; Preschoft 1970; Marzke 1971; Susman 1979; Rose 1988; Hunt 1991; Stern and Susman 1991; Richmond 1998, 2007; Shackelford and Trinkaus 2002; Yamanaka *et al*. 2005) however, a thorough understanding of this adaptation is still unresolved. The majority of this literature relates to the bending strength of terrestrial limb bones (Lanyon and Bourn 1979; Rubin and Lanyon 1982; Biewener 1983; Biewener *et al*. 1983, 1988; Biewener and Taylor 1986), although more recent studies assess degrees of curvature in relation to locomotor behaviour in the terrestrial limb bones of early hominins and other primates (Yamanaka *et al*. 2005; Richmond 2007).The impact of curvature is not fully resolved and its function may differ from bone to bone (Lanyon 1980, 1987; Rubin and Lanyon 1984; Bertram and Biewener 1988; Richmond 2007).

Specifically concerned with this project is Richmond's (2007) 2D finite element (FE) model based on biomechanical data of hand posture, muscle recruitment, and anatomical moment arms, that he used to analyse the role of curvature of the manual proximal phalanx of siamangs during suspensory grasping, in order to test whether curvature reduced overall strain. The study showed that during suspensory grasping, joint reaction forces load the distal articulation creating dorsal compression in the shaft, while flexors and extensor muscle forces pull the phalangeal midshafts palmarly in tension, effectively resisting the tendency of the substrate reaction forces to bend the phalanx 'open'. The study concluded that phalangeal curvature reduces overall strains during arboreal, suspensory activity with flexed digits since the curvature of the bone and the (compressive) joint reaction forces along its axis serve to minimize the effect of dorsal concave bending.

Understanding adaptations of curvature in metatarsals is limited by a lack of knowledge regarding the internal mechanics of the foot (Nester 2009), the true magnitude of applied force *in vivo* (Demes *et al*. 2001) and relative roles of applied axial, transverse and longitudinal forces to curved diaphyses (Yamanaka *et al*. 2005). The direction and degree of bending can be unpredictable when compared to biomechanical analyses that must estimate bending moments using external forces (e.g., substrate reaction forces), as demonstrated by experimental studies (Rubin and Lanyon 1982; Gross *et al*. 1992; Demes *et al*. 2001; Lieberman *et al*. 2004). Fortunately, however, quantitative plantar pressure data for *Homo* and *Pan* are available (Preuschoft 1970; Stokes *et al*. 1979; Ferris et al. 1995; Donahue *et al*. 1999; Wunderlich 1999; Vereecke *et al*. 2003). From these studies the relationships between function (metatarsal function during stance) and a bones functional adaptation (cortical thickness and curvature of metatarsals) can be explored, although as the next section reviews (1.2.2), are still controversial in their interpretation.

1.2.2. Bone functional adaptation

The laws that attempt to define cortical and trabecular bone adaptation to mechanical stimuli are well-researched (Roux 1881; Wolff 1896; Thompson 1917; Frost 1964; Heřt et al. 1971; Pauwels 1980; Rubin and Lanyon 1984; Rubin and McLeod 1998; Turner et al. 1995; Turner 1998), but still contentious in their conclusions (Pearson and Lieberman 2004; Ruff et al. 2006). Cortical bone varies in thickness both within individual cross sections of bone diaphyses, and along the longitudinal axis. Functional adaptations of cortical bone refer to changes in the structure and material organisation of a bone's cortical architecture (the cortex), in

response to loading outside of the normal stress/strain range, distribution and duration (figure 1.1) (Frost 1964, Lanyon 1982; Lanyon and Rubin 1984; Woo *et al*. 1981, Currey 1984; Schaffler and Burr 1984; Martin and Burr 1989; Biewener and Bertram 1993). One of the most important contributions from experimental research into bone's functional adaptation was made by Heřt *et al.* (1971) who established with a rabbit model that dynamic strain had a more influential response on bone formation than other stress strain relationships. The influence of dynamic strain was further verified by Lanyon and Rubin (1984) from their experimental analysis of an avian ulna. Using strain gages, the authors showed adaptation of cortical bone around the endosteal diameter and intra-cortical porosity. Adaptations observed in this isolated experiment were directly proportional to externally applied peak strain, a phenomenon later supported by Forwood (1998). Another important milestone was reached by Rubin and McLeod (1998) who experimented with correlations between applied strain distribution and site-specific remodelling activity in a turkey ulna.

Several bone remodelling studies have suggested bone deposition is stimulated by strain magnitude (Heřt *et al.* 1971; Churches and Howlett 1981; O'Conner *et al*. 1982), while others indicate that load frequency and the number of load cycles play a more influential role (Rubin and Lanyon 1984; Cullen *et al*. 2001; Gross *et al.* 1992; Judex *et al*. 1997, 2007), while awkward loading may also be more influential than is currently considered (Nordstrom *et al*. 1998; Daley *et al*. 2006; Zumwalt 2007; Garman *et al*. 2007). It seems likely that over the lifetime of an individual bone functional adaptations are influenced by all of these factors – strain frequency, strain magnitude, the loading history of bone

cells, muscular forces, bending forces, substrate reaction forces and gravitational forces (Nordstrom *et al*. 1998; Turner 1998; Burr *et al*. 2002; Zumwalt 2007; Garman *et al*. 2007; Demes 2007; Judex and Carlson 2009; Nester 2009). Because of the range of influences on bone functional adaptation some vastly different opinions about how to interpret the functional basis of skeletal variation have emerged.

Locomotor behaviour has been defined as an animal's dynamic interaction with its environment (Prost 1965), and this interaction appears to initiate the cascade of events that collectively, comprise a bone's adaptive response to function (i.e.; bone functional adaptations). Throughout life, bone is exposed to a multitude of internal and external forces in a variety of circumstances (Turner 1998; Pearson and Lieberman 2004; Ruff *et al*. 2006; Carlson *et al*. 2008) but despite this, non-mechanical factors are relevant too. Age, genetics, diet and hormones influence bone deformation and have a large effect on bone modelling and remodelling potentially effecting the analysis of bone by cross section (Rubin *et al*. 1992; Martin *et al*. 1998; Turner *et al*. 2000; Goodship and Cunningham 2001; Wergedal *et al*. 2005; Kontulainen *et al*. 2006; Xiong *et al*. 2006; Devlin and Lieberman 2007; Hartard *et al*. 2007; Robling *et al*. 2007; Cooper *et al*. 2008). Thus, it has been suggested that the role of bone, while providing strength and structure, is not purely mechanical, but instead is a compromise between physiological demands and mechanical support (Ruff *et al*. 2006).

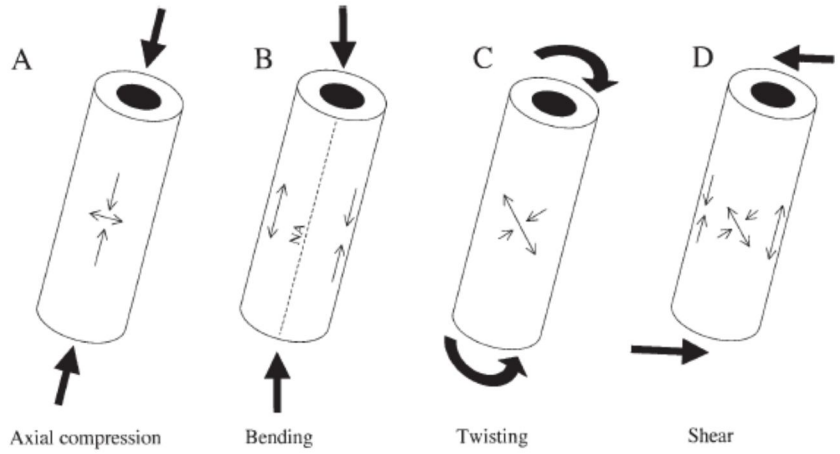


Figure 1.1: Beam views of the applied forces and strain distribution applied to long bones. Thick arrows represent the applied loads, while thin arrows represent the resulting strain. A = compression; B = bending; C = twisting; D = shearing. Schematic taken from Carter and Beaupré 2001.

1.2.3. Cortical bone thickness

Cortical bone thickness is one feature (along with robusticity, cross-sectional geometry, mass, trabeculae orientation and curvature) that enables the entire bone to withstand functional loading without failure (Lanyon 1987). An increase in the amount of cortical bone at any point on a diaphysis however, does not substantially increase rigidity unless it increases the external diaphyseal radius (Sparacello and Pearson 2010). Whether bone is habitually exposed to frequent or infrequent high magnitude loads, induced by internal or external forces, the cross-sectional area of cortical bone will adapt primarily to resist peak compressive loads (Preuschoft 2004; Ruff *et al*. 2006).

McLean and Marzke (1994) completed a comparative analysis of cortical bone thickness at several points along the shaft at anterior, posterior, medial and

lateral aspects of the fibulae of chimpanzees and humans. The authors reported proportionally thicker anterior cortex in chimpanzees than in humans with the lateral aspect exhibiting similarity in thickness at the midshaft. Positions of overall thicker cortical bone in chimpanzees are consistent with the orientation of the distal fibular articular facet, which accommodates for a more vertical and lesser weight-bearing load in humans (McLean and Marzke 1994). A thicker lateral cortex in humans was attributed to strong and repeated contraction of the peroneal muscles, which are thought to exert compressive stress on the lateral side in order to balance other extrinsic forces acting on the diaphysis (See: Swartz 1990 for insights into muscular loading in the forelimb of humans). Interspecific comparisons revealed a balanced cross section in the anteroposterior and mediolateral aspects, a similarity not observed in the human sample.

Bondioli and colleagues (Bondioli *et al*. 2010) contrasted cortical thicknesses of two *Homo* femora (modern human and fossil human from the Chancelade Late Upper Palaeolithic). Cortical bone thickness differed between the two specimens throughout the diaphysis: the modern human, for example, showed greater thickness in the proximal shaft medially, but the fossil specimen showed greater thickness laterally.

Morimoto *et al.* (2011) used morphometric mapping to analyse cortical bone thickness of femoral diaphyses in an ontogenetic series of wild and captive common chimpanzees (*Pan troglodytes troglodytes*). They only observed significant differences in the distal diaphysis where wild chimpanzees exhibited a higher proportion of mediolateral to anteroposterior cortical thickness than captive chimpanzees (Morimoto *et al*. 2011). Populations exhibited different patterns of

cortical bone thickness, perhaps as a consequence of differences in endosteal bone deposition or dietary differences, or alternatively different patterns may have reflected differences in loading conditions (Ruff *et al*. 1994; Pearson and Lieberman 2004).

Similar studies of thickness have not been undertaken on the metatarsals. Although not assessing cortical bone thicknesses, two comparative studies have examined the cross-sectional properties of metatarsal diaphyses. Marchi (2005) compared cross-sectional properties of the hand and foot bones of a large sample of hominoids concluding that their cross-sectional dimensions are correlated to broad locomotor modes. In this research, cross-sectional geometric properties distinguished between bipedal humans, knuckle-walking African apes and quadrumanous orang-utan with the most arboreal hominoids (chimpanzee and orang-utan) showing greater overall cortical area in the metacarpals and metatarsals relative to body mass (Marchi 2005). Inter-limb comparisons showed humans to have the most robust metatarsal 5 in accordance with the stress unloading mechanism traditionally described as the tripod (Elftman and Manter 1935; Roy 1988; Price and Price 1997). The three points of the tripod are metatarsophalangeal joint 1 and 5 and the tuber calcanei, a load distribution supported by pressure plate studies in humans (Cavanagh *et al*. 1987; Lundeen *et al*. 1994; Perry *et al*. 1995). Marchi's (2005) results are also in accordance with these data, showing greater cross-sectional geometric properties in metatarsal 5 of humans compared with other hominoids. Finally the results of this study provide a data set that can be compared to fossils as a useful indicator of broad locomotor modes in extinct hominins.

Griffin and Richmond (2005) were the first to systematically examine the relationship between mid-diaphyseal shaft strength and published plantar pressure studies to establish the impact of externally applied loads during functional activity. Mid-length cross-sectional properties (CA, Ix, Iy, Imax, Imin, J, Zx and Zy) were shown to be highest in metatarsal one in accordance with high pressure records recorded during varying types of bipedal locomotion. The lateral rays (2-5), however, produced varying results, showing that metatarsals 2-4 have weaker cross-sectional properties and structural properties relative to the applied loading regime, particularly in metatarsals 2 and 3, which coincide with high incidences of stress fractures that occur generally due to unusually high exposure to stress (as in prolonged marching in the armed forces or high levels of sport and physical activity).

1.2.4. Bipedal locomotion and footfall patterns in the human foot

During bipedal locomotion, humans vault over a stiff lower limb so that our centre of mass is at its lowest point at heel strike and rises to its highest point during toe-off (Cavagna et al., 1976; Lee and Farley, 1998). This allows for an efficient exchange of gravitational potential and kinetic energy. Specifically, the foot passes through three main phases during stance: heel strike, mid-stance and toe off (figure 1.2). At heel strike, the centre of pressure travels laterally along the longitudinal arch from the ankle joint (Ker *et al*. 1987) via the torque converter mechanism (Wolf *et al*. 2004). This is the mechanical distribution of force that acts to convert tibial rotation into forefoot pronation and supination via inversion and eversion via the subtalar and the ankle joints (Nester *et al*, 2007; Lundgren *et al*. 2008). At mid-stance, the centre of pressure shifts medially across the

dorsiflexing metatarsal heads (Close *et al*. 1967) to the distal segments of the phalanges initiating toe off, from where maximum propulsive power is exerted by the hallux, second and/or third toe (D'Août *et al.* 2009; Rolian *et al*. 2009; Crompton *et al.* 2010).



Figure 1.2: Schematic of the human foot during the three stages of stance; heel strike, mid-stance and toe off. Image taken from: www.ktsportsdoc.wordpress.com.

Although maximum propulsive force cannot be measured from pressure plate analysis, the aforementioned references provide biomechanical evidence as to the timing of maximally exerted propulsive force, commonly indicated by the colour red (Figure 1.3). This pattern is generally typical of shod Western populations, but variation in the path of the centre of pressure is also observed, including individuals who possess a mid-tarsal break rather than the more common metatarsal break (Vereecke *et al*. 2006a; D'Août *et al*. 2009; Crompton *et al.* 2010, 2011). The extent of intraspecific variation highlights the key role of the

metatarsals in the mediolateral transfer of the centre of pressure in the primates that have been tested for foot pressure related studies.

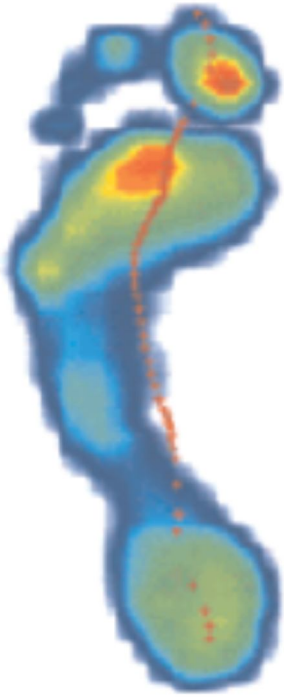


Figure 1.3: Schematic showing a typical peak pressure map for normal straight-legged bipedal walking. The red line represents the typical transfer of the centre of pressure ending at the hallux during toe off. The highest applied force is distinguished by the colour red seen here to being applied under metatarsal head 2-3 and the hallux. Moderate force is illustrated here by the colour yellow and can distinguish the transfer of force across the metatarsal heads from lateral (under metatarsal head 5) to medial (under metatarsal head 2) (Crompton., *et al.* 2008).

1.2.5. The mechanical function of the metatarsals in Homo

In humans metatarsals loading is initiated and sustained by the plantar aponeurosis at heel strike and throughout stance phase (Caravaggi *et al*. 2009). The ankle dorsiflexors and toe extensors actively tense the plantar aponeurosis along a line of fibres initiated from the medial slip to the mid-section of its five slips (Caravaggi *et al*. 2009). This mechanism results in early stiffening of the arch, ensuring that as the propulsive phase begins a substantial proportion of force is transferred to the ground by the foot (figure 1.4) (Caravaggi *et al*. 2009). The functional interaction displayed here may require that thicker, compression-resisting cortical bone should adapt to be maximal on the plantar aspect of metatarsals at the point of maximum geometry change (i.e., stress concentration), with a springy bony/soft tissue complex to resist tension on the dorsal aspect.

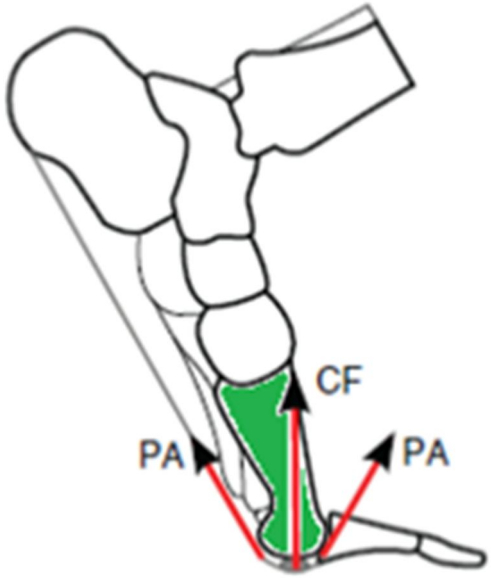


Figure 1.4: A schematic of the relationship between the internal forces of the plantar aponeurosis and the metatarsal heads (in green) during late stance phase and metatarsal 1 MTPJ (from Caravaggi *et al*. 2009 with permission). PA= tension in the plantar aponeurosis, CF=contact force between metatarsal heads and the plantar aponeurosis. As the $PA_{tension}$ pulls at the insertion on the plantar force plate and simultaneously at the proximal phalanx attachment site, the resulting force is the CF. The same CF is applied by the metatarsal heads into the contact force plate. Taken from Caravaggi *et al*. 2009.

Theoretical studies undertaken by Preuschoft *et al*. (1969, 1970) and Stokes *et al*. (1979) identify dorsoplantar bending and axial loads at the metatarsophalangeal joint at toe-off, suggesting these are primarily a product of substrate reaction forces experienced by the metatarsals at forefoot contact. Dorsally located compressive strains in metatarsal 2 were calculated to exceed that of the first metatarsal by a factor of 6.9 (Gross and Bunch 1989). These theoretical models are supported by more recent experimental studies on metatarsals 2 and 5, using physical gait simulators attached to cadaveric feet fitted with strain gauges (Ferris *et al*. 1995; Sharkey *et al*. 1995; Donahue and Sharkey 1999). Sharkey *et al*. (1995) and Donahue and Sharkey (1999) indicate that metatarsal 2 and 5 experience high compressive strain on the dorsal aspect during normal walking. They also observed that peak compressive strain occurred in the dorsal aspect of the metatarsal 2 diaphysis and peak tensile strain occurred in the lateral aspect of the metatarsal 5 diaphysis, with mean peak axial strains higher in all accounts in metatarsal 2 (Donahue and Sharkey 1999). In this specific model the authors were unable to simulate the stance roll over process in real time and as such, *in vitro* strains overestimated the values by approximately 15%. Relatedly, cadaveric models are unable to simulate the exact muscle contractile forces that are applied during life, particularly from the digital flexors that contribute to joint reaction forces along with a static plantar aponeurosis. This is due mainly to the inability in replicating the exact biomechanics of footfall in cadavers due mainly to a lack of blood flow that greatly increases stiffness, and no body weight applied throughout footfall. Further limitations of this method are discussed in section 1.4.7.

Arndt and colleagues (2002) combined plantar pressure, EMG and *in vivo* bone strain data in living humans showing that the dorsal aspect of metatarsal 2 primarily experiences bending and axial compression (Arndt *et al.* 2002). They also had subjects wear 20kg backpacks to measure the effect of fatigue in the *M. flexor digitorum longus.* They noted disproportionately high external loads along the diaphysis relative to its physical dimensions, as well as excessive bending moments, presumed to be a result of fatigue of the digital flexor muscles (Sharkey *et al*. 1995; Arndt *et al*. 2002). These studies confirm that an increase in external load carrying, coupled with fatigue of the plantar musculature, increases dorsal compressive strain in metatarsal 2. This supports the theoretical relationship between muscles and bone in the distribution of compressive and tensile forces.

1.2.6. Quadrupedal locomotion and footfall patterns in the Pan foot

The great apes (chimpanzees, gorillas, gibbons, orang-utans) practice a diverse array of locomotor behaviours including arm-swinging, vertical climbing, quadrumanous climbing, quadrupedal knuckle-walking and short bouts of terrestrial bipedal walking, skipping and running (Hunt *et al.*, 1996; Schmitt 2003). The most commonly practiced in the African apes however, is quadrupedalism, facilitated by a diagonal sequence footfall pattern whereby the hindfoot is followed by a contralateral forefoot (Muybridge 1887; Hildebrand 1967; Vilensky and Larson 1989; Cartmill *et al.*, 2002; Schmitt 2003) accompanied by relatively greater peak vertical applied forces in the foot than in the hands (Kimura et al., 1979; Reynolds, 1985; Demes *et al.*,1994; Polk, 2001, 2002; Schmitt and Lemelin, 2002; Schmitt 2003). This produces longer contact times and longer stride lengths compared with other mammals travelling at

dynamically similar speeds (Alexander and Maloiy 1984) with a more compliant quadrupedal walking style (Demes et al., 1990, 1994; Schmitt 1998, 1999; Wunderlich and Jungers 1998, Larney and Larson 2003).

The footfall pattern during quadrupedalism is similar across all great apes; however, as this study assesses only bonobos and chimpanzees, only pressure records from these species are discussed here. Bonobos and chimpanzees make initial contact almost simultaneously with the heel and lateral mid-foot. Weight is then transferred forward during mid-stance following a curved course along the lateral rays from where maximum propulsive power is exerted. Although propulsive force cannot be measured from pressure plates, it is inferred from pressure plate outputs based on highest point of pressure and represented usually by the colour red, at a given temporal stage of the footfall sequence, and when combined with maximum vertically applied force occurring at the same temporal stage. As in human bipedal locomotion, the metatarsals of non-human primates facilitate the transfer of the centre of pressure during stance.

1.2.7. The mechanical function of metatarsals in Pan

Although rare, non-human primates move bipedally both in the wild (Susman 1984) and in captivity (Vereecke *et al*. 2004). During chimpanzee bipedalism, the heel contacts the substrate, producing a sharp heel-strike transient (Crompton *et al*. 2008); propulsive force is exerted from the mid-foot rather than from the toes (as found in humans), thereby diminishing the transfer of the centre of pressure from lateral to medial across the metatarsal heads (figure 1.4) (Crompton *et al*. 2008). Wunderlich (1999) found peak metatarsal pressures under

the metatarsal heads of metatarsal 1 and 3 (Figure 1.4a) showing similarity in the function of the metatarsals between primates. On a climbing pole, peek metatarsal pressure occurs under metatarsal heads 2 and 3, followed by metatarsal head 1 and 5. This is supported by Marchi's (2005) study that finds the greatest bending rigidity in chimpanzee metatarsals 1 and 3.

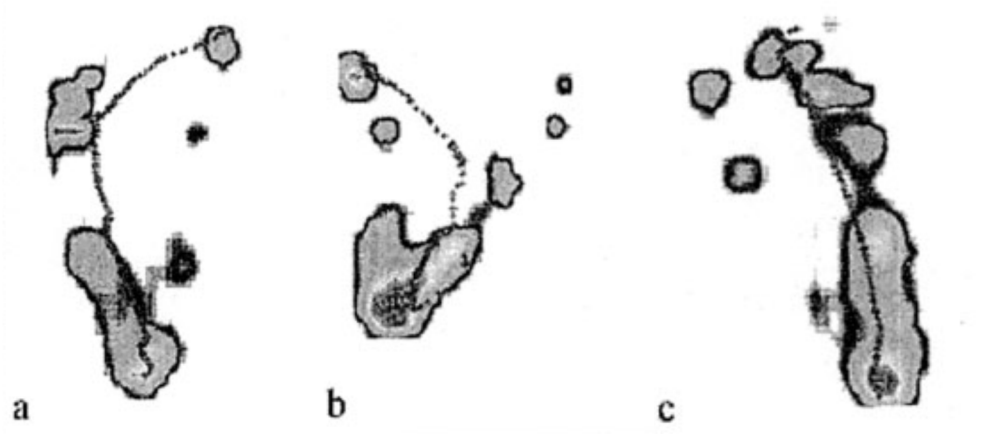


Figure 1.5: Examples of the plantar pressure distribution in bonobos (*P. paniscus*) during terrestrial locomotion. a (left foot), b and c (right foot) represent foot pressure distribution during quadrupedal walking. Initial contact is made by the heel with the centre of pressure moving anteriorly toward the metatarsal heads and lateral toes where it eventually turns medially toward the hallux. Footprint labelled 'a' indicates the curved and more typical transfer of centre of pressure. In b, a 'V' curve distribution of the centre of pressure is seen. In c, an almost straight distribution of the centre of pressure is depicted. Examples borrowed from Vereecke *et al*. (2003).

1.2.8. Interspecific variation in footfall patterns between primates

It is common in the palaeoanthropological literature to associate the development of a medial longitudinal arch with a mid-tarsal break (axis of plantarflexion), which serves as the traditional distinguishing feature between human and non-human ape feet (Elftman and Manter 1935; Lewis 1980). Lovejoy *et al*. (2009) argued that while living non-human great apes have compliant feet in order to grip branches in arboreal situations, and, because humans have developed a medial longitudinal arch apparently to immobilised the mid-foot, early hominins such as *Ardipithecus,* although lacking a medial longitudinal arch, likely retained a thick fibrous layer on the plantar aspect of the foot to provide a certain degree of rigidity. It is suggested that this retention improves the capacity of the lateral metatarsals to distribute propulsive forces from a more effective anterior position as demonstrated by the common occurrence of toe-off at metatarsal 2 (Lovejoy *et al*. 2009; Crompton *et al.* 2010). The absence of a mid-tarsal break in humans, however, is not a universal feature (Crompton *et al.* 2010; Crompton *et al*. 2011). Crompton and colleagues (2010), showed data from an individual who also lacked the traditional lateral to medial transfer of the centre of pressure, instead displaying an anterior shift of the centre of pressure to the second metatarsal, which is more similar to the path seen in chimpanzees (figure 1.4. C), showing that clinically normal individuals can a functioning lateral mid-foot pressure peak (Crompton *et al*. 2010).

Commonly in humans, foot pressure appears to be applied more consistently, particularly by the hallux, which plays a limited role in the transfer of propulsive forces evident in other primates, but acts more as a balancing agent

(Vereecke *et al*. 2003, 2006b; Crompton *et al*. 2010). Interestingly, flat-footed modern humans, or individuals raised as barefoot walkers, apply more plantar pressure under metatarsal heads 2 and 3 than the hallux (D'Août *et al.* 2009). However, the degree of hallucal abduction in non-human primates and a compliant foot does not prevent the practice of bipedal walking or running (Susman 1979; Vereecke et al. 2003, 2005, 2006 a,b; Crompton *et al*. 2008, 2010). Substantially robust metatarsals 2 and 3 in *Ardipithecus* suggest these bones may have played a more active role in transmitting accelerative forces in the parasagittal plane compared to the hallux, which with a high degree of abduction would provide better gripping capability (e.g., stability) while locomoting on branches (Lovejoy *et al*. 2009; Crompton *et al.* 2010). Adaptations in the modern human foot were built on a compliant arboreal template to provide for a variable gear organ able to accommodate irregular substrates and support changes in its stiffness relative to speed (D'Août *et al*. 2009; Crompton *et al.* 2010). This is supported by force plate data (Vereecke *et al*. 2003) that demonstrated less variation occurs between strides and individuals in human bipedalism than is observed in other hominoids.

1.3. Predictions and Hypotheses

When considering the integrated nature of the musculoskeletal system, I predict the following:

1) In humans, thicker, compression-resisting cortical bone will be positioned in the plantar cortex relative to other cortices (e.g., dorsal, medial, and

lateral). This may be due to the more consistently applied force from the plantar aponeurosis during footfall patterns (Caravaggi *et al*. 2009).

2) Maximum plantar thickness will coincide in location with the position of maximum geometry change on the plantar aspect (deepest point of the plant surface), particularly in metatarsals 1-3. This would support the assumption that high concentrations of stress require more material to provide structural support to the diaphysis (Preuschoft 1969, 1970, 1974; Mott 1996). These metatarsals in particular should show a correspondence due to their active role in the transfer of pressure and propulsion during footfall in all species in this sample (Vereecke *et al*, 2003; Griffin and Richmond 2005).

3) Given the differences in footfall patterns between *Pan* and *Homo*, there could be a difference in the relative positions of maximum thickness and the point of maximum geometry change. This could relate to bending in the oblique axis (Demes and Carlson 2009), or simply, the more variable nature of locomotion in *Pan*, suggesting relationships may occur in more than one cortex. In *Homo*, relationships between the two variables could be restricted to one cortex because of a more consistently applied loading regime.

Specifically, I hypothesise that maximum cortical bone thickness will correlate with the position of maximum change in geometry in each group;

2. CHAPTER 2 - Materials and Methods

2.1. Materials

Common chimpanzee (*Pan troglodytes schweinfurthii*) and bonobo (*P.paniscus*) metatarsal complexes from the Royal Museum of Central Africa in Terveren, Belgium (*P. t. schweinfurthii [n=22]; P. paniscus [n=15*) were subjected to computed tomography (CT) scanning by Dr. Tea Jashashvili in 2009. An additional sample of *Homo sapiens* metatarsal complexes from the Raymond Dart Collection, School of Anatomical Sciences, University of the Witwatersrand (*H. sapiens [n=22]*) were CT scanned by Dr. Jashashvili in 2010.

2.2. Methods

2.2.1. Introduction

Structural information on long bone diaphyseal morphology can be quantified in a number of different ways. For the purposes of this project, renderings of metatarsals were produced and analysed in Avizo 6.3 (1.9 Visualisation Sciences group, VSG, SAS). The protocol included digital application of landmarks to articular surfaces of proximal and distal ends of each metatarsal. Rather than using landmarks corresponding to homologous points between bones, as is typical in traditional geometric morphometrics, points representing defined biomechanical axes for individual bones were used.

2.2.2. Sampling methodology

For the purposes of this project, metatarsals from the left side were selected for analysis. In the absence of left side elements, right side elements were used after mirroring them in Avizo 6.3 (1.9 Visualisation Sciences group, VSG, SAS). *P. t. schweinfurthii* and *P. paniscus* metatarsal elements were CT scanned in Leuven, Belgium at the UZ Leuven Department of Radiology and some elements of *P. t. schweinfurthii* from the Department of Anthropology at the University of Minnesota (Minneapolis, MN, USA). Scan parameters were 140 kVp and 250 mAs energy, 0.6 mm collimation, 0.5 pitch, and a 512 x 512 pixel matrix. Images generated from scanned raw data were saved as a serial DICOM stack using a 0.3 mm reconstruction increment and "sharp" and "bone" reconstruction kernels. For the purposes of this project, the sharp filter reconstructed images were used. Image stacks were used to render each metatarsal in Avizo 6.3 (1.9 Visualisation Sciences group, VSG, SAS).

2.2.3. Segmentation methodology

Metatarsals were rendered (virtually reconstructed) using automated and semi-automated segmentation with a low threshold between (-400 and -750) HU. Using Avizo 6.3 (1.9 Visualisation Sciences group, VSG, SAS), bone elements were semi-automatically segmented; manual segmentation was used to disconnect renderings that were reconstructed as touching because, for example they had soft tissue still attached. Rendered images of individual metatarsals are 3D representations of each metatarsal, displayed as triangular mesh surfaces made from voxels in the CT data.

2.2.4. Orientation and resampling methodology

Accurately determining cross-sectional properties of bones requires the principal axes to be defined as precisely as possible. The methodology from Marchi (2005) was adapted for 3D imaging. In brief, this involved using Avizo 6.3 (1.9 Visualisation Sciences group, VSG, SAS) to orientate the axes of each metatarsal; proximodistal, mediolateral and anteroposterior, in order to obtain 17 equally-spaced cross sections from the diaphysis of metatarsal 1, and 21 equally-spaced cross sections from the diaphyses of metatarsals 2-5. Longitudinal axes were defined by manually applying 'landmarks' to the central points of the articular surfaces (e.g., figure 2.1D), then linking up the applied landmarks in Avizo 6.3 (1.9 Visualisation Sciences group, VSG, SAS) to define the three predefined axes (proximodistal, mediolateral and anteroposterior).

In order to define the longitudinal axes, rendered metatarsals were imported into Avizo 6.3 (1.9 Visualisation Sciences group, VSG, SAS) and aligned such that the proximal and distal articular surfaces were positioned in the same horizontal and vertical planes. Each rendering was positioned such that the proximal articulation surface was approximately parallel to the XY plane (figure 2.1A), the dorsal aspect approximately parallel to the XZ plane (figure 2.1B), and the medial aspect approximately parallel to the YZ plane (figure 2.1C). As a result, the Z axis indicates the axial direction of the rendering.

The proximal articular surface of the first metatarsal was aligned in the XY plane then rotated clockwise along the Z axis until the articulation groove was coincident with the Y axis (figure 2.1D). To align renderings in X and Y

directions, first landmark coordinate systems of the X and Y directions were rotated dorsoplantarly (X) then proximodistally (Y) such that in the X and Y planes proximal and distal landmarks were superimposed upon each other (i.e., in the same line of sight through the bone, figure 2.4a). For metatarsals 2, 3 and 4, the superior articular edge of the proximal articulation was aligned to the X axis, also by clockwise rotation about the Z axis (figure 2.1E). For metatarsal 5, the mediodorsal aspect of the proximal edge for the cuboid articulation was positioned horizontal to the Y axis, again by clockwise rotation of the diaphysis about the Z axis (figure 2.1F). The centres of articulating surfaces with the cuboid or cuneiforms were calculated with manual line measurements and landmarks were added.

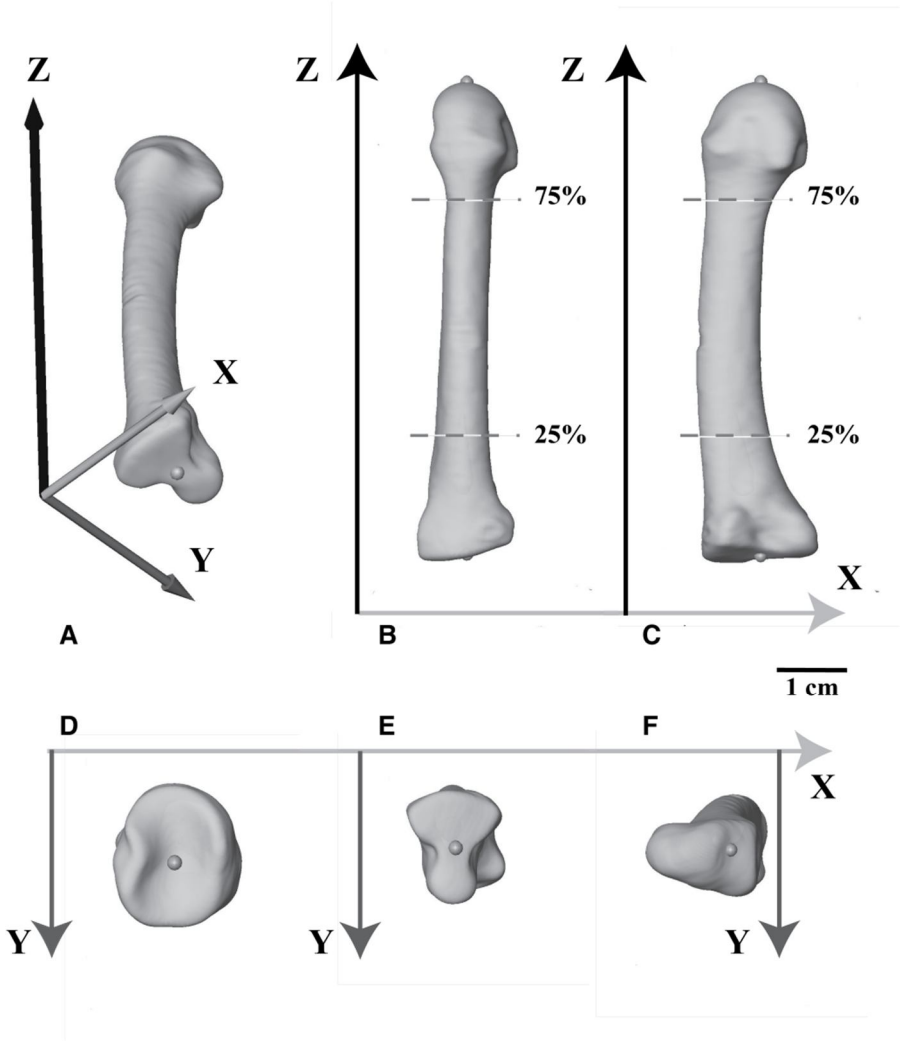


Figure 2.1: **A**: The proximal articular surface of metatarsal 3 (M3) rotated clockwise and approximately parallel to the XY plane. **B**: The dorsal aspect of M3 following rotation and being aligned approximately parallel to the XZ plane. **C**: The medial aspect of M3 following rotation and being aligned approximately parallel to the YZ plane. **D**: The proximal articular surface of the first metatarsal (M1) aligned in the XY plane with the diaphysis aligned along the ZY. **E**: Superior articular edge of the proximal articulation surface of metatarsals 2-4 aligned to the X axis. **F**: Mediodorsal aspect of the proximal articulation surface of metatarsal 5, aligned parallel to the Y axis by rotation along the Z axis.

Position adjustments in the coordinate system of the landmarks were transformed to the rendered surface. The difference between the XYZ coordinates of the original rendering and those from the surface rendering with the corrected position were calculated. The spatial difference between coordinates was used to rotate and translate the original DICOM stack into the adjusted position. Proximal and distal landmarks were used to define the area of the diaphysis to be analysed. Surface cuts were made along the total biomechanical length of each bone at regular intervals spaced 2.5% of the diaphysis apart, from 25% (proximal) to 65% (distal) for first metatarsals, and from 25% (proximal) to 75% (distal) for metatarsals 2-5 (figure 2.1B and C). The cropped, re-sliced DICOM stack was sampled in the Z direction using 17 cross sections from the first metatarsal and 21 for metatarsals 2-5. The process of creating a predetermined set of cross sections in diaphyses has a normalising influence on the data, as the distance along the diaphysis is referred to by cross section number rather than points defined by absolute millimetre measurements.

Non-parametric statistical analyses were selected to assess predictions because they are best-suited for comparisons between pre-defined values (see section 2.2.6 below for details). All images were standardised to a pixel size of 0.1mm and saved as 8-bit BMP files.

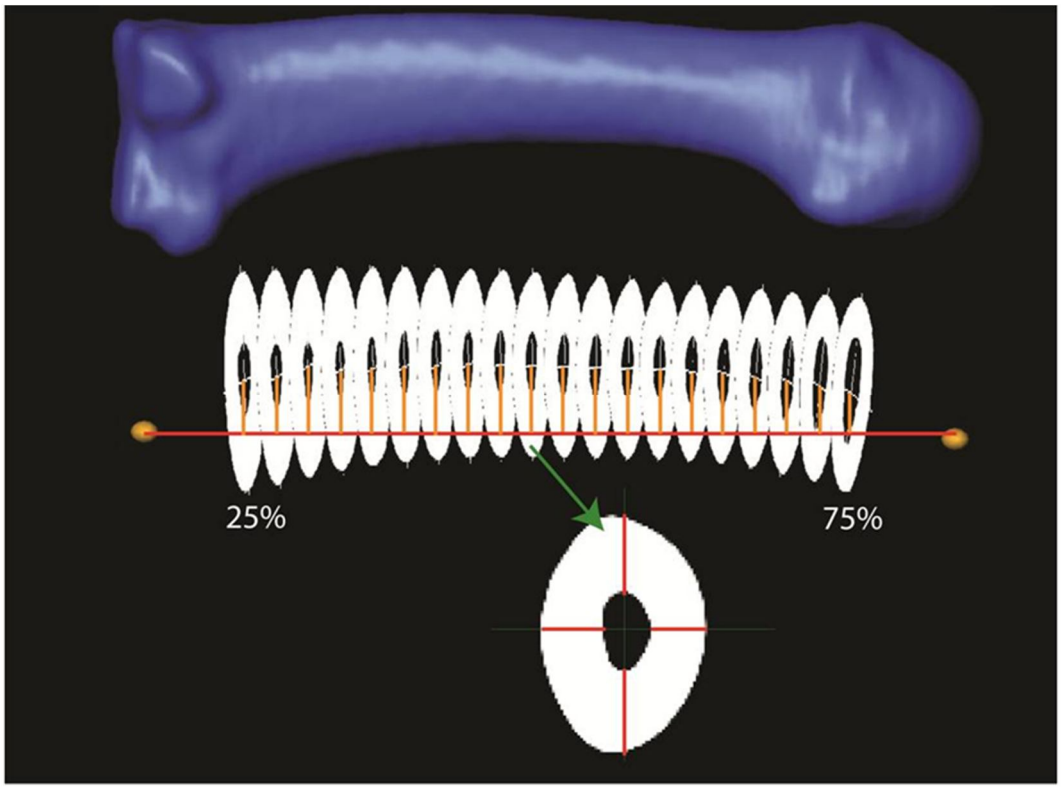


Figure 2.2: Representation of the technique employed by which cross sections are taken and analysed from a scanned metatarsal. Cross sections are taken every 2.5% from between 25%-75% of the biomechanical length of the diaphysis. The singular image at the bottom is one cross section with red lines indicating the anatomical directions of the cross section (plantar (bottom), dorsal (top), lateral (left) and medial (right). The yellow lines in each cross section represent the distance between the centroid and the longitudinal axis, i.e., the deepest point of the plantar surface.

2.2.5. Method for calculating cross-sectional properties

Data management: 5 absolute measurements were manually taken from each cross section (mm). Cortical bone thicknesses were measured at four anatomical regions (i.e., plantar, dorsal, medial and lateral cortices), while the location of plantar geometry change was measured on 59 bones in the sample set (Table 2.1). Each cross section is measured in an analogous fashion as morphological points on the base of metatarsals are more numerous and thus, more repeatable in future analysis (Figure 2.3). Aligning the bones according to diaphyseal landmarks would prove more difficult as there are fewer defined landmarks on any diaphysis compared to epiphyses, and is in line with current geometric morphometric techniques that have distinguished the epiphyses to be useful discriminators in morphological comparisons (Harmon 2007, 2009; Holliday *et al*. 2010). For all future studies relating to this data, the four measurements taken here will serve as the basis for calculation of a geometric mean (the average absolute measure from the four measurement locations in the cross section). This allows individual thickness values to be scaled before testing for inter-group variation, thereby increasing the statistical robusticity of the comparative thickness results.

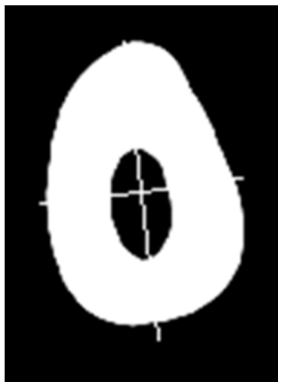
A)  B)  C) 

Figure 2.3: This figure represents three examples of the 5th cross section of metatarsal 2 taken from A) *Homo sapiens* (A13), B) *Pan paniscus* (20882) and C) *Pan troglodytes schweinfurthii* (15235).

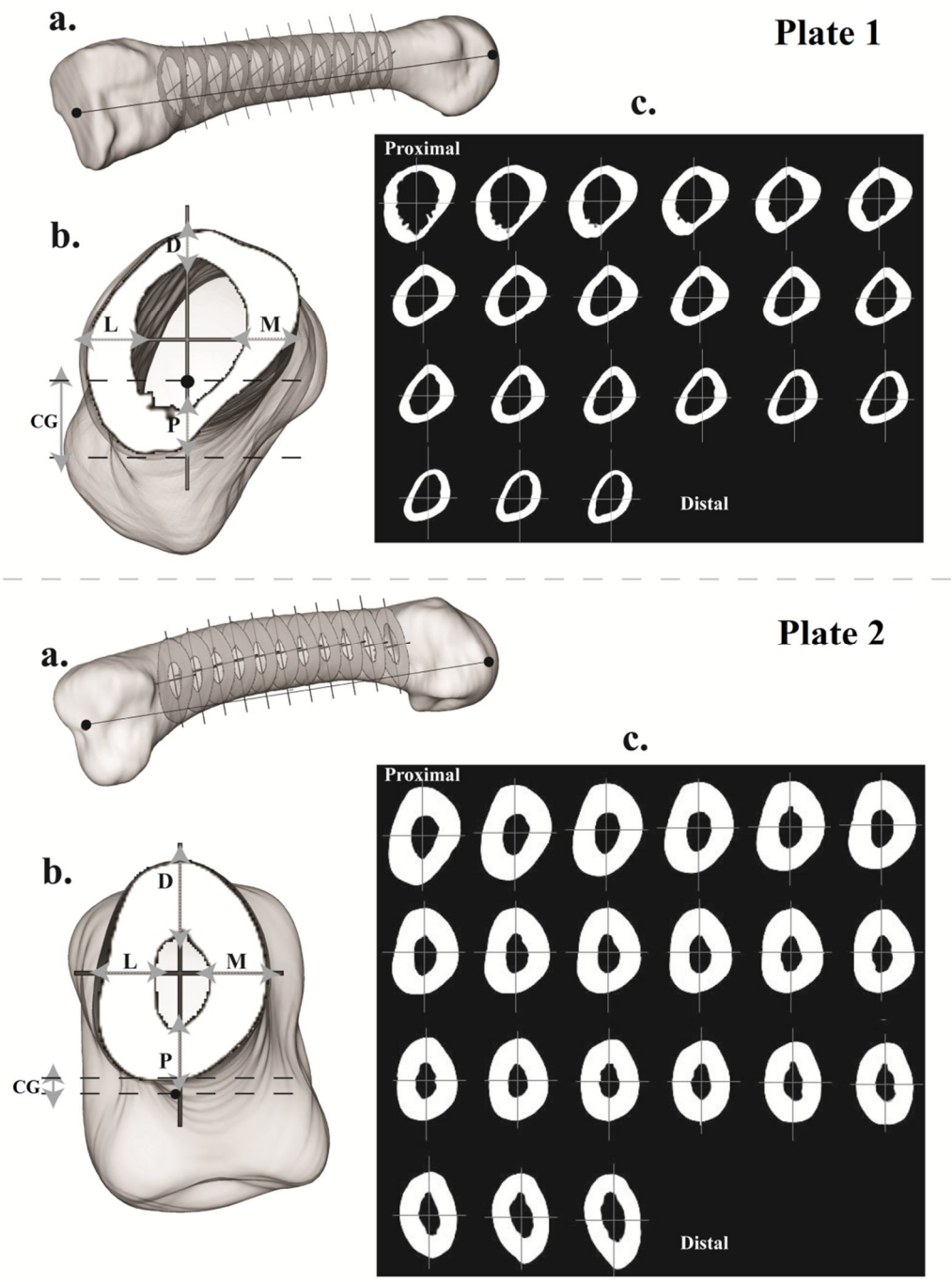


Figure 2.4: **Plate 1** represents *Pan paniscus* (20882). **Plate 2** represents *Homo sapiens* (A13); (**a**) depicts the method by which all 21 cross sections were taken (in this case from metatarsal 4), showing the cross- sectional positions along the diaphysis (number of cross sections reduced for clarity), and the landmarks

defining the longitudinal axis depicted as black dots; (**b**) depicts one cross section in position, viewed from the distal end of the metatarsal looking through the medullary cavity. The two examples depict the distance between the longitudinal axis (black dot) and the plantar surface (CG) and is an example of the measure taken for maximum change in geometry; (**c**). represents all 21 cross sections from metatarsal 4 to observe the obvious differences in cross-sectional shape between *Homo sapiens* and *Pan paniscus.*

Table 2.1: Total number of specimens per species and the total number of measurements taken per metatarsal, per cross section.

Variable	**M1 (16*)**	**M2 (21)**	**M3 (21)**	**M4 (21)**	**M5 (21)**	**TOTAL**
P.paniscus n=15						
Cv	255	315	315	315	315	
Pl	255	315	315	315	315	
Dr	255	315	315	315	315	
Md	255	315	315	315	315	
Lt	255	315	315	315	315	
Total	1275	1575	1575	1575	1575	7575
P.t.schweinfurthii n=22						
Cv	374	462	462	462	462	
Pl	374	462	462	462	462	
Dr	374	462	462	462	462	
Md	374	462	462	462	462	
Lt	374	462	462	462	462	
Total	1870	2310	2310	2310	2310	11110
H.sapiens n=23						
Cv	374	462	462	462	462	
Pl	374	462	462	462	462	
Dr	374	462	462	462	462	
Md	374	462	462	462	462	
Lt	374	462	462	462	462	
Total	1870	2310	2310	2310	2310	11110
					Total	**29,795**
* number of cross sections per metatarsal						
Cv= Curvature: Pl = Plantar: Dr = Dorsal: Md = Medial: Lt = Lateral						

Measuring cortical bone thickness: Cross sections were individually analysed using ImageJ (http://imagej.en.softonic.com/), a free open-source programme that, amongst other things, allows calculation of areas and pixel values. Principal axes of each cross section were defined by applying a moment calculation, marked on the cross section by a black cross (figure 2.2). One horizontal line was manually drawn through the centroid of each cross section to represent the mediolateral axis (X), and one vertical line through the centroid to represent the dorsoplantar axis (Y). This divided the cortex into four regions: plantar (Pl), dorsal (Dr), medial (Md) and lateral (Lt). Using the line tool in ImageJ, thickness in each region was manually measured on individual cross sections at the points where lines intersected the periosteal boundary (figure 2.2). For example, lateral cortical thickness was the distance from the outermost lateral surface of the cortex to the inner most surface of the cortex (i.e., red region of line in figure 2.2). An intraobservor error study was completed on 6 individuals, 2 from each species, reporting a mean difference for all respective measurements of 0.00146, or 0.105%.

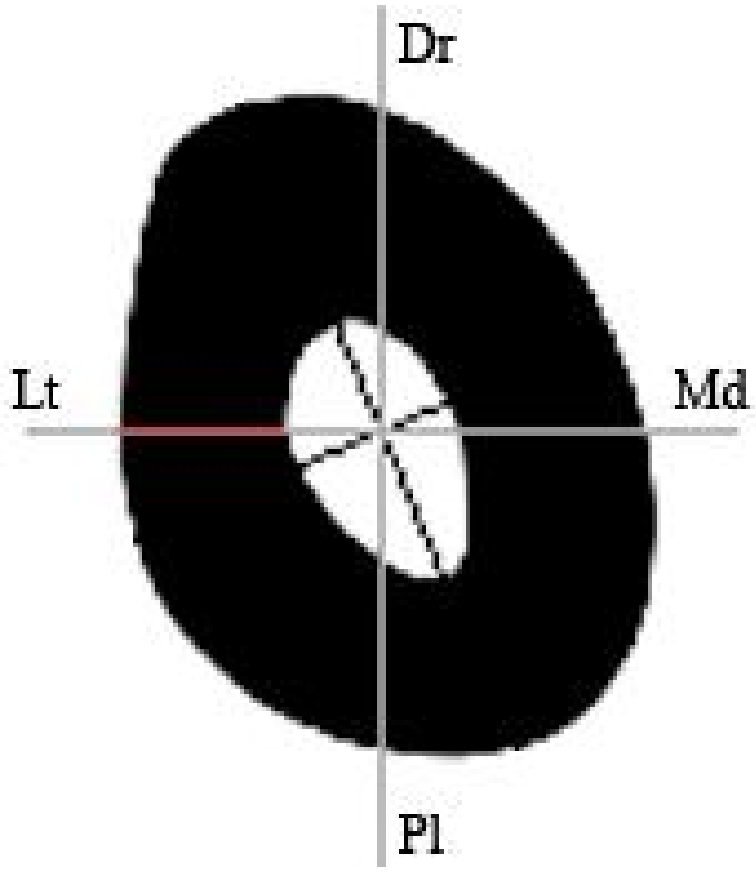


Figure 2.5: 6th cross section from left metatarsal 2, *P. t. schweinfurthii* (specimen #29073). The black cross in the medullary cavity represents the principal axes of metatarsal 2 (see section 2.2.4.). Grey lines represent anatomical axes (i.e., mediolateral and dorsoplantar), and indicates the points at which thickness measurements were taken. The red region of the line indicates lateral thickness. Pl = Plantar, Dr = Dorsal, Md = Medial, and Lt = Lateral. Figure is not to scale.

Measuring diaphyseal curvature (for maximum geometry change): The region of specific interest on the curved diaphysis can theoretically be considered as a stress concentrator, particularly on the plantar surface, since at the apex of the curve, geometry changes, and thus stress should be highly concentrated here, relative to other parts of the plantar surface (Pickley 1997). To quantify this theoretical point of stress concentration, a proxy location – the position of maximum curvature – was identified and calculated using Avizo 6.3 (1.9 Visualisation Sciences group, VSG, SAS). The method for determining the maximum change in geometry (i.e.; maximum curvature) involves measuring the distance from the longitudinal axis (defined by two points on the proximal and distal articular surfaces) to the plantar surface of the diaphysis. The cross section in which the greatest distance occurred thus indicated the greatest change in geometry (figure 2.6). In each cross section, the distance measurement was taken by first drawing a horizontal line through the middle of the projected landmark that defined the longitudinal axis (section 2.2.4, figures 2.1 and 2.2). The distance from this line to the plantar surface was measured. This method provides a proxy location for stress concentration since continuous assessment of the plantar surface was not practical. Also, because the change in geometry of the dorsal aspect of the diaphysis, or geometry of the medullary cavity, were not considered, the measurement is best considered as an estimate.

.

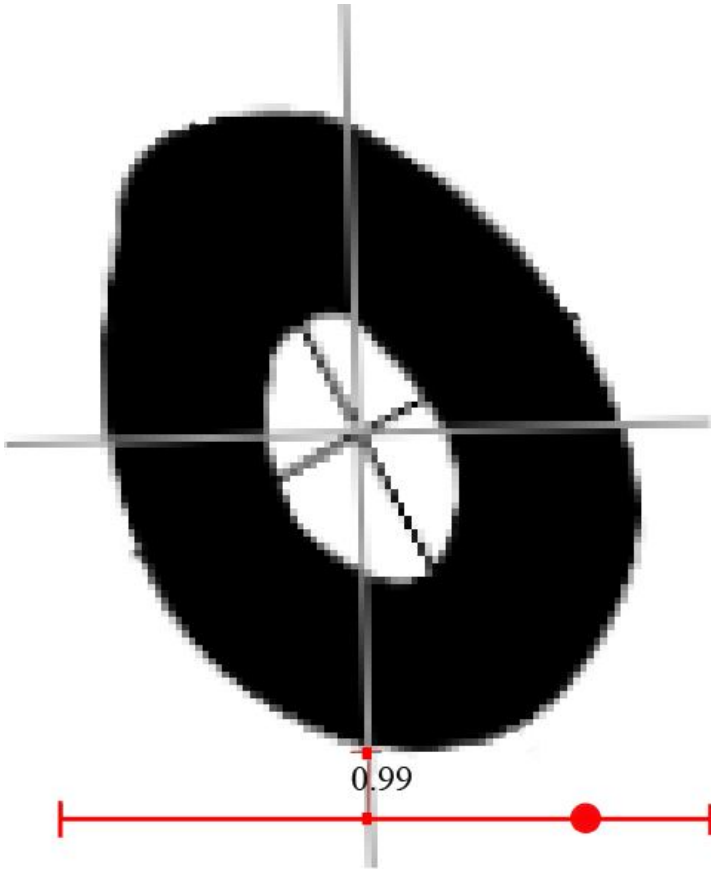


Figure 2.6: 6th cross section from left metatarsal 2, *P. t. schweinfurthii* (specimen #29073). The horizontal thick red line represents the longitudinal axis defined by the position of landmarks (e.g., dark red dot). The vertical thin red line indicates the maximum vertical distance between the longitudinal axis and the plantar surface (i.e. the proxy location of geometry change; 0.99mm). Figure is not to scale.

2.2.6. Analytical methodology

Descriptive analysis: Because values refer to cross section position, which is an ordinal scale variable rather than a continuous one (i.e., interval scale data),medians rather than means where chosen as the most appropriate indicator of central tendency. This required the use of non-parametric statistical tests (Siegel and Castellan 1988; Corder and Foreman 2009). The median cross section was calculated from all specimens by species, providing an indication of where (i.e., cross section position) maximum thickness and maximum geometry change of the diaphysis occurred (Table 2.2). Table 2.2 illustrates cross section position (CS = 9) at which maximum geometry change occurs in the plantar surface of metatarsal 1 for each specimen of *P. t. schweinfurthii*. Figure 2.4 illustrates data shown in Table 2.2 in a frequency distribution with a blue line representing the median value (CS 9). Figure 2.5 illustrates how the median for metatarsal 1 (CS 9) is represented within the metatarsal complex in *P. t. schweinfurthii* and in the results section (see Chapter 3).

Table 2.2: Cross section positions at which maximum geometry change occurs in metatarsal 1 of each specimen in *P. t. schweinfurthii*.

Specimen number	**CS**
Charlie	10
7426_#27	6
8341_#33	10
14579_#20	9
29074_#21	13
30845_#31	11
Flo	8
Gilka	11
8369_#34	5
11362_#32	9
Bee Madam	13
Jomeo	10
2916_32#	11
15235_20#	5
15350_31#	7
29073_19#	9
37663_34#	4
McBee	8
Melissa	11
OldFemale	8
Palias	8
Passion	6
	Median CS = 9

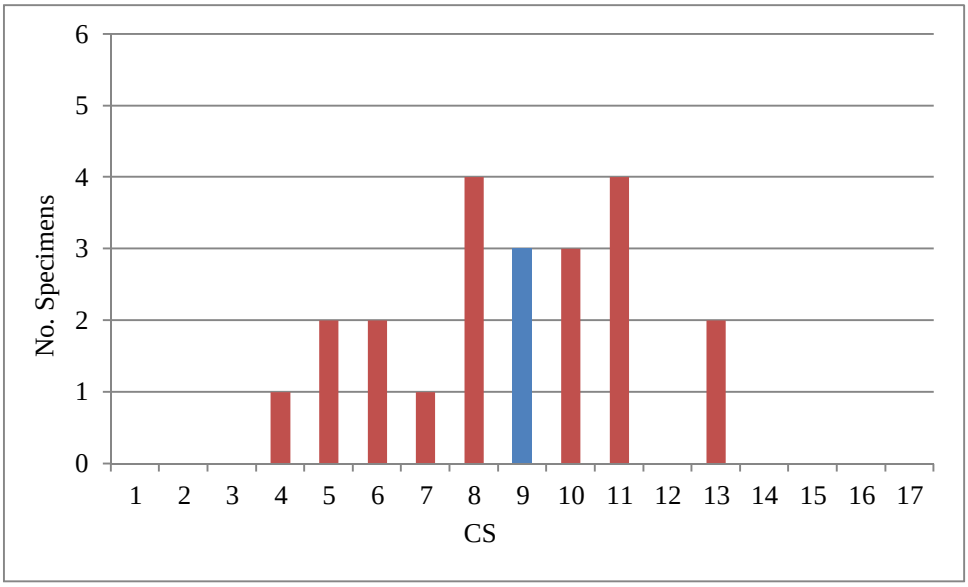


Figure 2.7: Frequency distribution of cross sections (CS) at which maximum geometry change occurs along the diaphysis of metatarsal 1 in *P. t. schweinfurthii*. The blue bar denotes the median.

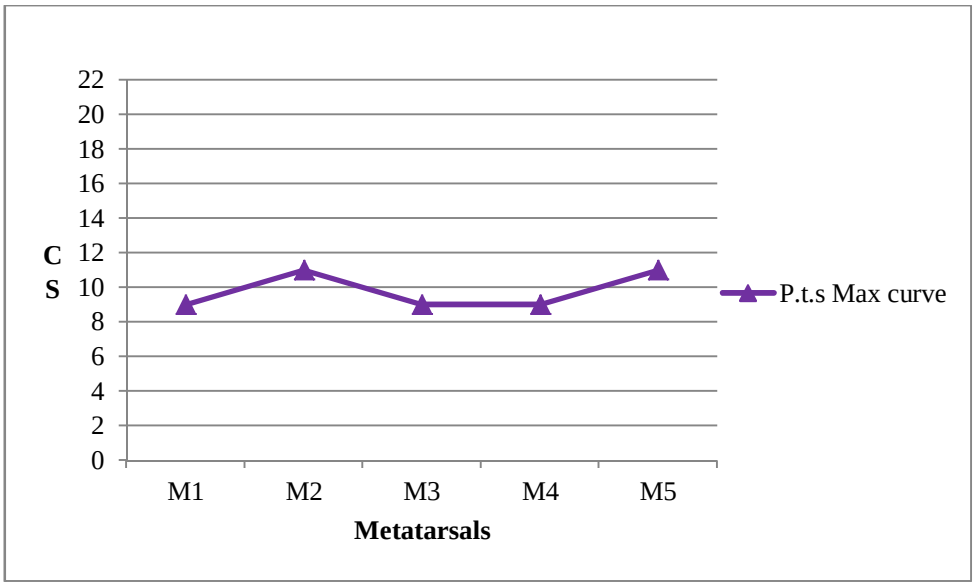


Figure 2.8: Location of the median cross section for maximum geometry change in all metatarsals in *P. t. schweinfurthii (P. t. s).*

Normalisation of the locations of maximum geometry change: Locating the maximum geometry change required normalisation[1], as the data set included both positive (i.e., plantar surface above the longitudinal axis) and negative (i.e., plantar surface below the longitudinal axis) values (figures 2.6 and 2.7).

Starting at cross section 0 (proximal most location), the first height value was subtracted from the other 16 or 21 values along the diaphysis in order to establish a zero point for each specimen. This facilitated comparisons of cross section locations at which maximum geometry change occurred. Figure 2.9 illustrates the changing position of the plantar surface for 6 specimens in *P. t. schweinfurthii*. It is clear that maximum geometry change occurs at different cross sections along the diaphysis in each individual, occurring both above and below the 0 axis. When represented like this, there is potential to interpret different 'types' of morphology, or to group particular individuals by a pattern of morphology seen through this representation. However, several distinct 'types' of curvature exhibit themselves across multiple individuals at the same time. Given this is a small subset of individuals, chosen randomly purely for ease of view, the observed differences in morphology that appear grouped in figures 2.9 and 2.10, may appear in the rest of the sample, however, alternatively, may also be representative of genetic variation within the sample. Figure 2.10 illustrates the same data, but after normalisation.

[1]Normalisation refers to division of multiple data sets (specimens) by a common variable in order to negate that variable's effect on the data, thus allowing underlying characteristics of the data sets to be compared and bringing them to a common scale (Surhone, *et al*.2010).

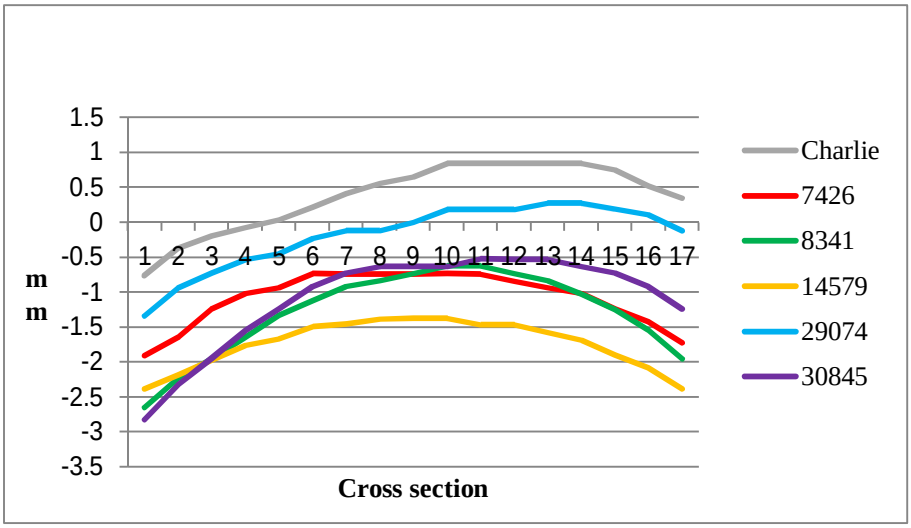


Figure 2.9: Example of non-normalised, raw values from 17 cross sections from 6 specimens of metatarsal 2, in *P. t. schweinfurthii*. The values defining the curves indicate the location of maximum change in geometry (Charlie-grey; 7426-red; 8341-green; 14579-orange; 29074-blue; 30845-purple).

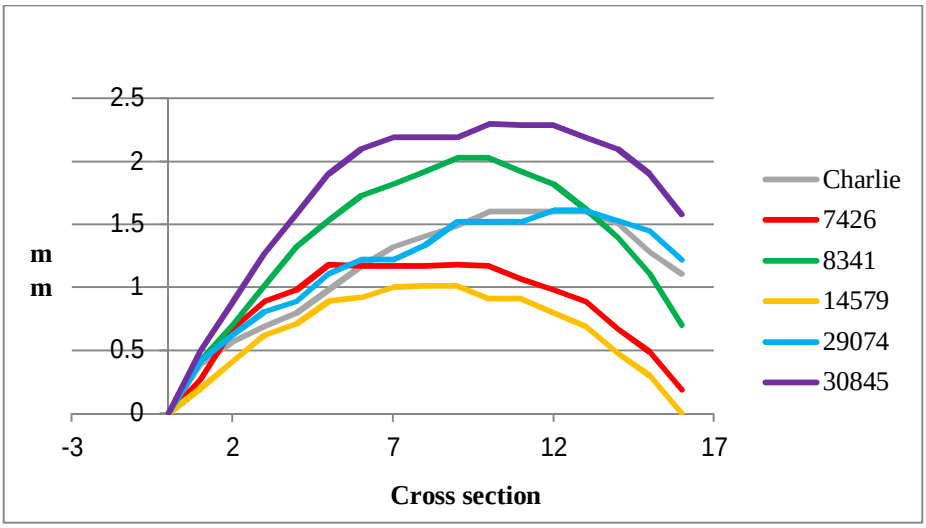


Figure 2.10: Example of normalised values from 17 cross sections from 6 specimens of metatarsal 2, in *P. t. schweinfurthii* representing values that define the location of maximum change in geometry (Charlie-grey; 7426-red; 8341-green; 14579-orange; 29074-blue; 30845-purple.

Statistical methodology: Non-parametric statistical analyses were performed with SPSS version 20 (IBM registered trademark). Analyses were performed on all bones between all cortices, and between relative positions of maximum thickness and geometry change within and between species. The non-parametric tests selected, test the example distribution shown in Table 2.2, but across all species.

To assess the intraspecific relationship of two variables (e.g.; plantar thickness by maximum geometry change in *P. paniscus*), a series of related-samples Wilcoxon signed rank test were applied.

To test interspecific relationships for multivariate comparisons (e.g.; plantar and lateral thickness by maximum curvature in *P. paniscus, H. sapiens* and *P. t. schweinfurthii*), an independent-samples Kruskal-Wallis one-way ANOVA was applied.

In all statistical analyses, the significance value that was used to denote statistical significance was 0.05. When $p < 0.05$, differences amongst groups were statistically significant. When $p > 0.05$, groups did not differ significantly in a variable.

3: CHAPTER 3 – Results

3.1. Intraspecific cortical bone thickness

3.1.1. Pan paniscus

Descriptive analysis:

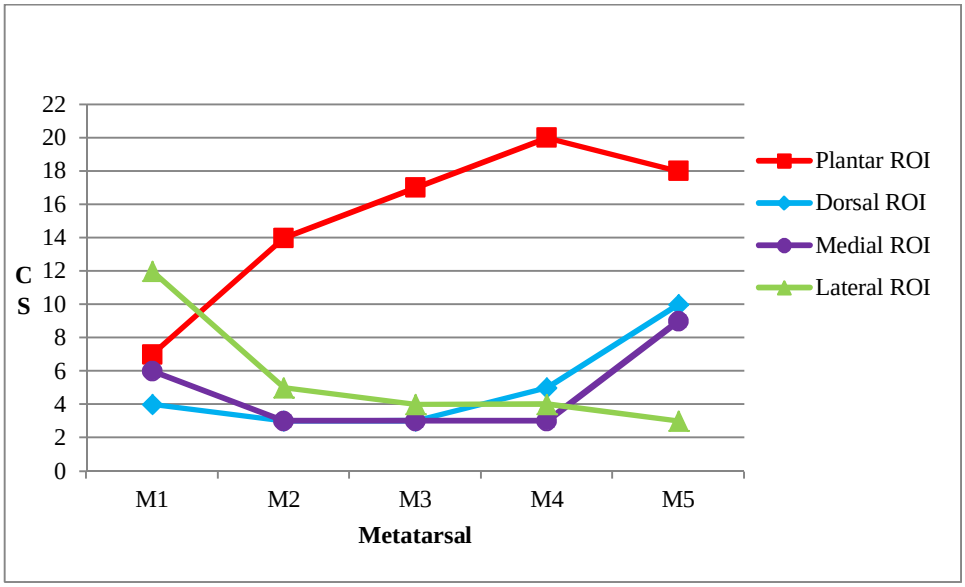


Figure 3.1: Cross sections (CS) containing ROI locations (median values) of maximal cortical thickness in metatarsal diaphyses (M1-5) of *P. paniscus*.

Plantar cortex: The position of maximum plantar thickness in metatarsals migrates gradually towards the distal end of the diaphysis when moving laterally amongst metatarsals of rays 1-4 (cross section (CS) 7, 14, 17, 20). In metatarsal 5, the trend in plantar thickness reverses itself, with the maximum moving proximally (CS 18) relative to maximum plantar thickness in metatarsal 4 (CS 20; Figure 3.1).

Dorsal cortex: The position of maximum dorsal thickness is nearer the proximal end of the diaphysis in metatarsals 1-4 (CS 4, 3, 3, 5, respectively). In metatarsal 5, the position of maximum dorsal thickness is relatively more distal and near the midshaft (CS 10; Figure 3.1).

Medial cortex: The position of maximum medial thickness exhibits a similar trend to maximum dorsal thickness. In metatarsal 1, medial thickness is positioned slightly more toward the midshaft (CS 6) than dorsal thickness. In metatarsals 2-4, however, the position of maximum medial thickness remains virtually in the same cross section as dorsal thickness (CS 3, 3, 3, respectively). In metatarsal 5, as with dorsal thickness, maximum medial thickness is more distally positioned toward the midshaft (CS 10; Figure 3.1).

Lateral cortex: The position of maximum lateral thickness exhibits an opposite trend across the metatarsus than maximum plantar thickness. In metatarsal 1, maximum lateral thickness is positioned near the midshaft (CS 12). Proceeding medially to laterally amongst metatarsals 2-5, the position of maximum lateral thickness remains proximally positioned across the complex (CS 3, 4, 4, 5, respectively; Figure 3.1) rather than distally.

Statistical analysis:

Table 3.1: *P*-values for Wilcoxon pairwise comparisons between positions of maximum thickness at all cortices in *P. paniscus.*

P. paniscus					
Cortical aspect	**MT1**	**MT2**	**MT3**	**MT4**	**MT5**
Plantardorsal	0.111	0.004**	0.006**	0.002**	0.003**
Plantarmedial	0.262	0.006**	0.023*	0.001**	0.003**
Plantarlateral	0.420	0.01*	0.024*	0.003**	0.003**
Dorsomedial	0.266	0.657	0.483	0.068	0.488
Dorsolateral	0.004**	0.078	0.285	0.875	0.054
Mediolateral	0.021*	0.132	0.858	0.027*	0.51

*Denotes values less than 0.05, **Denotes values less than 0.001

In metatarsal 1, positions of maximum cortical thickness were significantly different between dorsal and medial, and dorsal and lateral positions (Dr vs. Lt p=0.004; Md vs. Lt p=0.021).

In metatarsal 2, plantar positions of maximum cortical thickness were significantly different from dorsal, medial and lateral positions (Pl vs. Dr p=0.004; Pl vs. Md p=0.006; Pl vs. Lt p=0.010).

In metatarsal 3, plantar positions of maximum cortical thickness were significantly different from dorsal, medial and lateral positions (Pl vs. Dr p=0.006; Pl vs. Md p=0.023; Pl vs. Lt p=0.024).

In metatarsal 4, plantar positions of maximum cortical thickness were significantly different from dorsal, medial and lateral positions, while medial and

lateral positions differed significantly as well (Pl vs. Dr p=0.002; Pl vs. Md p=0.001; Pl vs. Lt p=0.003; Md vs. Lt p=0.027).

In metatarsal 5, plantar positions of maximum cortical thickness were significantly different from dorsal, medial and lateral positions, while medial and lateral positions differed as well (Pl vs. Dr p=0.003; Pl vs. Md p=0.003; Pl vs. Lt p=0.003; Md vs. Lt p=0.051).

3.1.2. Homo sapiens

Descriptive analysis:

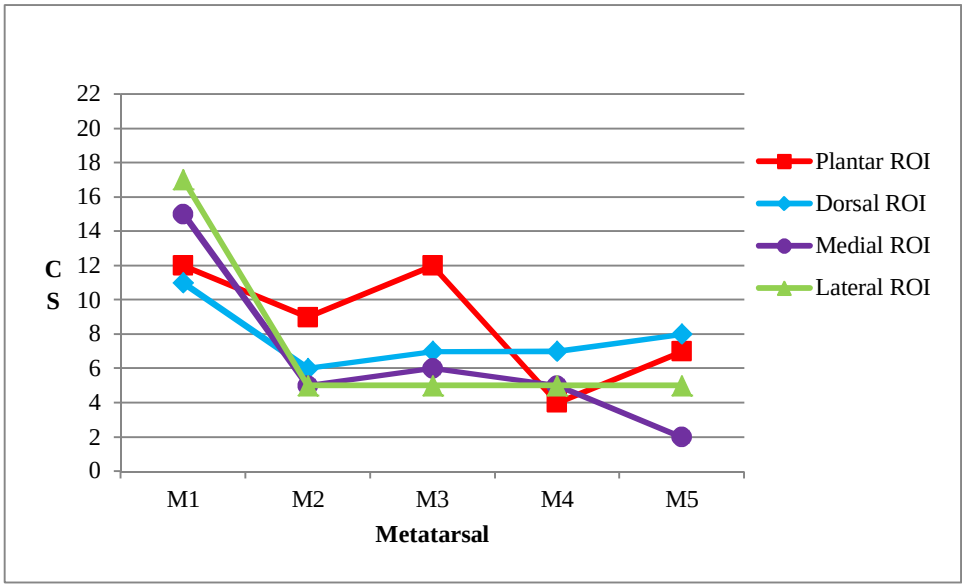


Figure 3.2: Cross sections (CS) containing ROI locations (median values) of maximal cortical thickness in metatarsal diaphyses (M1-5) of *H. sapiens*.

Plantar cortex: Positions of maximum thickness in metatarsals 1 and 3 are near the midshaft (CS 12). In metatarsal 2, maximum thickness is comparatively proximally-positioned (CS 9), and even more so in metatarsal 4 (CS 4). In

metatarsal 5, maximum thickness is positioned more distally than in metatarsal 4, but it is still in the proximal half of the diaphysis (CS 8; Figure 3.2).

Dorsal cortex: Position of maximum thickness in metatarsal 1 is near the midshaft (CS 11). Within metatarsals 2-5, maximum thickness migrates distally toward the midshaft while moving laterally amongst rays (CS 6, 7, 7, 8, respectively; Figure 3.2). Maximum thickness in these rays never quite reaches the comparatively more distal location observed in metatarsal 1.

Medial cortex: Position of maximum thickness moves relatively proximally through metatarsals 2-5 (Figure 3.2). In metatarsal 1, the point of maximum thickness is situated distally (CS 15) relative to the more proximal positions in metatarsals 2-5 (CS 5, 6, 5, 2, respectively).

Lateral cortex: The position of maximum thickness in metatarsal 1 is at the distal aspect (CS 17). The position of maximum thickness in other metatarsals is comparatively more proximal, and does not change in metatarsals 2-5 (CS 5, 5, 5, 5, respectively; Figure 3.2).

Statistical analysis:

Table 3.2: *P*-values for Wilcoxon pairwise comparisons between positions of maximum thickness at all cortices in *H. sapiens.*

H. sapiens					
Cortical aspect	**MT1**	**MT2**	**MT3**	**MT4**	**MT5**
Plantardorsal	0.512	0.520	0.134	0.717	0.512
Plantarmedial	0.065	0.394	0.097	0.224	0.003**
Plantarlateral	0.003**	0.295	0.005**	0.296	0.016*
Dorsomedial	0.001**	0.982	0.936	0.016*	0.007**
Dorsolateral	0.001**	0.277	0.007**	0.009**	0.011**
Mediolateral	0.110	0.378	0.026*	0.627	0.474

*Denotes values less than 0.05, **Denotes values less than 0.001

In metatarsal 1, positions of maximum cortical thickness were significantly different between plantar and lateral, dorsal and medial, and dorsal and lateral positions (Pl vs. Lt p=0.003; Dr vs. Md p=0.001; Dr vs. Lt p=0.001).

In metatarsal 2, positions of maximum cortical thickness exhibited no significant differences between the cortical locations .

In metatarsal 3, positions of maximum cortical thickness were significantly different between plantar and lateral, dorsal and lateral, dorsal and medial positions (Pl vs. Lt p=0.005; Dr vs. Lt p=0.007; Dr vs. Md p=0.026).

In metatarsal 4, positions of maximum cortical thickness were significantly different between dorsal and lateral, and between dorsal and medial positions (Dr vs. Lt p=0.009; Dr vs. Md p=0.016).

In metatarsal 5, positions of maximum cortical thickness were significantly different between dorsal and lateral, and between dorsal and medial

positions (Pl vs. Md p=0.003; Pl vs. Lt p=0.016; Dr vs. Lt p=0.011; Dr vs. Md p=0.007).

3.1.3. Pan troglodytes schweinfurthii

Descriptive analysis:

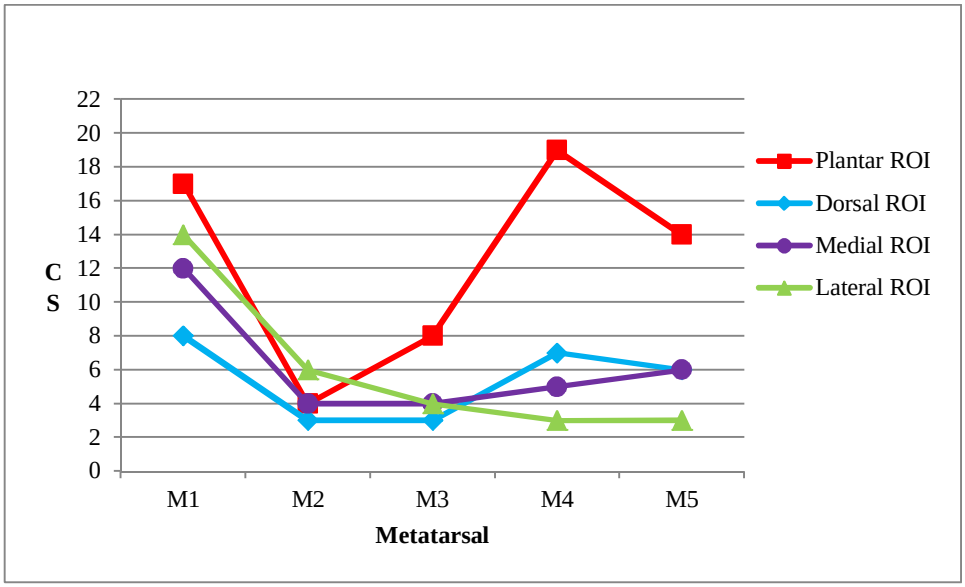


Figure 3.3: Cross sections (CS) containing ROI locations (median values) of maximal cortical thickness in metatarsal diaphyses (M1-5) of *P. t. schweinfurthii*.

Plantar cortex: Position of maximum thickness is highly variable between metatarsals. In metatarsals 1 and 4, position of maximum thickness is at the distal end (M1-CS 17; M4-CS19). In contrast, maximum thickness occurs in the proximal region of metatarsal 2, and in metatarsal 3 just before the midshaft (M2-CS 3; M3-CS 8). In metatarsal 5, position of maximum thickness is more distal in the diaphysis (CS 14; Figure 3.3).

Dorsal cortex: A plot of the position of maximum thickness exhibits a slight 'U' shape for metatarsals 2-4 (CS 8, 3, 3, 7, respectively). In metatarsal 5, there is a slight shift in position back toward the proximal end of the diaphysis (CS 6; Figure 3.3).

Medial cortex: Positions of maximum thickness in metatarsals 2-5 are proximally-situated (CS 4, 4, 5, 6, respectively; Figure 3.3). Position of maximum thickness in metatarsal 1 is near the midshaft (CS 12).

Lateral cortex: Position of maximum thickness moves from a distal position in metatarsal 1 to a comparatively proximal position in metatarsal 5 (CS 14, 6, 4, 3, 3, respectively; Figure 3.3).

Statistical analysis:

Table 3.3: *P*-values for Wilcoxon pairwise comparisons between positions of maximum thickness at all cortices in *P. t. schweinfurthii.*

P. t. schweinfurthii					
Cortical aspect	**MT1**	**MT2**	**MT3**	**MT4**	**MT5**
Plantardorsal	0.002**	0.102	0.001**	0.001**	0.001**
Plantarmedial	0.047*	0.445	0.075	0.001**	0.001**
Plantarlateral	0.264	0.313	0.003**	0.001**	0.001**
Dorsomedial	0.028*	0.671	0.056	0.022*	0.227
Dorsolateral	0.001**	0.006**	0.213	0.002**	0.002**
Mediolateral	0.089	0.033*	0.619	0.109	0.011*

*Denotes values less than 0.05, **Denotes values less than 0.001

In metatarsal 1, positions of maximum cortical thickness were significantly different between plantar and dorsal, plantar and medial, dorsal and medial, and dorsal and lateral positions (Pl vs. Dr p=0.002; Pl vs. Md p=0.047; Dr vs. Md p=0.000; Dr vs. Lt p=0.028).

In metatarsal 2, positions of maximum cortical thickness were significantly different between dorsal and lateral, and between medial and lateral positions (Dr vs. Lt p=0.006; Md vs. Lt p=0.033).

In metatarsal 3, plantar position of maximum cortical thickness was significantly different from dorsal and lateral positions (Pl vs. Dr p=0.001; Pl vs. Lt p=0.003).

In metatarsal 4, plantar position of maximum cortical thickness was significantly different from dorsal, medial and lateral positions, while dorsal position also was significantly different from medial and lateral positions (Pl vs. Dr p=0.001; Pl vs. Md p=0.001; Pl vs. Lt p=0.001; Dr vs. Md p=0.022; Dr vs. Lt p=0.022).

In metatarsal 5, plantar position of maximum cortical thickness was significantly different from dorsal, medial and lateral aspects, while lateral position also was significantly different from dorsal and medial positions (Pl vs. Dr p=0.001; Pl vs. Md p=0.000; Pl vs. Lt p=0.000; Dr vs. Lt p=0.002; Md vs. Lt p=0.011).

3.2. Interspecific cortical bone thickness

3.2.1. Interspecific comparison of maximum plantar thickness location:

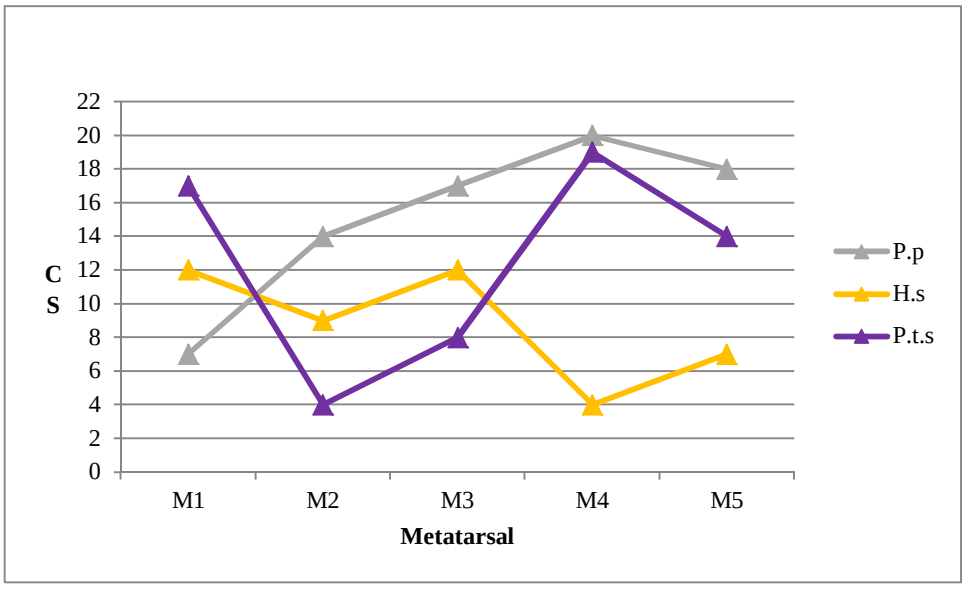


Figure 3.4: Cross sections (CS) containing ROI locations (median values) of maximum cortical thickness on the plantar surface in metatarsal diaphyses (M1-5) of *P. paniscus (P.p), H. sapiens (H.s) and P. t. schweinfurthii (P.t.s).*

In metatarsal 1, *P. t. schweinfurthii* has the most distally-positioned (CS 17) maximum plantar thickness, while *P. paniscus* has the most proximally-positioned (CS 7) thickness of the three taxa. Amongst bonobos and common chimpanzees, positions of maximum plantar thickness exhibit a similar pattern between the other metatarsals (2, 3, 4 and 5) compared to humans. This pattern exhibits a general trend toward the distal aspect, sharing a similar point at metatarsal 4, however, in metatarsal 5 the position is more proximally placed in *P. t. schweinfurthii*. In metatarsal 2, *P. t. schweinfurthii* exhibits the most proximally-positioned thickness (CS 4), while *P. paniscus* exhibits the most distally-positioned thickness (CS 14) of the three taxa. In metatarsals 1 and 2,

maximum plantar thickness locations in *H. sapiens* (CS 12 and 9, respectively) fall between these locations in *P. paniscus* and *P. t. schweinfurthii.* Absolute interspecific correspondence in actual cross sections occurs only in the distal region of metatarsal 4 in *P. paniscus* (CS 20) and *P. t. schweinfurthii* (CS 19). In *H. sapiens*, locations of maximum plantar thickness in metatarsal 4 and 5 are uniquely at the proximal end (CS 4, 7, respectively; Figure 3.4).

Statistical analysis:

Table 3.4: *P*-values for Kruskal-Wallis tests of positions of maximum thickness at plantar cortices between all species.

Interspecific plantar thickness *p*-values				
MT1	**MT2**	**MT3**	**MT4**	**MT5**
0.093	0.199	0.225	0.001**	0.001**

*Denotes values less than 0.05, **Denotes values less than 0.001

Positions of maximum cortical thickness at the plantar cortices were significantly different between species in metatarsals 4 and 5 (M4 p=0.000; M5 p=0.001). The Kruskal-Wallis test does not permit post-hoc testing of specific pairwise comparisons, however, based on the values plotted in figure 3.4, it is reasonable to suggest that the locations in *H. sapiens* differ from the locations of both species of *Pan*. The two species of *Pan*, however, trace a similar pattern through metatarsals 2-4 in that position progresses distally. At metatarsals 2 and 3, there is a dramatic difference in the position of maximum plantar thickness, although a distally moving trend is consistent.

.

3.2.2. Interspecific comparison of maximum dorsal thickness location:

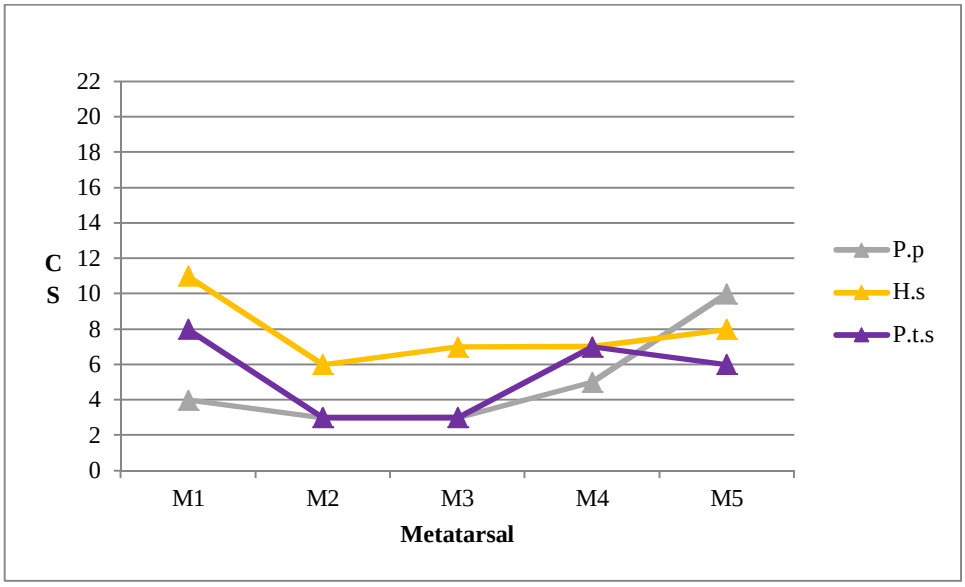


Figure 3.5: Cross sections (CS) containing ROI locations (median values) of maximal cortical thickness on the dorsal surface in metatarsal diaphyses (M1-5) of *P. paniscus (P.p), H. sapiens (H.s) and P. t. schweinfurthii (P.t.s).*

In all species, positions of maximum dorsal thicknesses are distributed in the proximal half of the diaphysis. Position of maximum dorsal thickness is most distal in metatarsals 1-4 in *H. sapiens.* Position of maximum dorsal thickness is largely similar between species in metatarsals 4 and 5. The three species converge most closely in distribution of dorsal thickness in metatarsal 4, particularly when comparing *H. sapiens* and *P. t. schweinfurthii* (CS 5, 7, respectively).

Statistical analysis:

Table 3.5: *P*-values for Kruskal-Wallis tests between positions of maximum thickness at dorsal cortices between all species.

Interspecific dorsal thickness *p* values				
MT1	**MT2**	**MT3**	**MT4**	**MT5**
0.038*	0.008**	0.001**	0.258	0.91

*Denotes values less than 0.05, **Denotes values less than 0.001

Positions of maximum cortical thickness at the dorsal cortices were significantly different between species in metatarsals 1, 2 and 3 (M1 p=0.038; M2 p=0.008; M3 p=0.000). The Kruskal-Wallis test does not permit post-hoc testing of specific pairwise comparisons. At least in metatarsals 2 and 3, the locations of maximum cortical thickness in *H. sapiens* are more distally positioned relative to *Pan*, while the two species of *Pan* retain a similar position (figure 3.5). Conservatively, it is possible that in metatarsal 1, humans and bonobos differ, and it may or may not be the common chimpanzee sample that is driving the taxonomic difference.

3.2.3. Interspecific comparison of maximum medial thickness location:

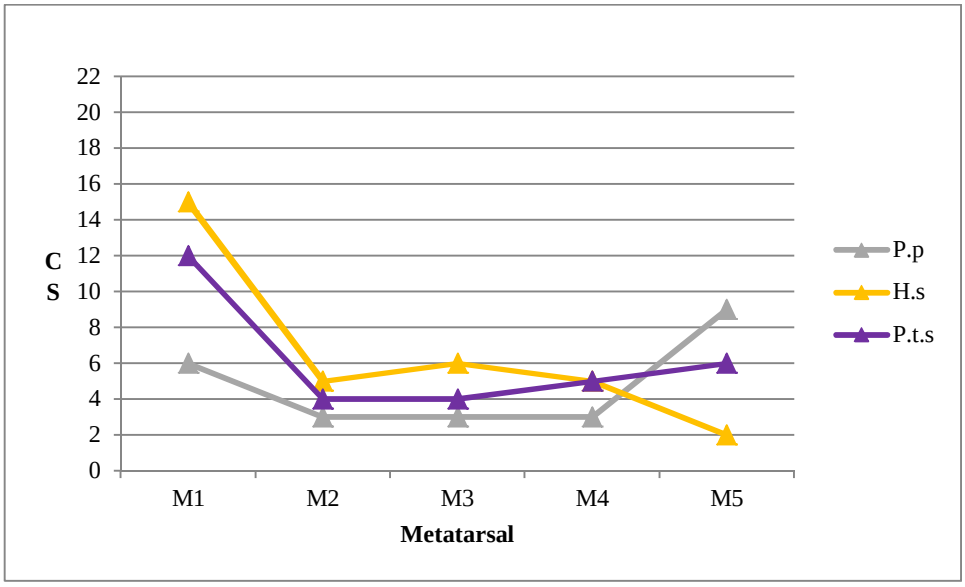


Figure 3.6: Cross sections (CS) containing ROI locations (median values) of maximum cortical thickness on the medial surface in metatarsal diaphyses (M1-5) of *P. paniscus (P.p), H. sapiens (H.s) and P. t. schweinfurthii (P.t.s).*

Positions of maximum medial thickness in metatarsal 1 are distributed along the diaphysis such that *H. sapiens* exhibits the most distal position (CS - 15) and *P. paniscus* the most proximal position (CS - 6). A relatively proximal position of maximum medial thickness applies across species for metatarsals 2, 3 and 4 positions, where locations occur within 3 slices of each other. As in the dorsal cortex thickness location, the three species correspond most closely in metatarsal 4 for medial thickness position, for which *H. sapiens* and *P. t. schweinfurthii* share the same cross section position (CS - 5). For metatarsal 5, the three species show an opposite trend compared to metatarsal 1: *P. paniscus* displays the most distal position and *H. sapiens* the most proximal position (Figure 3.6).

Statistical analysis:

Table 3.6: *P*-values for Kruskal-Wallis between positions of maximum thickness at medial cortices between all species.

Interspecific medial thickness *p* values				
MT1	**MT2**	**MT3**	**MT4**	**MT5**
0.003**	0.038*	0.392	0.225	0.011*

*Denotes values less than 0.05, **Denotes values less than 0.001

Positions of maximum cortical thickness at the medial cortices were significantly different between species in metatarsals 1, 2 and 5 (M1 p=0.003; M2 p=0.038; M5 p=0.011). While Kruskal-Wallis test does not permit post-hoc testing of specific pairwise comparisons, statistically significant pairwise comparisons in figure 3.6 appear in metatarsals 2-4 between the two species of Pan, and between all three species in metatarsals 2 and 4.

3.2.4. Interspecific comparison of maximum lateral thickness location:

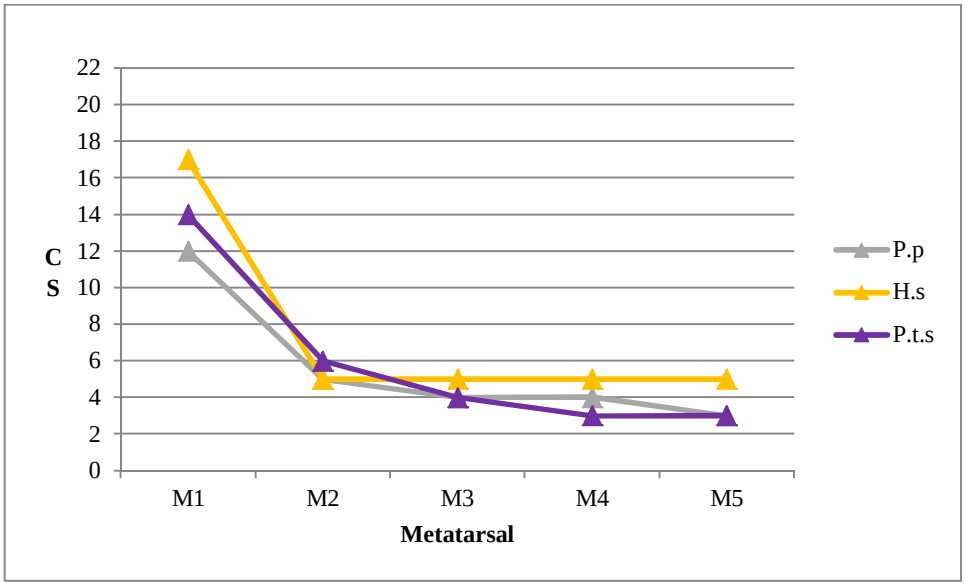


Figure 3.7: Cross sections (CS) containing ROI locations (median values) of maximal cortical thickness on the lateral surface in metatarsal diaphyses (M1-5) of *P. paniscus (P.p), H. sapiens (H.s) and P. t. schweinfurthii (P.t.s).*

Positions of lateral maximum thickness have nearly identical locations in metatarsal 1 for each of the three species, occurring within 5 cross sections across the three groups (CS 12, 14, 17). All exhibit positions in the distal half of the diaphysis. *H. sapiens* occupies the most distal position (CS 17), while *P. paniscus* displays the comparatively most proximal position (CS 12). In metatarsals 2, 3, 4 and 5, all positions of lateral maximum thickness are in the proximal half of diaphyses, occurring within 2 cross sections.

Statistical analysis:

Table 3.7. *P*-values for Kruskal-Wallis between positions of maximum thickness at lateral cortices between all species.

Interspecific lateral thickness *p* values				
MT1	**MT2**	**MT3**	**MT4**	**MT5**
0.005**	0.353	0.823	0.381	0.234

*Denotes values less than 0.05, **Denotes values less than 0.001

Positions of maximum cortical thickness in medial cortices of metatarsal 1 were significantly different between species (p=0.005). No other significant differences were observed between species.

3.2.5. Interspecific comparison of all cortices thicknesses across species:

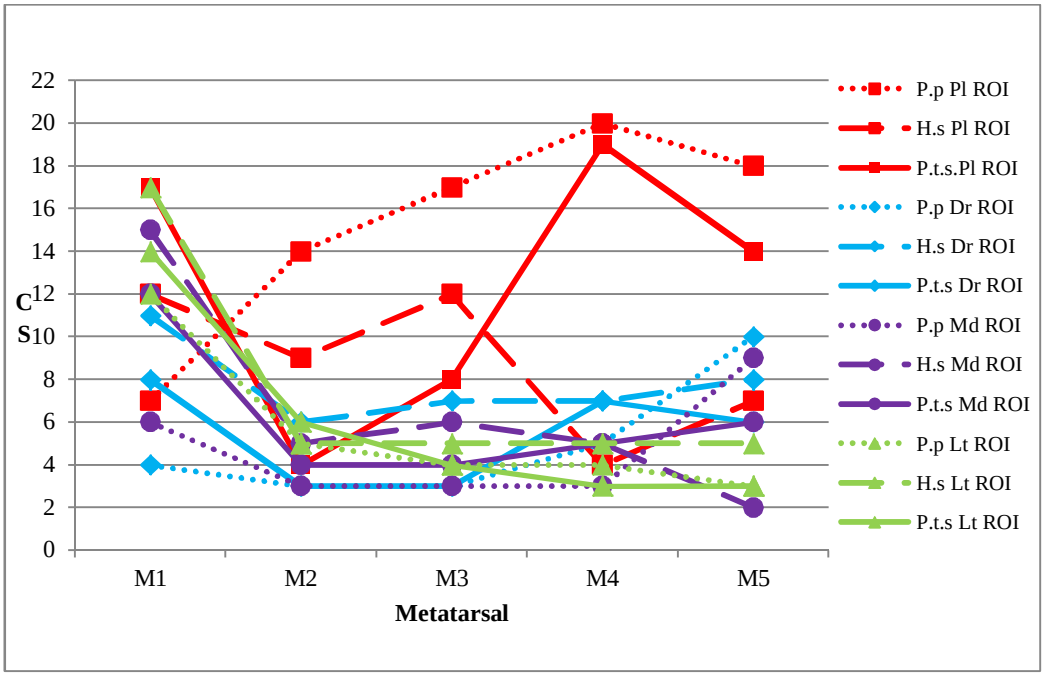


Figure 3.8: Illustration of interspecific relationships in maximum thicknesses in all four cortices (plantar – Pl, dorsal – Dr, medial – Md, lateral - Lt. ROI locations). Note: the greatest interspecific divergence of thickness positions in metatarsal 1 is in the plantar cortex. Note also the consistently more distal position of plantar thickness across the metatarsus in *P. paniscus (P.p)*, across metatarsals 1-3 in *H. sapiens (H.s)*, and metatarsals 2-5 in *P. t. schweinfurthii (P.t.s)* compared to other cortices in each taxa. Furthermore, note that in metatarsals 2-5 the dorsal, medial and lateral positions of maximum thickness reside proximal to the midshaft in all three groups.

Each group exhibits positions of median maximum plantar thickness that are variably distributed along the diaphysis and throughout the metatarsal complex (Figure 3.8). In all taxa for dorsal, medial, and lateral cortices, positions of maximum thickness in all metatarsals usually occur in the proximal half of the

diaphysis (before CS 10; Figure 3.12). In metatarsal 1, positions of maximum thickness in all cortices are widely distributed along the diaphysis from proximal and distal.

3.3. Position of maximum change in geometry

3.3.1. Pan paniscus

The position occurs in the midshaft region of the diaphysis and maintains this general position in metatarsals 1-5 (CS 8, 12, 9, 10, 11, respectively; Figure 3.9).

3.3.2. Homo sapiens

The position occurs in the midshaft region of the diaphysis and remains within 3 cross sections across metatarsals 1-5 (CS 11, 12, 11, 11, 14 respectively). The biggest shift in position occurs between metatarsals 4 and 5 (CS - 11, 14, respectively; Figure 3.9).

3.3.3. Pan troglodytes schweinfurthii

The position occurs in the midshaft region of the diaphysis and remains within 2 cross sections across metatarsals 1-5 (CS 9, 11, 9, 9, 11, respectively; Figure 3.9).

3.3.4. Interspecific comparisons of maximum geometry change

Descriptive analysis:

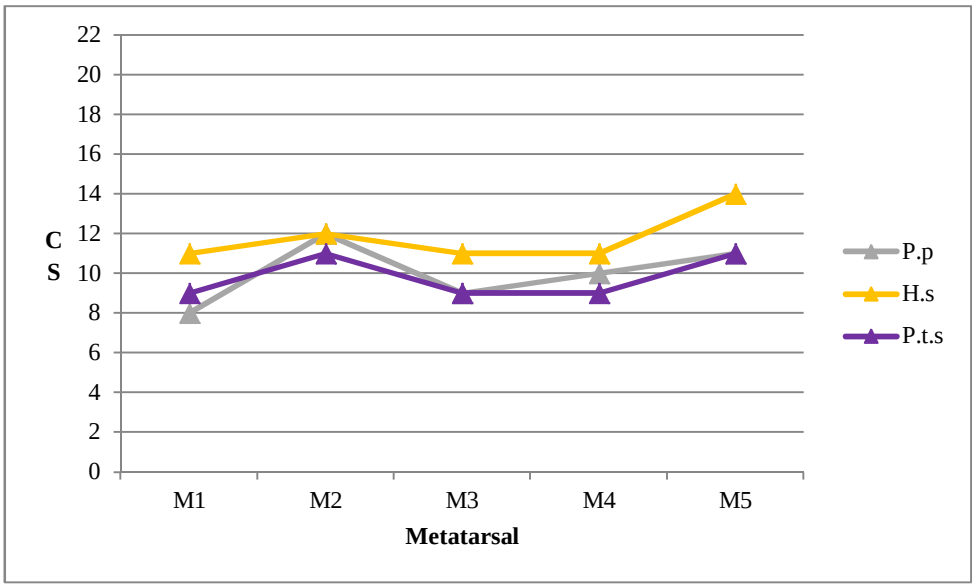


Figure 3.9: Group comparisons of cross sections (CS) containing ROI locations (median values) of maximum change in geometry on the plantar surface in metatarsals (M1-5) of *P. paniscus (P.p), H. sapiens (H.s) and P. t. schweinfurthii (P.t.s).*

The positions correspond between species at the midshaft essentially mirroring each other across the complex from metatarsals 1-5. *H. sapiens* display a slightly more distally-positioned location compared to *P. paniscus* and *P. t. schweinfurthii*, which both exhibit locations within a single cross section of each other for each metatarsal (CS 11, 12, respectively; Figure 3.9).

Statistical analysis:

Table 3.8: *P*-values for Kruskal-Wallis tests between positions of maximum geometry change in all species across metatarsals.

***p* values: All taxa**				
MT1	**MT2**	**MT3**	**MT4**	**MT5**
0.007**	0.082	0.112	0.001**	0.906

*Denotes values less than 0.05, **Denotes values less than 0.001

Table 3.9: *P*-values for Kruskal-Wallis between positions of maximum geometry change in *P. paniscus and P. t. schweinfurthii* across metatarsals.

p* values: *Pan				
MT1	**MT2**	**MT3**	**MT4**	**MT5**
0.553	0.017*	1.000	0.003**	0.839

*Denotes values less than 0.05, **Denotes values less than 0.001

The positions of maximum geometry change were significantly different between species in metatarsals 1 and 4 (Kruskal-Wallis; M1 p=0.007; M4 p=0.001). Within *Pan*, positions of maximum geometry change are significantly different between *P. paniscus* and *P. t. schweinfurthii* in metatarsals 2 and 4 (Man Whitney-U; M2 p=0.017; M4 p=0.003).

3.4. Relationship between positions of maximum thicknesses versus maximum geometry change.

In the following statistical tests, the predicted relationship is the null-hypothesis – similarity in (cross section) location of thickness and geometry change. Thus, predictions are supported when statistically significant differences in locations are not found ($p > 0.05$).

3.4.1. Pan paniscus

Descriptive analysis:

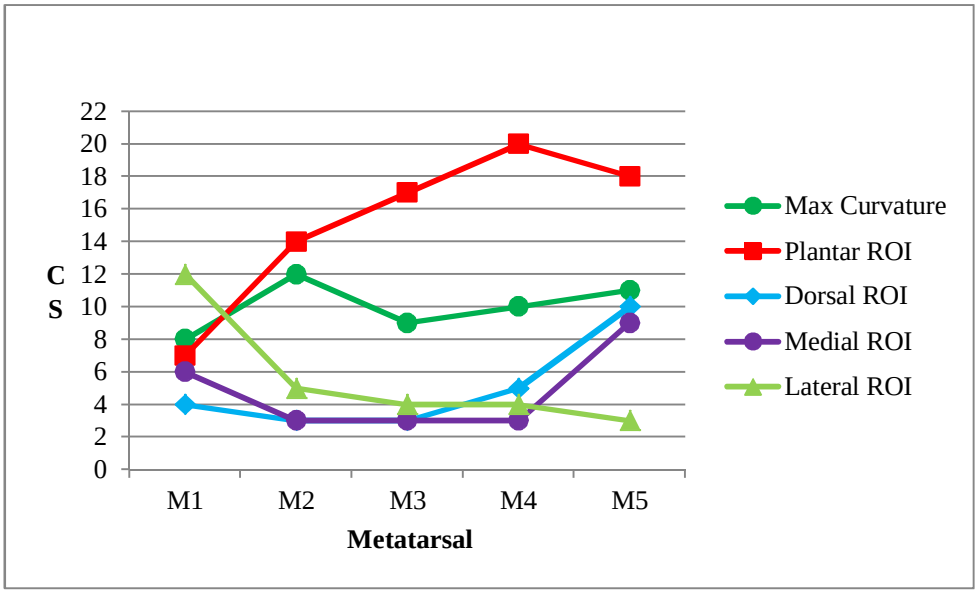


Figure 3.10: Cross sections (CS) containing ROI locations (median values) of maximum change in geometry compared to all anatomical cortices in metatarsal (M1-5) of *P. paniscus.*

Plantar thickness versus maximum geometry change: Position of maximum thickness corresponds with the position of maximum geometry change on the proximal aspect of metatarsal 1 to within one cross section (CS 7, 8, respectively).

In metatarsal 2, position of maximum thickness corresponds with the position of maximum geometry change to within 2 cross sections (CS 14, 12, respectively). Position of maximum thickness and maximum geometry change do not correspond in metatarsals 3, 4 and 5. The greatest distance between these positions occurs in metatarsal 4 where positions are over 10 cross sections apart (CS 10 vs. 20; Figure 3.10).

Dorsal thickness versus maximum geometry change: Position of maximum thickness corresponds with the position of maximum geometry change (near the midshaft) in metatarsal 5 to within one cross section (CS 10, 11, respectively). Position of maximum thickness and maximum geometry change do not correspond in metatarsals 1, 2, 3 and 4. The greatest distance between these positions occurs in metatarsal 2 (CS 3 vs. 12; Figure 3.10).

Medial thickness versus maximum geometry change: Position of maximum thickness corresponds with the position of maximum geometry change (near the midshaft) in metatarsal 1 (CS 6, 8, respectively) and metatarsal 5 in both cases to within two cross sections (CS 8, 10, respectively). Positions of maximum dorsal thickness and maximum geometry change do not share similarity in positions in metatarsals 2, 3 and 4. The greatest distance between positions occurs in metatarsal 2 (CS 3 vs. 12; Figure 3.10).

Lateral thickness versus maximum geometry change: Position of maximum thickness does not correspond with maximum geometry change in any metatarsal diaphysis (Figure 3.10).

Statistical analysis:

Table 3.10: *P*-values for Wilcoxon pairwise comparisons of maximum thickness and maximum geometry change locations in *P. paniscus* across metatarsals.

Wilcoxon *p* values					
P. paniscus	**MT1**	**MT2**	**MT3**	**MT4**	**MT5**
Plantar/curvature	0.649	0.733	0.439	0.009*	0.020*
Dorsal/curvature	0.010**	0.001**	0.001**	0.050	0.267
Medial/curvature	0.587	0.001**	0.063	0.001**	0.105
Lateral/curvature	0.108	0.002**	0.032*	0.250	0.004**

*Denotes values less than 0.05, **Denotes values less than 0.001

Statistical analyses were used to test distributions of relative positions of maximum thicknesses and maximum geometry change. In metatarsal 1, positions were not statistically different in the plantar (p=0.649), medial (p=0.587), and lateral cortices (p=0.108). In metatarsal 2, positions were not statistically different in the plantar cortex (p=0.733). In metatarsal 3, positions were not statistically different in plantar (p=0.053) and medial cortices (p=0.063). In metatarsal 4, positions were not statistically different in the dorsal (p=0.05) and lateral cortices (p=0.025). In metatarsal 5, positions were not statistically different in plantar (p=0.232), dorsal (p=0.267) and medial cortices (p=0.105; Table 3.9).

3.4.2. Homo sapiens

Descriptive analysis:

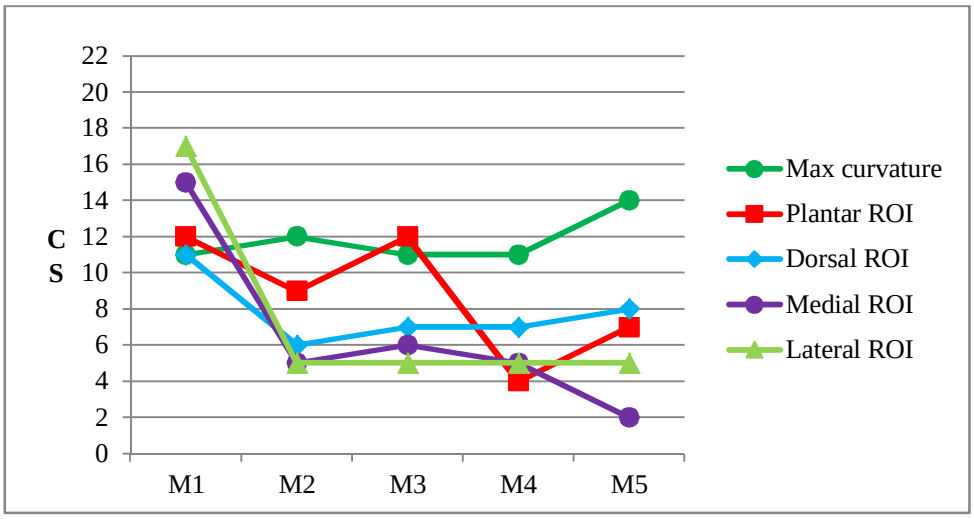


Figure 3.11: Cross sections (CS) containing ROI locations (median values) of maximum change in geometry compared to all anatomical cortices compared to all cortices in metatarsals 1-5 of *Homo sapiens.*

Plantar thickness versus maximum geometry change: Position of maximum thickness corresponds with position of maximum geometry change (near the midshaft) in metatarsals 1 and 3 to within one cross section (CS 12, 11, respectively). In metatarsal 2, position of maximum thickness corresponds with position of maximum geometry change to within 3 cross sections (CS 9, 12, respectively). In metatarsals 4 and 5, positions of maximum plantar thickness and maximum geometry change follow a similar pattern, but do not correspond in locations (i.e., separated by 7 cross sections) (Figure 3.11).

Dorsal thickness versus maximum geometry change: Position of maximum thickness corresponds with position of maximum geometry change (near the

midshaft) in metatarsal 1 to within one cross section (CS 11, 12, respectively). In metatarsal 2, positions do not correspond as maximum thickness is positioned somewhat proximally and maximum geometry change is positioned more distally (CS 6, 12, respectively). Positions of maximum thickness and maximum geometry change also do not correspond in metatarsals 3, 4 or 5, (M3 and M4 CS 7, 11; M5 CS 8, 14; Figure 3.11).

Medial thickness versus maximum geometry change: Position of maximum thickness does not share a similar position with maximum geometry change in any metatarsal. The position of maximum thickness is positioned proximally, while maximum geometry change is positioned more distally showing no correspondence in metatarsals 1, 2, 3, 4 or 5 (Figure 3.11).

Lateral thickness versus maximum geometry change: Position of maximum thickness does not correspond to the position of maximum geometry change in any metatarsal (Figure 3.11).

S*tatistical analysis:*

Table 3.11: *P*-values for Wilcoxon pairwise comparisons of maximum thickness and maximum geometry change locations in *H. sapiens* across metatarsals

Wilcoxen *p* values					
H. sapiens	**MT1**	**MT2**	**MT3**	**MT4**	**MT5**
Plantar/curvature	0.883	0.014**	0.184	0.002**	0.001**
Dorsal/curvature	0.125	0.002**	0.001**	0.001**	0.004*
Medial/curvature	0.005**	0.001**	0.005**	0.002**	0.001**
Lateral/curvature	0.001**	0.001**	0.001**	0.001**	0.001**

*Denotes values less than 0.05, **Denotes values less than 0.001

In metatarsal 1, positions of maximum thickness and geometry change were not statistically different at plantar (p=0.883) and dorsal cortices (p=0.125). In metatarsal 3, positions were not statistically different at the plantar cortex (p=0.184; Table 3.11).

3.4.3. Pan troglodytes schweinfurthii

Descriptive analysis:

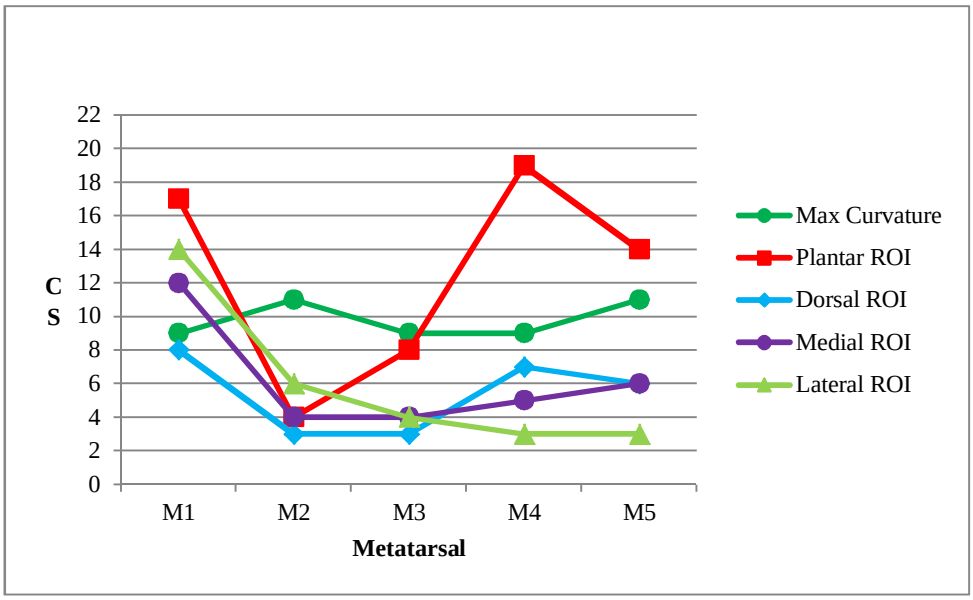


Figure 3.12: Cross sections (CS) containing ROI locations (median values) of maximum change in geometry compared to all anatomical cortices compared to all cortices in metatarsals (M1-5) of *P. t. schweinfurthii*.

Plantar thickness versus maximum geometry change: Position of maximum thickness corresponds with position of maximum geometry change in metatarsal 3 (near the midshaft) to within one cross section (CS 8, 9, respectively). There is no correspondence between positions of maximum thickness and maximum geometry change in metatarsals 1, 2, 4 or 5 (Figure 3.12).

Dorsal thickness versus maximum geometry change: Position of maximum thickness corresponds with position of maximum geometry change in metatarsal 1 to within one cross section (CS 8, 9, respectively). In metatarsal 4, position of maximum dorsal thickness corresponds to position of maximum geometry change

within 2 cross sections (CS 7, 9, respectively). There is no correspondence between positions of maximum dorsal thickness and maximum geometry change in metatarsals 2, 3 or 5 (Figure 3.12).

Medial thickness versus maximum geometry change: There is no correspondence between positions of maximum thickness and maximum geometry change across the metatarsus (Figure 3.12).

Lateral thickness versus maximum geometry change: Position of maximum thickness does not correspond to the position of maximum geometry change across the metatarsus (Figure 3.12).

Statistical analysis:

Table 3.12: Pairwise comparisons of maximum thickness and maximum geometry change in *P. t. schweinfurthii* across metatarsals.

Wilcoxon *p* values					
P. t. schweinfurthii	**MT1**	**MT2**	**MT3**	**MT4**	**MT5**
Plantar/curvature	0.003**	0.011*	0.745	0.001**	0.454
Dorsal/curvature	0.667	0.001**	0.001**	0.558	0.002*
Medial/curvature	0.060	0.001**	0.022*	0.001**	0.001**
Lateral/curvature	0.001*	0.016*	0.011*	0.001**	0.001**

*Denotes values less than 0.05, **Denotes values less than 0.001

In metatarsal 1, positions were not statistically different in the dorsal (p=0.667) and medial cortices (p=0.060). In metatarsals 2, 3 and 5, positions were not statistically different in the plantar cortex (p=0.066, p=0.745; p=0.454, respectively). In metatarsal 4, positions were not statistically different in the dorsal cortex (p=0.394; Table 3.12).

3.5. Summary of results

The analyses presented here documented patterns in the locations of maximum cortical thickness of the metatarsals using four regions of interest (plantar, dorsal, medial, and lateral cortices). The pattern of maximum geometry change on the plantar surface also was documented. Finally, correspondence between the locations of maximum cortical thickness and maximum geometry change on the plantar surface (i.e., a theoretical point of high stress concentration) was tested.

3.5.1 Main intraspecific results:

a) In *P. paniscus,* positions of maximum thickness were significantly different across the metatarsal complex in metatarsals 2-4, predominantly at plantar cortices (Table 3.1). Positions of maximum thickness in plantar and medial cortices corresponded with maximum geometry change (Table 3.10).
b) In *H. sapiens,* positions of maximum thickness were significantly different across the metatarsal complex in plantar, lateral and medial cortices (Table 3.2). Positions of maximum thickness in plantar and dorsal cortices corresponded with maximum geometry change in metatarsals 1 and 3 (Table 3.11).
c) In *P. t. schweinfurthii,* positions of maximum thickness were significantly different in all cortices across the metatarsus (Table 3.3). Positions of maximum thickness in plantar and dorsal cortices

corresponded with maximum geometry change across the metatarsus (Table 3.12).

3.5.2 Main interspecific results:

a) Relatively speaking, plantar thickness is distally positioned in all species compared to other cortices. A lack of relationship between position of plantar thickness and position in other cortices may be related to the plantar surface responding differentially to stress concentration (Figure 3.8).
b) Comparing bonobos and common chimpanzees, metatarsals 3-5 exhibit similar differences in maximum thicknesses (Table 3.1, 3.3). In the bonobo metatarsal 2, however, differences in thicknesses are significant, but this is not observed in common chimpanzees. Positions of thicknesses are significantly different in the dorsal aspect of metatarsals 1-3 (Table 3.5) and in the plantar aspect in metatarsals 4-5 (Table 3.4) in all species, not just between bonobos and common chimpanzees. Positions of medial and lateral thickness are not significantly different (Table 3.5, 3.6) in all species, not just between bonobos and common chimpanzees.
c) Positions of maximum geometry change are not significantly different between all species at metatarsals 2, 3 and 5 (Table 3.8) and mirror a similar pattern in all species across the metatarsus. Bonobos and common chimpanzees share a similar distribution in maximum geometry change across the midshaft region, particularly in metatarsals 1, 3 and 5 (Figure 3.9).

d) Relationships between positions of maximum thickness and maximum geometry vary throughout the metatarsals and between species, but correspond most often (13 out of 30 times) at plantar and dorsal cortices. Specifically, positions of maximum plantar thickness correspond with the position of maximum change in geometry more often in *H. sapiens*, observed in 4 out of 5 occasions (metatarsals 1, 2, 3 and 5) and in *P. paniscus*, compared to *P. t. schweinfurthii*, which has correspondence in 3 out of 5 (metatarsals 2, 3 and 5) instances.

4. CHAPTER 4 – Discussion, Conclusions and Evaluations

4.1. Discussion

The study assessed two structural properties of all metatarsals (1-5) of bonobos, common chimpanzees, and humans in order to quantify relative positions of maximum thickness and maximum geometry change on the plantar surface. An important caveat must first be made that while functional analyses have frequently suggested that bone curvature may be a response to loading regimes experienced during life, such a link has not yet been conclusively established. Indeed, the actual loading regimes experienced by metatarsals *in vivo* are likely to be highly complex, varying along the length of the metatarsal and throughout one individual life time. It is beyond the scope of this dissertation to address the extent to which this widely used interpretive paradigm is warranted, if for no other reason than it would not be reliable to do so on the basis of the two variables measured. Rather, this dissertation seeks to assess whether the interspecific similarities and differences that have been demonstrated in this study regarding the distribution of maximum cortical thickness and maximum geometry change are broadly compatible with this interpretive paradigm.

4.1.1. Intraspecific comparisons of the positions of maximum thicknesses

P. paniscus and P. t. schweinfurthii: Patterns in the location of maximum thicknesses highlight a different response of the plantar cortex compared to all other cortices in bonobos and common chimpanzees versus humans. Plantar thickness systematically occupies a more distal position across metatarsals 2-5 in

bonobos (figure 3.8) and metatarsals 4-5 in common chimpanzees. This may suggest that a (localized) stress concentration in the plantar cortex may be present more distally in the plantar aspect of the metatarsus than in other cortices in *Pan*. It could be suggested that given this correspondence, and within the limitations of the irregular geometry of metatarsal cross sections, stress concentration may affect the plantar cortex of the metatarsus more overall, than the other cortices. This result could be associated with grasping during suspensory behaviour in that the substrate reaction force may be higher causing a boney adaptive response during this behaviour than in other types of locomotion (to thoroughly test this hypothesis however, statistical assessment via the geometric mean would be required). However, variance in absolute thickness differences between cortices, showing plantar thickness to be the thickest overall, would need to be analysed through the use of an overall geometric mean as a scaling factor (not done here). However, as the maximum change in geometry in dorsal, medial and lateral cortices were not measured here, assessment of non-plantar surface local relationships (correspondence) are not possible, and the correlation in such locations remains theoretical despite the observation of relationships between thicknesses.

Positions of maximum thickness are variably distributed along the diaphysis between the four cortices, which theoretically could be a response to the wide variety of bending regimes to which *Pan* metatarsal bones are exposed during locomotion (Demes et al. 1998, 2001). Similarities in maximum thickness locations across cortices occur most frequently on the plantar and medial aspects of metatarsals 1 and 2, and on the medial aspect of metatarsals 3-5 in both species

of *Pan*. *Pan* metatarsals may experience variably applied loads in transverse and sagittal planes, which could invoke an adaptation to resisting bending in oblique axes (according to the arguments of Demes *et al*. 1998, 2001 and Demes and Carlson 2009), implying that a functionally efficient correspondence may occur at a 45° angle, i.e.; the plantarmedial cortex. Additionally, similar positions of maximum thickness in the medial and lateral aspects may be in response to transverse bending, or alternatively, in response to the transfer of the centre of pressure from lateral to medial, particularly in metatarsals 4 and 5 (Wunderlich 1999; Vereecke *et al*. 2003). Furthermore, it may be that bone is adapting to the greatest bending rigidity in the plantarmedial – to – dorsolateral direction, however actual assessment of this was beyond the scope of this study. This study was designed to assess the absolute distribution of bone by cross section, by comparing the four anatomical cortices. This provided results of a finer resolution than if bending rigidity had been assessed, as each measure is a true reflection of cross-sectional geometry measures.

Homo sapiens: Regarding differences in positions of maximum thickness, the main differences appear between metatarsal 1 and metatarsal 5. In the human foot, metatarsals on the medial and lateral margins show an opposing correspondence represented by non-significant *p* values (Table 3.2). This distinction is not apparent in the two *Pan* species, which might signal a major functional distinction in loading regimes, however, further extensive biomechanical modelling validated by strain studies would be needed to confirm this possibility.

Across all metatarsals, similarities in positions of maximum thickness along the diaphyses occur predominantly in the plantar and dorsal cortices, which are consistent with *in-vivo* (cadaver) studies that have measured high compressive strains on the dorsal surface, particularly in metatarsals 2 and 5 during normal walking (Donahue and Sharkey 1999). Positions of maximum cortical thickness on the plantar aspect were not found to be significantly differently located along the diaphysis from those on the dorsal aspect using the statistical methods employed here. Hence, these results with specific reference to the plantar surface could provide support for a hypothesis where cortical bone might be thicker on the plantar aspect to provide greater resistance to compression associated with pre-loading of the plantar aponeurosis across the metatarsal complex (Caravaggi *et al*. 2009). Regarding the irregular shape of cross sections, these results support predictions that elongated or expanded cross sections in the direction of the principal axis are associated with loading in that axis (Lovejoy *et al*. 1976; Jungers and Minn 1979; Burr *et al*. 1982). This pattern is consistent with the literature of a general dorsoplantar loading regime of human metatarsals (e.g., Griffin and Richmond 2005) and may be representative of bending rigidity through a cross section. Assessment of this feature may confirm the signal seen using thickness measurements in specific cortical locations.

Positions of maximum thickness of the medial and lateral cortices coincide in positions, as do plantar and dorsal cortices, although the former coincide in position less frequently than the latter (Table 3.2) perhaps in response to the mediolateral bending component through certain parts of stance phase (Griffin

and Richmond 2005). This is consistent with *in-vivo* (cadaver) studies that suggest lower, more variable strains occur on the medial and lateral cortices during normal human walking (Donahue and Sharkey 1999). More variable or lower magnitude transverse strains would not theoretically induce a strong adaptive response for an increase in cortical bone, particularly at a localised position on the diaphysis (Carlson *et al*. 2005).

4.1.2 Interspecific comparisons of the position of maximum thicknesses:

In metatarsal 1, positions of maximum thicknesses are widely distributed in different positions in all cortices along the diaphysis of sample groups. In humans, the first metatarsal head is more in contact with the ground than in *Pan*, as the toe-off mechanism is employed more consistently during bipedal locomotion. The Genus level difference in positions of maximum thickness in metatarsal 1 may indicate a different transfer of the path of the centre of pressure between groups (sections 1.2.4, 1.2.5). In metatarsal 1, maximum thickness in all cortices occurs at the distal aspect in *H. sapiens* (from CS 11-17), suggesting support for the hypothesis that thicker cortical bone might be distributed distally in order to bear high propulsive forces during the latter half of stance phase at toe-off. It is possible, given that the present sample is from shod human individuals, that this may reflect the constrained forces/loads experienced by a redistribution of forces due to footwear.

In *P. paniscus*, *H. sapiens* and *P. t. schweinfurthii*, maximum positions of dorsal, medial and lateral thicknesses are distributed proximally to the midshaft in metatarsals 2-4 (figure 3.8). While in metatarsal 5 the same three cortices have

thickest points in the proximal half of the diaphysis (figure 3.8), positions of maximum dorsal and medial thickness are more distally-positioned in *P. paniscus* relative to *P. t. schweinfurthii* (CS - 9, 10; CS - 6, 8 respectively). To the extent that maximum thickness locations indicate bending loads, this finding suggests that bending loads may be more proximally concentrated in the common chimpanzee than bonobo at these two aspects, suggesting that bending strength is being resisted at different aspects of the shaft across species. Perhaps the difference in bending loads is partly a response to different dorsomedial muscle arrangements and their effects on loads experienced locally in the metatarsal diaphyses. However, documenting the location of muscle attachment sites and torsion, and their localized loading patterns related to these sites is beyond the scope of the present analysis. Further study is necessary to address this possibility and assessment of torsion is currently underway as part of another study.

Available foot pressure data from bonobos suggest that, all other things being equal, initial contact between the foot and the ground is made concurrently by the heel and lateral mid-foot during terrestrial quadrupedalism (Vereecke *et al*. 2003; D'Août *et al*. 2004). In *Pan*, the results are broadly consistent with foot pressure results suggesting that bone may be thickest proximally, where it might increase structural support for resisting joint reaction forces applied from the transverse tarsal joint region at initial contact. In *Homo*, this pattern could suggest that despite the transfer of the centre of pressure from lateral to medial, structural support is required at the proximal region where high bending stress or ground reaction forces are experienced between heel strike and mid-stance.

Further analysis could include an assessment of whether there is a trend in declining or increasing thickness from the midshaft of the diaphysis to the proximal or distal end, however, this is currently beyond the scope of this thesis. Comparing the positions of maximum thickness in metatarsals, particularly the differences in positions of maximum plantar thickness in the two species of *Pan* relative *H. sapiens*, to fossil hominin metatarsals, could provide such comparisons in determining taxonomic assignments of fossil specimens. These comparisons also could be the basis for building inferences into foot functional morphology in various hominin groups.

4.1.3. Interspecific comparisons of the relationships between positions of maximum geometry change

Curvature in long bones has been theorised to distribute the highest loads at the midshaft of the diaphysis (Preuschoft 1969, 1970), and/or, to improve loading predictability to reduce the risk of bone failure (Bertram and Biewener 1988). Maximum geometry change on the plantar surface in all three species shares a similar position across the metatarsus (Figure 3.9). Internal stress might thus be concentrated at the position of maximum change in geometry on the plantar surface in the midshaft region, as, all things being equal, metatarsal morphology may act to distribute the highest loads to the midshaft of the diaphysis (Preuschoft 1969, 1970) and loads throughout the diaphysis differentially.

The position of maximum geometry change in *H. sapiens* occupies a *slightly* more distal position relative to *Pan*. The minor positional differences are separated by no more than three cross sections at any metatarsal (i.e., 7.5% of

diaphyseal length). With the exception of metatarsal 2, there is no point at which *Homo* are closer in position to *Pan*, than the two species are to one another. These results could be interpreted in a number of ways. Firstly, the slight difference in position may represent the difference in the track of the path of centre of pressure in *H. sapiens* and *Pan*, suggesting that in this case, morphology could be adapted to foot function.

Secondly, the similarity in positions may indicate simply that the path of transfer of the centre of pressure may not drive morphological adaptation, or at least has not yet driven adaptive morphological changes since the evolutionary divergence of *Pan* and *Homo*. If on the other hand it was assumed that bone morphology has come to reflect the characteristics of the mean species path of the centre of pressure, then positional similarity would imply that there is not enough difference in the mean path of transfer of the centre of pressure between species to select for morphological distinction. The latter would be consistent with the proposition based on pressure records, namely that overlap exists in foot pressure studies of bonobo, chimpanzee and modern humans (D'Août *et al.* 2009; Crompton *et al*. 2010). A third possibility could be the relative difference in the superimposition of digital flexor compressive forces and bending moments relative to different substrate reaction forces, suggesting there could be a greater or lesser contribution of substrate reaction between species. This would be almost impossible to quantify however and is well beyond the scope of this study.

4.1.4. Interspecific comparisons of the relationships between the positions of maximum thickness and maximum geometry change

In comparing positions of maximum thicknesses of the plantar, dorsal, medial, and lateral cortices to geometry changes on the plantar surface, correspondence amongst locations were not widespread. It could be suggested that bone loading in the metatarsal diaphysis may be extremely localized within all taxa, perhaps represented by the similarity in position of geometry change presented here. In order to better understand this relationship, comparison of local positions of maximum thicknesses and geometry changes specific to cortex (i.e., dorsal maximum thickness with dorsal maximum geometry change, medial max thickness with medial max geometry change, and lateral maximum thickness with lateral maximum geometry change) would be helpful. Additionally, understanding the absolute differences in thickness measurements between cortices (i.e., whether plantar thickness is comparatively more or less thick in Homo than in Pan), would be helpful in understanding where relative positions of thickness differ across taxa.

The paradigm of a relationship between morphology and stress/strain can only be extended so far since bone has other functions apart from resisting internal and external forces resulting from everyday activity including locomotion. Further, bone is not homogenous because material properties vary across and within bones and can act both to compensate, and to exaggerate geometric properties/trends (Currey 2002). Again, bone is not continuously re-modelled only for the purpose of reducing strain, which in turn reduces stress (Goodship and Cunningham 2001; Ruff *et al*. 2006). Metatarsal morphology

represents a compromise between avoidance of the risk of bone failure and the cost of producing new bone. Thus, all things being equal, the theoretical relationship between cortical thickness and geometry change is likely to represent a compromise within, and between metatarsals, as part of the wider functionality (digital flexor/extensor forces and bending stresses) of the foot complex.

Bertram and Biewener (1988) suggested that curvature in terrestrial mammalian long bones might be expected to improve loading consistency, effectively making the loading regime more predictable. If their proposal is correct, we might note that in *Pan* there should appear to be a strong relationship between position of maximum cortical thickness and position of maximum geometry change on the plantar surface, which by extension might suggest that the distribution of bone in this area may contribute to loading predictability. In this case, positions of maximum thickness sometimes correspond to positions of maximum change in geometry in *P. paniscus*: in metatarsal 1 at the plantar, medial and lateral aspects, at the plantar aspect in metatarsal 2, at the plantar and medial aspects of metatarsal 3, at the dorsal and lateral aspects of metatarsal 4, and in metatarsal 5 at the dorsal and medial aspects. In *P. t. schweinfurthii*, positions of maximum thickness and maximum change in geometry on the plantar aspect correspond less frequently: at the dorsal and medial aspect in metatarsal 1, at the plantar aspect of metatarsal 3 and 5, and at the dorsal aspect of metatarsal 4. Corresponding positions are thus variable across the metatarsal complexes similarly, which could be a reflection of the variable loads experienced during daily locomotor activity, and hence the exposure to high

bending loads in the oblique axis, and in response to an increase in the predictability of a variable loading regime (Bertram and Biewener 1988).

The broad occurrence of this relationship across the metatarsus in *Pan* is not observed in *H. sapiens.* As a habitually terrestrial mammal that might be expected to experience a more consistent anteroposterior loading regime in response to a more two-dimensionally arranged support, it is more intuitive that this relationship would exist in less cortices relative to *Pan*, which probably experience more variable loading and changes in direction due to variability in supports. In *H. sapiens*, position of maximum plantar and dorsal thicknesses and maximum geometry change correspond in metatarsal 1, the metatarsal involved predominantly in propulsion. Correspondence is also observed between maximum thickness of the plantar cortex and maximum geometry change of the plantar surface in metatarsal 3. Correspondence in metatarsal 1 suggests that locations of maximum geometry change and thickness may reflect locations of consistently encountered/experienced high forces during toe-off. Furthermore, this pattern is consistent in accordance with the plantar-to-dorsal loading regime suggested by others (Bertram and Biewener 1988; Griffin and Richmond 2005).

The case in metatarsal 3 supports the hypothesis that the highest yielding (Von Mises) stress is born under the metatarsal head of metatarsal 3 during normal standing (Cheung *et al*. 2005). This could suggest that corresponding positions of maximum plantarmedial thickness and point of maximum change in geometry, may act to add structural support at the point of highest von Mises stress. This interpretation is predicted from an FEA model that applied plantar tissue stiffening during standing and recorded the highest yielding stress under

the head of the third metatarsal. This relationship is also likely to be in response to pre-loading of the plantar aponeurosis throughout stance phase (Caravaggi *et al*. 2009) where combined corresponding positions of plantar cortical bone thickness and change in geometry may provide structural strength in response to high compressive forces applied before, and throughout stance phase by the plantar aponeurosis, and also substrate reaction forces generating bending. Furthermore, metatarsal 3 could theoretically act as a stable, neutral 'axis' in the foot, as metatarsals 1 and 2 are stabilised medially and metatarsals 4 and 5 are stabilised laterally, consequently, metatarsal 3 is theoretically less 'mobile' than the metatarsals on either side. If recruited into this role of serving as a neutral axis, then metatarsal 3 may require further structural support signified by a relationship between maximum position of plantar thickness and maximum position of change in geometry on the plantar surface. Finally, this pattern or correspondence between positions of maximum plantar thickness and maximum change in geometry on the plantar surface in metatarsals 1 and 3 is reasonable considering that ankle joint reaction force is transferred primarily from the hindfoot to the forefoot through the talonavicular and cuneonavicular joint during mid-stance, consequently applying a higher load and stress/strain magnitude to metatarsals 1-3 in humans (Cheung *et al*. 2005; Caravaggi *et al*. 2009; Qian *et al*. 2010).

In humans, significant differences between positions of maximum thickness and position of maximum geometry change on the plantar surface were measured in metatarsals 2 and 5. Explanation for this relationship could be drawn from Richmond's (2007) siamang phalanx model. Richmond's model proposes

that total compressive forces created by joint reaction forces tend to balance the tensile force on the plantar surface during concave open bending, but is slightly additive with the compressive force that is applied to the dorsal surface. However, because the plantar surface is concave and the dorsal surface convex, this combination of forces essentially straightens the curved bone making the joint reaction/bending loads even more balanced. Under an equivalent metatarsal paradigm, the lack of significant difference between locations of maximum plantar thickness and maximum geometry change that occur here in metatarsals 2 and 5, despite high levels of strain during normal walking, could be attributable to the superimposition of two axial compressive forces that could be responsible for counteracting tensile plantar strain and apply compressive dorsal strain, effectively minimising bending stress.

4.2. Conclusions

This study assessed relative positions of maximum cortical thickness across four cortices and its relationship to the position of maximum change in geometry on the plantar surface. The relationships presented here distinguish the human position (plantar-dorsal) from positions in bonobos and chimpanzees (mostly medial) and may prove useful as a quantitative feature for the assessment of fossil metatarsals in determining the distinction between hominins and *Pan*.

Based on this study, positions of maximum plantar thickness are more distally distributed in the two species of *Pan* relative to humans suggesting the possibility of a more distally applied bending regime during more variably employed locomotor behaviours such as vertical climbing, grasping and leaping.

The locomotor (functional) difference may be phenotypically manifested by a positional difference that represents an adaptive response in the forefoot to grasping and climbing in *Pan* that differs from the adaptive response exhibited in the forefoot of humans.

Positions of maximum thickness in the dorsal, medial and lateral aspects of the metatarsus between species are similar, and usually located proximal to the midshaft of the diaphysis. The position of maximum geometry change on the plantar surface is consistently similar between all three taxa in this study, being positioned in the midshaft region of the diaphysis in accordance with the ability of curvature to predictably constrain high loads at the midshaft of the diaphysis (Preuschoft 1969, 1970; Bertram and Biewener 1988). In humans, the position of maximum change in geometry is slightly more distally located than in *Pan*, which is separated by no more than three cross sections (i.e., about 7.5% length) at any metatarsal.

The observed discrepancies here may simply be an adaptive response of bones to the marked difference in curvature between humans and *Pan*. As hypothesised by Winkler over 150 years ago (see Timoshenko 1960), any curved, mortised beam will displace the locus of the centroid for the neutral axis potentially explaining the difference in the positions of maximum change in geometry. Correspondence between positions of maximum cortices thickness and maximum change in geometry on the plantar surface correspond differently between all three taxa. The two sub species of *Pan* exhibit correspondence at different cortices, sometimes corresponding at three of the four cortices across the metatarsus, theoretically suggesting that this variability may be representative

of loading and bending variability experienced during the variety of practiced locomotor behaviour. Correspondence in positions of maximum thickness and maximum geometry change on the plantar surface in humans is rather limited, occurring in metatarsal 1 in line with the plantar-dorsal primary loading regime (Bertram and Biewener 1988), and in line with the first metatarsal being recruited most consistently to apply propulsive force in the latter half of stance phase during toe-off (Ker *et al*. 1987). This same correspondence is also observed in metatarsal 3, which is in accordance with the highest applied von Mises stress during normal standing (Cheng *et al*. 2005). These results, however, are limited in their scope because only two characteristics of the cross sections have been examined.

On the basis of what appears to be the most advanced quasi-static modelling to date in humans (Qian *et al*. 2010), highest absolute stress concentrations have been found to be on the lateral side of metatarsal 1 and the medial aspect of metatarsal 3, not in line with the positions of maximum bone thickness (plantar and dorsal), or positions of maximum change in geometry on the plantar surface presented here. Position of highest stress/strain concentration within the metatarsals *in vivo* are the net result of a complex interaction of forces and loading conditions applied by the many soft tissues in the foot complex that would not be resolvable in a simplified two dimensional FEA mesh analysis. 3D dynamic, or at least quasistatic FEA validated by in vivo strain studies, is a good option in modelling the complex dynamic situation occurring in the foot during static and dynamic movement. Unlike direct estimation of loading (e.g., strain studies), FEA is non-invasive and accounts for the high number of ligaments and

muscles acting on bones during locomotor behaviour, although requires real world validation through EMG, MRI or stress/studies (Nester 2009, Qian *et al.* 2010). This approach is well beyond the scope of this project and should be the next stop in extracting more comprehensive results and a more comprehensive understanding of the relationship between cortical bone adaptation and morphology. Equivalent cross-sectional geometric analyses, at the very minimum, and FEA of the metatarsals in their full *in-vivo* context, would be useful and more fully able to assess the results in the context of metatarsal curvature.

4.3. Evaluation

This study had some limitations that can be addressed in future work;

-Only locations of maximum properties are discussed rather than exploring the distribution of absolute magnitudes of thicknesses along the length of the diaphysis. It would be interesting to establish the relationship between absolute maximum thickness at each cross section (e.g., occurrence at medial, plantar, lateral, or dorsal cortex) and track its movement along the diaphysis in order to establish by what magnitudes changes in thickness occur from one cross section to the next along the diaphysis, and whether overall thickness changes from one cortex to another along the diaphysis. Visualizing this using thickness maps, for example, could be very informative.

-It would be interesting to establish absolute difference between cross sections in terms of much broader biomechanical parameters (e.g., joint reaction forces, substrate reaction forces and the effects of soft tissue stiffening on the

plantar pressure distribution and plantar pressure contact area) in order to establish the relative importance of the positions of thickness and maximum stress concentration.

- It would be interesting to make comparisons between geometric properties (e.g., cortical area, second moments of area, polar moment of area and section moduli, associated with stress/strain patterns that are predicted by finite element models assessing the effects of soft tissue stiffening on stress distribution in the plantar surface of the metatarsals during different gaits (Cheng *et al*. 2005).

- It would be interesting to re-scale all of the absolute measures to the geometric mean of the four thickness measurements in each cross section in order to assess the absolute values of thicknesses, rather than the position of the cross section that represents the thickest bone. This would be useful in terms of tracking changes in thickness relative to changes in bone geometry along the diaphysis, as well as provide a more specific inter-species comparison.

REFERENCES:

Alexander, R. M. and Maloiy, G. M. 1984. Stride lengths and stride frequencies of primates. *Journal of Zoology, London.* 202, 577-582.

Arndt, A., Ekenman, I., Westblad, P. and Lundberg, A. 2002. Effects of fatigue and load variation on metatarsal deformation measured in vivo during barefoot walking. *Journal of Biomechanics*, 35:621-8.

Bertram, J.E.A. and Biewener, A.A. 1988. Bone curvature: sacrificing strength for load predictability? *Journal of Theoretical Biology*, 131:75-92.

Biewener, A.A. 1983. Locomotory stresses in the limb bones of two small mammals: the ground squirrel and chipmunk. *Journal of Experimental Biology*, 103:131-154.

Biewener, A.A. 1990. Biomechanics of mammalian terrestrial locomotion. *Science*, 250:1097-1103.

Biewener, A.A. and Bertram, J.E.A. 1993. Skeletal strain patterns in relation to exercise training during growth. *Journal of Experimental Biology*, 185:51-69.

Biewener, A.A. and Taylor, C.R. 1986. Bone strain: a determinant of gait and speed? *Journal of Experimental Biology*, 123:383-400.

Biewener, A.A., Thomason, J. and Lanyon, L.E. 1983. Mechanics of locomotion and jumping in the forelimb of the horse (Equus): in vivo stress developed in the radius and metacarpus. *Journal of Zoology London*, 201:67-82.

Biewener, A.A., Thomason, J.J. and Lanyon, L.E. 1988. Mechanics of locomotion and jumping in the horse (Equus): in vivo stress in the tibia and metatarsus. *Journal of Zoology London*, 214:547-565.

Bennett, M. R., Harris, J.W.K., Richmond, B. R., Braun, D.R., Mbua, E., Kiura, P., Olago, D., Kibunjia, M., Omuombo, C., Behrensmeyer, K. A., Huddart, D. and Gonzalez, S. 2009. Early Hominin foot morphology based on 1.5-million-year-old footprints from Ileret, Kenya. *Science*, 323:1197-1201.

Bondioli, L., Bayle, P., Dean, C., Mazurier, A., Puymerail, L., Ruff, C., Stock, J-T., Volpato, V., Zanolli, C. and Macchiarelli, R. 2010. Technical note: morphometric maps of long bone shafts and dental roots for imaging topographic thickness variation. *American Journal of Physical Anthropology*, 142:328-344.

Burr, D. B., Robling, A. G. and Turner, C. H. 2002. Effects of biomechanical stress on bones in animals. *Bone*, 30:781-786.

Caravaggi, P., Pataky, T. C., Goulermas, J. Y., Savage, R. and Crompton, R. H. 2009. A dynamic model of the windlass mechanism of the foot: evidence for early stance phase preloading of the plantar aponeurosis. *Journal of Experimental Biology*, 212:2491-2499.

Carlson, K. J., Demes, B., and Franz, T. M. 2005. Mediolateral forces associated with quadrupedal gaits of lemurids. *Journal of the Zoological Society London*. 266: 261-273.

Carlson, K. J., Sumner, D.R., Morbeck, M.E., Nishida, T., Yamanaka, A. and Boesch, C. 2008. The role of non-behavioural factors in adjusting

long bone diaphyseal structure in free-ranging chimpanzees. *International Journal of Primatology*, 29:1401-1420.

Carrano, 2001. Implications of limb bone scaling, curvature and eccentricity in mammals and non-avian dinosaurs. *Journal of Zoology London*, 254:41-55

Carter, D.R. 1981. The relationship between in vivo strains and cortical bone remodeling. *Critical Review in Biomechanical Engineering*, 8: l-28.

Carter, D.R. and Beaupré, G.S. 2001. *Skeletal function and form.* Cambridge University Press, Cambridge, UK.

Cartmill, C., Lemelin, P. and Schmitt, D. 2002. Toward a predictive theory of symmetrical gaits. *Zoological Journal of the Linnaen Society,* 136, 401-420.

Cavagna, G. A., Thys, H. and Zamboni, A. 1976. Sources of external work in level walking and running. *Journal of Physiology London.* 262, 639-657.

Cavagna, G. A., Heglund, N. C. and Taylor, C. R. 1977. Mechanical work in terrestrial locomotion: two basic mechanisms for minimizing energy expenditure. *American Journal of Physiology*, 233, R243-261.

Cheng, J, T-M., Zhang, M., Leung, A, K-L. and Fan, Y-B. 2005. Three-dimensional finite element analysis of the foot during standing-a material sensitivity study. *Journal of Biomechanics*, 38: 1045-1054.

Churches, A.E. and Howlett, C.R. 1981. The response of mature cortical bone to controlled time varying loading. In, Cowin, S.C. (Ed). *Mechanical*

properties of bone, Volume 45. Pp. 69-80. American Society of Mechanical Engineers.

Close, J.R., Inman, V.T., Poor, P.M. and Todd, F.N. 1967. The function of the subtalar joint. *Clinical Orthopedic Related Research,* 50:159–179.

Coffing, K.E. 1998. *The metatarsals of Australopithecus afarensis: locomotor and behavioural implications of cross-sectional geometry*. Ph.D. Dissertation, Johns Hopkins University, Baltimore.

Cooper, D.M., Ahamed, Y., Macdonald, H.M. and McKay, H.A. 2008. Characterising cortical density in the mid-tibia: intra-individual variation in adolescent girls and boys. *British Journal of Sports Medicine,* 42:690-5.

Corder, G.W. and Foreman, D.I. 2009. *Nonparametric Statistics for Non-Statisticians: A Step-by-Step Approach,* Pg 5-85. Wiley.

Cowin, S.C. 1983. The mechanical and stress adaptive properties of bone. *Annals of Biomedical Engineering,* 11:263-295.

Crompton, R.H., Vereecke, E.E. & Thorpe, S.K.S. 2008. Locomotion and posture from the common hominoid ancestor to fully modern hominins, with special reference to the last common panin/hominin ancestor. *Journal of Anatomy,* 212:501-543.

Crompton, R.H., Sellers, W. I. & Thorpe, S.K.S. 2010. Arborality, terrestriality and bipedalism. *Philosophical transactions of the Royal Society B,* 365:3301-3314.

Crompton, R.H., Pataky, T.C., Savage, R., D'Août, K., Bennett, M.R., Day, M.H., Bates, K., Morse, S. and Sellers, W. I. 2011. Human-like external

function of the foot and fully upright gait confirmed in the 3.66 million year old Laetoli hominin footprints by topographical statistics, experimental footprint-formation and computer simulation. *Journal of the Royal Society Interface,* doi:10.1098/rsif.2011.0258.

Cullen, D.M., Smith, R.T. and Akhter, M.P. 2001. Bone-loading response varies with strain magnitude and cycle number. *Journal of Applied Physiology,* 91:1971-1976.

Currey J. 1984. *The mechanical adaptations of bones.* Princeton University Press, Princeton, Il, USA.

Currey, J.D. *Bones: structure and mechanics.* 2002. Princeton University Press. Princeton Il, USA.

Currey, J.S. 2003.The many adaptations of bone. *Journal of Biomechanics,* 36, 10:1487-1495.

Daley, M.A., Usherwood, J.R., Felix, G. and Biewener, A.A. 2006. Running over rough terrain: guinea fowl maintain dynamic stability despite a large unexpected change in substrate height. Journal of Experimental Biology, 209: 171-187.

D'Août, K., Vereecke, E., Schoonaert, K., De Clercq, D., Van Elsacker, L., and Aerts, P. 2004. Locomotion in bonobos (Pan paniscus): differences and similarities between bipedal and quadrupedal terrestrial walking, and a comparison with other locomotor modes. *Journal of Anatomy,* 204, 5:353-361.

D'Août, K., Pataky, T. C., De Clercq, D. and Aerts, P. 2009. The effects of habitual footwear use: foot shape and function in native barefoot walkers. *Footwear Science*, 1:81-94.

DeSilva, J.M. 2009. Functional morphology of the ankle and the likelihood of climbing in early hominins. *Proceedings of the National Academy of Sciences, USA*, 106: 16, 6567-6572.

DeSilva, J.M. 2010. Revisiting the midtarsal break. *American Journal of Physical Anthropology,* 141:245-258.

Devlin, M. J. and Lieberman, D. E. 2007. Variation inestradiol level affects cortical bone growth in response tomechanical loading in sheep. *Journal of Experimental Biology*, 210:602-613.

Demes, B. 2007. In vivo bone strain and bone functional adaptation. *American Journal of Physical Anthropology,* 133:717-722.

Demes, B., Jungers, W. L. and Nieschalk, U. 1990. Size- and speed-related aspects of quadrupedal walking in slender and slow lorises. In *Gravity,Posture and Locomotion in Primates.* Eds. F. K. Jouffroy, M. H. Stack, and C. Niemitz, pp. 175-198. Florence: Il Sedicesimo.

Demes, B., Larson, S. G., Stern, J. T., Jr, Jungers, W. L., Biknevicius, A.R. and Schmitt, D. 1994. The kinetics of primate quadrupedalism: hindlimb drive reconsidered. *Journal of Human Evolution,* 26: 353-374

Demes, B. and Carlson, K.J. 2009. Locomotor variation and bending regimes in Capuchin limb bones. *American Journal of Physical Anthropology*, 139:558-571.

Demes, B., Stern, J.T. Jr., Hausman, M.R., Larson, S.G., McLeod, K.J. & Rubin, C.T. 1998. Patterns of strain in the macaque ulna during functional activity. *AmericanJournal of Physical Anthropology*, 106:87-100.

Demes, B., Qin, Y.X., Stern, J.T., Larson, S.G. and Rubin, C.T. 2001. Patterns of strain in the macaque tibia during functional activity. *American Journal of Physical Anthropology*, 116:257-265.

Donahue, S.W. and Sharkey, N.A. 1999. Strains in the Metatarsals During the Stance Phase of Gait: Implications for Stress Fractures. *Journal of Bone and Joint Surgery America*, 81:1236-44.

Doran, D.M., 1993. Comparative locomotor behavior of chimpanzees and bonobos: the influence of morphology on locomotion. *American Journal of Physical Anthropology,* 91: 83-98.

Doran, D.M., 1997. Ontogeny of locomotion in mountain gorillas and chimpanzees, *Journal of Human Evolution*, 32: 323-344.

Elftman, H. and Manter, J. 1935. Chimpanzee and human feet in bipedal walking. *American Journal of Physical Anthropology*, 20:69-79.

Ferris, L., Sharkey, N.A., Smith, T.S., Matthews, D.K. 1995. Influence of extrinsic plantar flexors on forefoot loading during heel rise. *Foot and Ankle International*, 16:464-473.

Forwood, M.R., Bennett, M.B., Blowers, A.R. and Nadorfi, R.L. 1998. Modification of the In vivo four-point loading model for studying mechanically induced bone adaptation. *Bone*, 23, 3:307-310.

Frost, H.M. 1964. *The Laws of Bone Structure*. Pp. 1-165. Charles C. Thomas, Springfield, IL, USA.

Frost, H.M. 1972. *The Physiology of Cartilaginous, Fibrous and Bony Tissues.* Pp. 1-249. Charles C. Thomas, Springfield, IL, USA.

Frost, H.M. 1973. *Bone Modeling and Skeletal Modeling Errors.* Pp. 1-214. Charles C. Thomas, Springfield, IL, USA.

Frost, H.M. 1979. A chondral modeling theory. *Calcified Tissue International*, 28:181-200.

Frost, H.M. 1986. *Intermediary Organization of the Skeleton.* Vol. I, Pp. 1-316; Vol 11, Pp. 1-334. C.R.C. Press, Boca Raton, FL, USA.

Frost, H.M. 1988. Structural adaptations to mechanical usage: A three-way rule for lamellar bone modeling. *Veterinary and Comparative Orthopedics Traumatology*, 1:7-17; 2:80-85.

Garman, R., Gaudette, G., Donahue, L.R., Rubin, C. and Judex, S. 2007. Low level accelerations applied in the absence of weight bearing canenhance trabecular bone formation. *Journal of Orthopedic Research*, 5, 6:32-40.

Gambhir, M.L. 2009. *Fundamentals of solid mechanics: a treatise on strength of materials*. Pp-825-847. PHI Learning, PVT. Ltd. Baba-Barkha Nath Printers, New Delhi.

Goodship, A.E. and Cunningham, J.L. 2001. Pathophysiology of functional adaptation of bone in remodeling and repair in vivo. In: Cowin, S.C. (Ed). *Bone mechanics handbook*, 2nd ed. Pp 26-31. Boca Raton: CRC Press.

Griffin, N.L. 2005. Recent evolution of the human foot. In Wood, B. A. & Klenerman, L. (Eds)., *The Human Foot: a companion to clinical studies*. Pp. 27-79. Springer.

Griffin, N.L. and Richmond, B.G. 2005. Cross-sectional geometry of the human forefoot. *Bone*, 37:253-260.

Griffin, N.L. and Richmond, B.G. 2010. Joint orientation and function in great ape and human proximal pedal phalanges. *American Journal of Physical Anthropology*, 144:116-123.

Gross, T.S. and Bunch, R.P. 1989. A mechanical model of metatarsal stress fracture during distance running. *American Journal of Sports Medicine*, 17, 5:669-673.

Gross, T.S., McLeod, K.J. and Rubin, C.T. 1992. Characterizing bone strain distributions in vivo using three triple rosette strain gages. *Journal of Biomechanics*, 25:1081–1087.

Hartard, M., Kleinmond, C., Wiseman, M., Weissenbacher, E.R., Felsenberg, D. and Erben, R.G. 2007. Detrimental effect of oral contraceptives on parameters of bone mass and geometry in a cohort of 248 young women. *Bone*, 40:444–50.

Heřt, J., Lišková, M. and Landa, J. 1971. Reaction of bone to mechanical stimuli. Part 1. Continuous and intermittent loading of tibia in rabbit. *Folia Morphologica*, 19:290-300.

Hildebrand, M. (1967). Symmetrical gaits of primates. *American Journal of Physical Anthropology*, 26: 119-130.

Holt, B.M., Ruff, C.B. and Trinkaus, E. 2004. The Wolff's law debate: throwing out the water, but keeping the baby. *American Journal of Physical Anthropology [Suppl]*, 38:115–116.

Hunt, K.D. 1991. Positional behavior in the Hominoidea. *International Journal of Primatology,* 12:95-118.

Hunt, K.D., Cant, J.G.H., Gebo, D.L., Rose, M.D., Walker, S.E. and Youlatos, D. Standardised descriptions of primate locomotor mode and postural modes. *Primates,* 37, 4:363-387.

Jee, W.S.S. 1988. The Skeletal Tissues. In: L. Weiss, (Ed). *Cell and Tissue Biology*, Pp. 21, 1-254. Urban and Schwarzenberg, Baltimore, USA.

Jouffroy, F.K. and Lessertisseur, J. 1960. Les specializations anatomiques de lamain chez les Singes a progression suspendue. *Mammalia,* 24:93-151.

Judex, S., Gross, T.S. and Zernicke, R.F. 1997. Strain gradients correlate withsites of exercise-induced bone-forming surfaces in the adultskeleton. *Journal of Bone and Mineral Research,* 12, 10:1737-1745.

Judex, S., Lei, X., Han, D. and Rubin, C. 2007. Low-magnitude mechanical signals that stimulate bone formation in the ovariectomized rat are dependent on the applied frequency but not on the strain magnitude. *Journal of Biomechanics,* 40:1333-1339.

Judex, S. and Carlson, K.J. 2009. Is bone's response to mechanical signals dominated by gravitational loading? *Medicine and Science in Sports and Exercise,* 9:2037-2043.

Jungers, W.L. & Minns, R.J. 1979. Computed tomography and biomechanical analysis of fossil long bones. *American Journal of Physical Anthropology*, 50:285-290.

Ker, R.F., Bennett, M.B., Bibby, S.R., Kester, R.C. & Alexander, R. McN. 1987. The spring in the arch of the human foot. *Nature*, 325:147-148.

Kimura, T., Okada, M. and Ishida, H. 1977. Dynamics of primate bipedalism as viewed from the force of the foot. *Primates*, 18:137–147.

Kimura, T., Okada, M. and Ishida, H. 1979. Kinesiological characteristics of primate walking: its significance in human walking. In *Environment, Behaviour, and Morphology: Dynamic Interactions in Primates.* Eds. M. Morbeck, H.Preuschoft and N. Gomberg, pp. 297-312. New York: Gustav Fischer.

Kimura, T. 1985. Bipedal and quadrupedal walking of primates: comparative dynamics. In: Kondo, S., Ishida, H., Kimura, T., Okada, M., Yamazaki, N. and Prost, J.H. (Eds*). Primate morphophysiology, locomotor analyses and human bipedalism*. Tokyo: University of Tokyo Press. p 81–104.

Kontulainen, S.A., Macdonald, H.M. and McKay, H.A. 2006. Change in cortical bone density and its distribution differs between boys and girls during puberty. *Journal of Clinical Endocrinological Metabolism*, 91:2555-2561.

Lanyon, L.E. and Bourne, S. 1979. The influence of mechanical function on the development and remodeling of the tibia. *Journal of Bone and Joint Surgery [America]*, 61:263-273.

Lanyon. L. E. 1980. The influence of function on the development of bone curvature: an experimental study on the rat tibia. *Journal of Zoology London,* 192:457-466.

Lanyon, L.E. 1982. Biomechanical properties of bone and response of bone to mechanical stimuli: functional strain as a controlling influence on bone modelling and remodelling behaviour. In: Hall, B.K., (Ed). *Bone*. Pp 79-108. Boca Raton: CRC Press. USA.

Lanyon, L.E. 1987. Functional strain in bone tissue as an objective and controlling stimulus for adaptive bone remodelling. *Journal of Biomechanics,* 20, 11-12:1083-1093.

Lanyon, L.E. and Baggott, D.G.1976. Mechanical function as an influence on the structure and form of bone. *Journal of Bone and Joint Surgery*, 58B:436-443.

Lanyon, L.E. and Rubin, C.T. 1984. Static vs. dynamic loads as an influence on bone remodelling. *Journal of Biomechanics*, 17:897-905.

Larney, E. and Larson, S. G. 2003. Limb compliance during walking: comparisons of elbow and knee yield across quadrupedal primates and in other mammals. *American Journal of Physical Anthropology(Supplement)* 1: 135.

Latimer, B.M., 1991. Locomotor adaptations in Australopithecus afarensis: the issue of arboreality. In: Coppens, Y., Senut, B. (Eds). *Origines de la Bipédie chez les Hominidés.* Pp. 169-176. CNRS, Paris. France.

Lee, C. R. and Farley, C. T. 1998. Determinants of the center of mass trajectory in human walking and running. *Journal of Experimental Biology,* 201: 2935-2944.

Les, C.M., Stover, S.M., Keyak, J.H., Taylor, K.T. and Willits, N.H. 1997. The distribution of material properties in the equine third metacarpal bone serves to enhance sagittal bending. *Journal of Biomechanics*, 30:355-61.

Lewis, O. J. 1980. The joints of the evolving foot part II, the intrinsic joints. *Journal of Anatomy*, 131:275-298.

Lieberman, D., Polk, J. and Demes, B. 2004. Predicting long bone loading from cross-sectional geometry. *American Journal of Physical Anthropology,* 123:156-71.

Lovejoy, C. O., Latimer, B., Suwa, G., Asfaw, B. and White,T. D. 2009. Combining prehension and propulsion: the foot of Ardipithecus ramidus. *Science*, 326:721-728.

Lundgren, P., Nester, C., Liu, A., Arndt, A., Jones, R., Stacoff, A., Wolf, P. and Lundberg, A. 2008. Invasive in-vivo measurement of rear-, mid- and forefoot motion during walking. *Gait Posture*, 28, 1: 93-100.

MacLatchy, L.M., Gebo, D., Kityo, R. and Pilbeam, D.2000. Postcranial functional morphology of *Morotopithecusbishopi*, with implications for the evolution of modern ape locomotion. *Journal of Human Evolution*, 39:159-183.

Madar, S.I., Rose, M.D., Kelley, J., MacLatchy, L. and Pilbeam, D. 2002. New *Sivapithecus*postcranial specimens from the Siwaliks of Pakistan. *Journal of Human Evolution*, 42:705-752.

Marchi, D. 2005. The cross-sectional geometry of the hand and foot bones of the Hominoidea and its relationship to locomotor behaviour. *Journal of Human Evolution*, 49:743-761.

Marchi, D. 2008. Relationships between lower limb cross-sectional geometry and mobility: the case of a Neolithic sample from Italy. *American Journal of Physical Anthropology*, 137:188–200.

Marchi, D. 2010. Articular to diaphyseal proportions of human and great ape metatarsals. *American Journal of Physical Anthropology*, 143:198-207.

Martin, R.B. and Burr, D.B. 1989. *Structure, function, and adaptation of compact bone*. Raven Press. NY. USA

Martin, R. B., Burr, D. B. and Sharkey, N. A. 1998. *Skeletal Tissue Mechanics*. Springer-Verlag, NY. USA

Martens, A.M. 1985. *Mechanical properties of human bone*. Ph.D. thesis, University of Louvain, Leuven.

Marzke, M.W. 1971. Origin of the human hand. *American Journal of Physical Anthropology*, 34:61-84.

McLean, S.P. and Marzke, M. 1994. Functional significance of the fibula: Contrasts between humans and chimpanzees. *Folia Primatologica*. 63:107-114.

Morimoto, N., Ponce de León, M. and Zollikofer, P.E. 2011. Exploring femoral diaphyseal shape variation in wild and captive chimpanzees by means of morphometric mapping: A test of Wolff's law. *The Anatomical Record,* 294:589-609.

Mott, R.L. 1996. *Applied strength of materials. 3rd edition.* Prentice Hall Inc. Upper Saddle River, NJ. USA

Muybridge, E. 1887. *Animals in Motion.* London: Chapman and Hall.

Nester, C.J., Liu, A.M., Ward, E., Howard, D., Cocheba, J., Derrick, T. and Patterson, P. 2007. In vitro study of foot kinematics using a dynamic walking cadaver model. *Journal of Biomechanics,* 40: 9, 1927-37.

Nester , C.J. 2009. Lessons from dynamic cadaver and invasive bone pin studies: do we know how the foot really moves during gait? *Journal of Foot and Ankle Research,* 2: 18-25.

Nordstrom, P., Pettersson, U. and Lorentzon, R. 1998. Type of physicalactivity, muscle strength, and pubertal stage as determinants ofbone mineral density and bone area in adolescent boys. *Journal of Bone and Mineral Research,* 13, 7:1141-1148.

O'Connor, J.A., Lanyon, L.E. and MacFie, H. 1982. The influence of strain rate on adaptive bone remodelling. *Journal of Biomechanics,* 15:767-781.

Oxnard, C.E., 1963. Locomotor adaptations in the primate forelimb. *Symposium for the Zoological Society London, No. 10 (the Primates),* 165-182.

Pauwels, F., 1965. *Gesammelte Abhandlungen zur funktionellen Anatomie des Bewegungsapparates*. Springer, Berlin Heidelberg, NY, USA.

Pauwels, F. 1980. *Biomechanics of the locomotor apparatus: contributions on the functional anatomy of the locomotor apparatus.* Springer-Verlag. Berlin.

Pearson, O.J. and Lieberman, D.E. 2004. The aging of Wolff ’s ‘‘law": ontogeny and responses to mechanical loading in cortical bone. *Yearbook of Physical Anthropology*, 47:63-99.

Pilkey, W. D, 1997. *Peterson's Stress Concentration Factors*, 2nd Edition. Wiley-Interscience, NY, USA.

Plato, C.C., Wood, J.L. and Norris, A.H., 1980. Bilateral asymmetryin bone measurements of the hand and lateral handdominance. *American Journal of Physical Anthropology*, 52:27-31.

Polk, J. D. 2001. The influence of body size and body proportions on primate quadrupedal locomotion. PhD dissertation, State University of New York at Stony Brook.

Polk, J. D. 2002. Adaptive and phylogenetic influences on musculoskeletal design in Cercopithecine primates. *Journal of Experimental Biology,* 205: 3399-3412.

Preuschoft, H. 1969. Statische Untersuchungen am Fuss der Primaten. I. Statik der Zehen und des Mittelfusses. *Z. Anat. Entwickl.-Gesch*. 129:285-345.

Preuschoft, H. 1970. Functional anatomy of the lower extremity. In: Bourne, G.H. Ed., *The Chimpanzee*, vol. 3. Pp. 221-294. Karger, Basel. NY, USA.

Preuschoft, H. 1974. Body posture and mode of locomotion in fossil primates: method and example: Aegyptopithecuszeuxis. *Symposium for the*

Fifth Congregation of the International Primatological Society. Pp. 345-359.

Preuschoft, H. 2004.Mechanicsm for the acquisition of habitual bipedality: are there biomechanical reasons for the acquisition of upright, bipedal posture. *Journal of Anatomy*, 204:363-384.

Prost, J. 1965. A definitional system for the classification of primate locomotion. *American Anthropologist*, 67:1198-1214.

Qian, Z-H., Ren, L., Ren, L-Q. and Boonpratatong, A. 2010. A three-dimensional finite element musculoskeletal model of the human foot complex. In, Lim, C.T. and Goh, J.C.H. (Eds), *IFMBE Proceedings: 6th World Congress of Biomechanics, WCB 2010. Volume 31*. Springer, Berlin.

Reilly, D.T. and Burstein, A.H. 1975. The elastic and ultimate properties of compact bone tissue. *Journal of Biomechanics*, 8:393-405.

Reynolds, T. R. 1985. Stresses on the limbs of quadrupedal primates. *American Journal of Physical Anthropology*, 67: 351-362.

Richmond, B.R. 1998. *Ontogeny and biomechanics of phalangeal form in primates.* Ph.D. Dissertation, State University of New York at Stony Brook.

Richmond, B.R. 2007. The biomechanics of phalangeal curvature. *Journal of Human Evolution*, 53, 6:678-690.

Robling, A. G., Warden, S. J., Shultz, K. L., Beamer, W. G., and Turner, C. H. 2007. Genetic effects on bone mechanotransduction in congenic mice harboring bone size and strength quantitative trait loci. *Journal of Bone and Mineral Research*, 22:984-991.

Rolian, C., Lieberman, D.E., Hamill, J., Scott, J.W. and Werbel, W. 2009. Walking, running and the evolution of short toes in humans. *The Journal of Experimental Biology*, 212:713-721.

Rose, M.D., 1988. Functional anatomy of the cheiridia. In: Schwartz, J. (Ed). Pp. 299-309. *Orang-utan Biology*. Oxford University Press, Oxford. UK.

Roux, W. 1881. *Der Kampf der TheileimOrganismus.* Leipzig: Engelmann. Berlin. GR.

Roy, T.A., Ruff, C.B. and Plato, C.C. 1994. Hand dominance andbilateral asymmetry in the structure of the second metacarpal. *American Journal of Physical Anthropology*, 94:203-211.

Rubin, C. and Lanyon, L. 1982. Limb mechanics as a function of speed and gait: a study of functional strains in the radius and tibia of horse and dog. *Journal of Experimental Biology,*17:352-358.

Rubin, C.T. and Lanyon, L.E. 1984. Regulation of bone formation by applied dynamic loads. *Journal of Bone and Joint Surgery*, 66A:397-402.

Rubin, C.T. and McLeod, K.J. 1998. Non-linear dependence of loading intensity and cycle number in the maintenance of bone mass and morphology. *Journal of Orthopaedic Research*, 16, 4:482-489.

Rubin, C.T., Bain, S.D. and McLeod, K.J. 1992. Suppression of the Osteogenic Response in the Aging Skeleton. *Calcified Tissue International*, 50:306-313.

Ruff, C.B. 2002. Long bone articular and diaphyseal structure in Old World monkeys and apes. I: locomotor effects. *American Journal of Physical Anthropology*, 119:305-342.

Ruff, C.B. and Runestad, J. 1992. Primate limb bone structural adaptations. *Annual Review in Anthropology*, 21:407-433.

Ruff, C.B., Walker, A. and Trinkaus, E. 1994. Postcranial robusticity in Homo. III: Ontogeny. *American Journal of Physical Anthropology*, 93:35-54.

Ruff, C.B., Trinkaus, E. and Holliday, T.W. 1997. Body mass and encephalization in Pleistocene Homo. *Nature*, 387:173-176.

Ruff, C. B., Holt, B. and Trinkaus, E. 2006. Who's afraid of the big bad Wolff?: "Wolff's law" and bone functional adaptation. *American Journal of Physical Anthropology*, 129:484-498.

Rybicki, E.F. and Kanninen, M.F. 1977. A finite element calculation of stress intensity factors by a modified crack closure integral. *Engineering Fracture Mechanics*. 9, 11:931-938.

Savvidis, E. and Stabrey, H. 1996. ExperimentellermitteIteWerkstoffdaten von humane Oberschenkelknochen und Analyse der richtungsabh¨angigen Bean- spruchbarkeit. *ZeitschriftfürOrthopädie und Unfallchirurgie*, 134:445-451.

Schaffler, M. and Burr, D.B. 1984. Primate cortical bone microstructure: relationship to locomotion. *American Journal of Physical Anthropology*, 65:191-197.

Schaffler, M.B., Burr, D.B., Jungers, W.L. and Ruff, C.B. 1985. Structural and mechanical indicators of limb specialization in primates. *Folia Primatologica*, 45:61-75.

Schmitt, D. 1998. Forelimb mechanics during arboreal and terrestrial quadrupedalism in Old World Monkeys. In *Primate Locomotion: Recent Advances* (Eds). E. Strasser, J. G. Fleagle, A. L. Rosenberger and H. M. McHenry. Pp. 175-200. New York: Plenum Press.

Schmitt, D. 1999. Compliant walking in primates. *Journal of Zoology* 247, 149-160.

Schmitt, D. and Lemelin, P. 2002. The origins of primate locomotion: gait mechanics of the woolly opossum. *American Journal of Physical Anthropology,* 118: 231-238.

Schmitt, D. 2003. Insights into the evolution of human bipedalismfrom experimental studies of humans and other primates. *Journal of Experimental Biology*, 206:1437-1448.

Shackelford. L.L and Trinkaus, E. 2002. Late Pleistocene human femoral diaphyseal curvature. *American Journal of Physical Anthropology,* 118:359-370.

Sharkey, N.A., Ferris, L., Smith, T.S. and Matthews, D.K. 1995. Strain and loading of the second metatarsal during heel lift. *Journal of Bone and Joint Surgery*. 77-A, 1050-1057.

Siegel, S. and Castellan, N. J. Jr. 1988. *Nonparametric statistics for the behavioural sciences.* 2nd edition. McGraw–Hill. NY, USA.

Sparacello,V.S. and Pearson, O.M. 2010. The importance of accounting for the area of the medullary cavity in cross-sectional geometry: A test based on the femoral midshaft. *American Journal of Physical Anthropology*, 143, 4:612-624.

Stern Jr., J.T. 2000. Climbing to the top: a personal memoir of *Australopithecus afarensis*. *Evolutionary Anthropology*. 9:113-133.

Stern Jr., J.T. and Susman, R.L. 1991. "Total morphological pattern" versus the "magic trait": conflicting approaches to the study of early hominid bipedalism. In: Coppens, Y., Senut, B. (Eds.), *Origines de la Bipédie chez les Hominidés*. Pp. 99-111.CNRS, Paris.

Stokes, I., Hutton, W. and Stott, J. 1979. Forces acting on the metatarsals during normal walking. *Journal of Anatomy*, 129:579-90.

Susman, R.L. 1979. Comparative and functional morphology of hominoid fingers. American *Journal of Physical Anthropology*, 50:215-236.

Susman, R.L., Stern, J.T. and Jungers, W.L. 1984. Arboreality and bipedality in the Hadar hominids. *Folia Primatologica*, 43:113-156.

Sverdlova, N.S. and Witzel, U. 2010. Principles of determination and verification of muscle forces in the human musculoskeletal system: muscle forces to minimise bending stress. *Journal of Biomechanics*, 43:387-96.

Swartz, S.M. 1990. Curvature of the forelimb bones of anthropoid primates: Overall allometric patterns and specialisations in suspensory species. *American Journal of Physical Anthropology*, 83:477-498.

Szivek, J.A., Johnson, E.M. and Pagee, F.P. 1992. In vivo strain analysis of the greyhound femoral diaphysis. *Journal of Investigative Surgery*, 5, 2:91-108.

Timoshenko, S.P. 1921. On the correction for shear of the differential equation for transverse vibrations of prismatic bars. *Philosophical Magazine,* 41: 744–746

Timoshenko, S. P. 1922. On the transverse vibrations of bars of uniform cross-section. *Philosophical Magazine,* 43: 125–131

Thompson, D.W. 1917. *On Growth and Form*. Cambridge University Press, Cambridge, UK.

Trinkaus, E. and Ruff. C. 1999. Diaphyseal Cross-sectional Geometry of Near Eastern Middle Palaeolithic Humans: The Tibia. *Journal of Archaeological Science,* 26: 289-1300.

Turner, C. H. 1998. Three rules for bone adaptation to mechanical stimuli. *Bone*, 23:399-407.

Turner, C. H., Owan, I., and Takano, Y. 1995. Mechanotransduction in bone: Role of strain rate. *American Journal of Physiology*, 269:438-442.

Turner, C. H., Hsieh, Y. F., Muller, R., Bouxsein, M. L., Baylink, D. J., Rosen, C. J., McCrann, M.E., Donahue, L.R. and Beamer, W.G. 2000. Genetic regulation of cortical and trabecular bone strength and microstructure in inbred strains of mice. *Journal of Bone and Mineral Research*, 15:1126-1131.

Tuttle, R.H. 1969. Quantitative and functional studies on the hands of the Anthropoidea. *Journal of Morphology*, 128:309-364.

Uhthoff, H. 1987. *Current Concepts of Bone Fragility*. Springer-Verlae. Berlin.

Vereecke, E. E., D'Août, K., DeClercq, D., van Elsacker, L. and Aerts, P. 2003. Dynamic plantar pressure distribution during terrestrial locomotion of Bonobos (*Pan paniscus*). *American Journal of Physical Anthropology,* 120:373-383.

Vereecke, E. E., D'Août, K. and De Clercq, D. 2004. The relationship between speed, contact time and peak plantar pressure in terrestrial walking of bonobos. *Folia Primatologica,* 75:266-278.

Vereecke, E. E., D'Août, K., DeClercq,D., Van Elsacker, L. and Aerts, P. 2005. Functional analysis of the gibbon foot during terrestrial bipedal walking: plantar pressure distributions and 3D ground reaction forces. *American Journal of Physical Anthropology,* 128:659-669.

Vereecke, E. E., D'Août, K. and Aerts, P. 2006a. Speed modulation in hylobatid bipedalism: a kinematical analysis. *Journal of Human Evolution,* 51: 513-526.

Vereecke, E. E., D'Août, K. and Aerts, P. 2006b. The dynamics of hylobatid bipedalism: evidence for an energy-saving mechanism? *Journal of Experimental Biology*, 209:2829-2838.

Vilensky, J. A. and Larson, S. G. 1989. Primate Locomotion: Utilization and control of symmetrical gaits. *Annual Review of Anthropology.* 18: 17-35.

Wallace, I.J. and Demes, B. 2008. Symmetrical gaits of Cebusapella: implications for the functional significance of diagonal sequence gait in primates. *Journal of Human Evolution*, 54:783-794.

Ward, C. V., Kimbel, W. H. and Johanson, D. C. 2011. Complete fourth metatarsal and arches in the foot of Australopithecus afarensis. *Science* 331:750-753.

Wergedal, J. E., Sheng, M. H., Ackert-Bicknell, C. L., Beamer, W. G., and Baylink, D. J. 2005. Genetic variation in femur extrinsic strength in 29 different inbred strains of mice is dependent on variations in femur cross-sectional geometry and bone density. *Bone*, 36:111-122.

Winkler, E. 1867. *Die Lehre von der Elastisita¨t und Festigkeit,* Prague, Dominicus.

Wolf, P., Stacoff, A. and Stussi, E. 2004. Modelling of the passive mobility in human tarsal gears: implications from the literature. *The Foot*, 24:23-34.

Wolff, J. 1986. *The law of bone remodelling* [translated from the 1892 original, Das Gesetz der Transformation der Knochen, by P. Maquet and R. Furlong]. Berlin: Springer Verlag.

Woo, S.L.Y., Kuei, S.C., Amiel, D., Gomez, M.A., Hayes, W.C., White, F.C. and Akeson, W.H. 1981. The effect of prolonged physical training on the properties of the long bone: a study of Wolff's law. *Journal of Bone and Joint Surgery America*, 63:780-787.

Wunderlich, R. E. and Jungers, W. L. 1998. Force distribution on the digits during knuckle-walking. *American Journal of Physical Anthropology,(Suppl)* 105, 26:236.

Wunderlich, R.E., 1999. *Pedal form and plantar pressure distribution in anthropoid primates*. Ph.D. Dissertation. State University of New York at Stony Brook.

Xiong, D. H., Shen, H., Xiao, P., Guo, Y. F., Long, J. R., Zhao, L. J., Liu, Y-Z., Deng, H-Y., Li, J-L., Recker, R.R. and Deng, H-W. 2006. Genome-wide scan identified QTLs underlying femoral neck cross-sectional geometry that are novel studied risk factors of osteoporosis. *Journal of Bone and Mineral Research*, 21:424-437.

Yamanaka, A., Gunji, H. and Ishida, H. 2005. Curvature, length, and cross-sectional geometry of the femur and humerus in anthropoid primates. *American Journal of Physical Anthropology*, 127:46-57.

Zipfel, B., DeSilva, J.M., Kidd, R.S., Carlson, K.J., Churchill, S.E. and Berger, L.R. 2011. The foot and ankle of Australopithecus sediba. *Science*, 333:1417-1420

Zumwalt, A. 2006. The effect of endurance exercise on the morphology of muscle attachment sites. *Journal of Experimental Biology*, 209, 3:444-54.

APPENDIX A: Variability tables, all species, all specimens, all metatarsals showing minimum, maximum, mean and standard deviations

Interspecific variability table: minimum, maximum, mean & standard deviation in mm for plantar thickness in *P. paniscus*																				
	MT1				MT2				MT3				MT4				MT5			
Specimen	Min	Max	Mean	SD	Min	Max	Mean	SD	Min	Max	Mean	SD	Min	Max	Mean	SD	Min	Max	Mean	SD
15296	1.4	2.18	1.75	0.22	0.02	1.9	1.61	0.37	1.55	2.15	1.85	0.17	1.15	2.4	1.78	0.3	1.15	1.85	1.47	0.23
20882	1.77	2.42	2.07	0.18	2.15	2.8	2.34	0.18	1.93	2.85	2.44	0.25	1.75	2.48	2.17	0.22	1.38	2.48	1.98	0.35
27698	1.97	2.5	2.28	0.14	2.35	2.8	2.53	0.13	2	2.93	2.36	0.24	1.7	2.53	2.08	0.24	1.87	2.5	2.15	0.19
29035	1.77	2.33	2.03	0.17	1.6	2.3	1.98	0.23	1.68	2.45	2.09	0.27	1.5	2.45	1.93	0.32	1.25	2.15	1.68	0.29
29040	1.82	2.68	2.12	0.24	2.07	2.53	2.35	0.14	2.5	2.93	2.7	0.13	2.07	3.6	2.51	0.31	1.6	2.8	2.09	0.38
13202	1.28	1.85	1.57	0.17	1.27	1.97	1.59	0.21	1	1.67	1.33	0.21	1	1.6	1.31	0.16	0.83	1.43	1.12	0.18
15294	2.53	3.3	2.76	0.26	2.57	3.07	2.9	0.14	1.9	2.4	2.06	0.11	1.9	2.4	2.06	0.11	1.47	2.03	1.83	0.14
15295	1.7	2.37	1.96	0.18	1.55	2.18	1.8	0.18	1.6	2.3	1.9	0.16	1.65	2.35	2.11	0.18	1.33	2.18	1.75	0.19
29044	2	2.87	2.34	0.26	2.07	3	2.63	0.31	1.77	2.83	2.36	0.24	1.6	3.18	2.35	0.44	1.63	1.97	1.75	0.09
29052	1.63	2.33	2.06	0.19	1.83	2.4	2.05	0.19	1.98	2.93	2.31	0.29	1.87	2.67	2.14	0.18	1.5	2.5	1.92	0.22
20881	1.82	2.32	2.1	0.16	2.31	2.68	2.5	0.11	2.27	3.33	2.62	0.23	1.92	2.84	2.39	0.2	1.71	2.53	2.02	0.25
29042	1.82	2.63	2.26	0.2	2.12	2.81	2.43	0.21	2.12	2.8	2.38	0.2	2.01	2.65	2.26	0.19	0	2.61	2.04	0.52
29045	2.01	2.73	2.24	0.2	2	2.45	2.31	0.1	2.01	3.09	2.47	0.32	1.94	2.32	2.11	0.11	1.6	2.36	1.93	0.26
29060	2	2.55	2.22	0.16	1.65	2.12	1.87	0.12	1.59	2.23	1.89	0.19	1.37	2.3	1.78	0.24	1.3	2.15	1.62	0.21
27696	1.62	2.47	1.97	0.24	1.51	2.14	1.73	0.16	1.21	2.1	1.54	0.21	1.51	1.97	1.71	0.13	1.29	1.93	1.55	0.2

Interspecific variability table: minimum, maximum, mean & standard deviation in mm for dorsal thickness in *P. paniscus*																				
	MT1				MT2				MT3				MT4				MT5			
Specimen	Min	Max	Mean	SD	Min	Max	Mean	SD	Min	Max	Mean	SD	Min	Max	Mean	SD	Min	Max	Mean	SD
15296	1.05	1.68	1.38	0.14	1.27	2.43	1.99	0.37	1.1	2.38	1.69	0.37	1.25	1.67	1.46	0.11	1.12	1.57	1.36	0.12
20882	1.72	2.48	2.16	0.25	1.85	3.02	2.41	0.39	1.8	2.63	2.27	0.2	1.63	2.33	2.04	0.15	1.7	2.18	1.9	0.11
27698	1.83	2.53	2.25	0.21	1.9	4	2.95	0.73	1.83	3.07	2.58	0.39	1.83	2.6	2.24	0.19	1.7	2.53	2.03	0.25
29035	1.76	2.33	2.09	0.14	1.33	3.23	2.28	0.63	1.53	2.15	1.88	0.18	1.53	2.65	1.85	0.31	1.55	2	1.72	0.13
29040	2.18	2.47	2.31	0.1	1.8	3.47	2.7	0.58	1.8	3	2.48	0.36	1.7	2.67	2.3	0.26	1.7	2.23	1.96	0.16
13202	1.38	1.83	1.63	0.12	1.3	2.47	1.9	0.31	1	1.63	1.27	0.18	0.93	1.5	1.28	0.2	0.8	1.27	1.01	0.13
15294	2.23	2.67	2.49	0.1	2.3	3.9	3.08	0.56	1.63	2.47	2	0.27	1.63	2.47	2	0.27	1.5	2.17	1.89	0.19
15295	1.53	1.97	1.81	0.12	1.3	2.7	2.24	0.41	1.28	2.73	2.09	0.48	1.63	2.1	1.88	0.1	1.25	1.83	1.57	0.16
29044	1.87	2.6	2.23	0.16	2.53	4.13	3.17	0.51	2.2	2.8	2.51	0.17	2.1	3.13	2.34	0.22	1.8	2.2	2.02	0.13
29052	1.8	2.5	2.14	0.2	1.73	3.5	2.6	0.44	1.4	2.95	2.17	0.48	1.8	2.57	2.13	0.23	1.43	2.3	1.98	0.2
20881	1.77	2.52	2.13	0.2	2.05	3.65	3.2	0.4	1.8	3.12	2.35	0.44	2.08	2.58	2.36	0.12	1.6	2.38	2	0.18
29042	1.79	2.72	2.44	0.22	2.02	3.22	2.8	0.39	2.07	3.11	2.62	0.36	2.19	3.01	2.55	0.24	0	2.24	1.91	0.45
29045	1.95	2.4	2.19	0.15	1.76	2.72	2.4	0.25	1.71	2.53	2.11	0.24	1.71	2.17	1.91	0.13	1.41	1.98	1.67	0.14
29060	1.67	2.55	2.07	0.29	1.7	2.71	2.28	0.34	1.4	2.87	2.24	0.44	1.31	2.32	1.9	0.25	1.34	1.82	1.59	0.13
27696	1.74	2.24	2.04	0.12	1.51	3.41	2.56	0.64	1.18	2.61	1.9	0.42	1.47	2.23	1.85	0.23	1.29	2.51	1.75	0.31

Interspecific variability table: minimum, maximum, mean & standard deviation in mm for medial thickness in *P. paniscus*																				
	MT1				MT2				MT3				MT4				MT5			
Specimen	Min	Max	Mean	SD	Min	Max	Mean	SD	Min	Max	Mean	SD	Min	Max	Mean	SD	Min	Max	Mean	SD
15296	0.95	1.93	1.44	0.3	1.45	2.3	1.96	0.24	1.1	1.63	1.39	0.15	1.2	1.93	1.64	0.21	1	1.78	1.43	0.21
20882	1.78	2.92	2.07	0.25	1.68	2.4	2.11	0.2	1.52	2	1.83	0.13	1.68	2.53	2.15	0.26	1.6	2.05	1.8	0.11
27698	1.8	2.8	2.28	0.3	1.9	2.85	2.29	0.29	1.5	2.5	2.15	0.27	1.8	2.37	2.15	0.17	1.73	2.43	2.12	0.19
29035	1.77	2.2	2.02	0.13	1.67	2.2	1.93	0.18	1.6	2	1.77	0.11	1.6	1.98	1.82	0.12	1.63	2.25	1.95	0.17
29040	2.07	2.99	2.44	0.26	2.3	3.37	2.77	0.35	1.83	2.47	2.22	0.19	1.87	2.53	2.18	0.17	1.7	2.43	2.07	0.2
13202	1.48	1.98	1.64	0.14	1.3	2.67	1.79	0.42	0.9	1.37	1.12	0.12	1.07	1.9	1.37	0.23	0.8	1.2	0.99	0.08
15294	2.2	2.53	2.41	0.08	2.67	3.67	3.05	0.29	1.53	2.13	1.86	0.17	1.53	2.13	1.86	0.17	1.57	1.97	1.74	0.11
15295	1.5	1.97	1.71	0.14	1.38	2.85	2.15	0.41	1.08	1.98	1.69	0.26	1.53	2.48	2.05	0.27	1.25	1.95	1.66	0.16
29044	1.8	3.37	2.65	0.52	2.2	2.83	2.52	0.19	1.83	2.4	2.16	0.15	1.95	2.23	2.08	0.07	1.77	2.2	1.94	0.12
29052	1.93	2.7	2.35	0.23	1.63	2.73	2.42	0.33	1.4	2.2	1.91	0.26	1.5	2.57	2.06	0.25	1.63	2.23	1.87	0.16
20881	1.68	2.48	2.17	0.2	1.99	2.8	2.46	0.22	1.6	2.21	1.96	0.14	1.62	3.28	2.44	0.51	1.6	2.51	2.12	0.25
29042	1.67	2.57	2.18	0.3	2.27	3.12	2.65	0.26	1.79	2.13	1.95	0.09	1.69	2.33	2.1	0.19	0	2.18	1.89	0.45
29045	1.92	2.39	2.05	0.1	2.08	3.06	2.4	0.27	1.4	2.32	1.92	0.24	1.58	2.31	1.94	0.21	1.59	1.99	1.79	0.1
29060	1.55	2.2	1.83	0.2	1.7	2.5	2	0.24	1.5	2.01	1.73	0.14	1.28	2.02	1.71	0.18	1.47	2.03	1.75	0.16
27696	1.88	2.32	2.13	0.15	1.57	2.31	1.95	0.26	1.5	1.82	1.65	0.09	1.7	2.18	1.9	0.13	1.28	1.9	1.56	0.16

Interspecific variability table: minimum, maximum, mean & standard deviation in mm for lateral thickness in *P. paniscus*																				
	MT1				MT2				MT3				MT4				MT5			
Specimen	Min	Max	Mean	SD	Min	Max	Mean	SD	Min	Max	Mean	SD	Min	Max	Mean	SD	Min	Max	Mean	SD
15296	1.43	2.13	1.74	0.17	1.42	1.83	1.66	0.13	1.17	1.65	1.53	0.13	1.13	1.75	1.51	0.16	0.93	1.9	1.45	0.27
20882	1.69	2.18	2.01	0.14	1.6	1.95	1.78	0.11	1.67	1.93	1.8	0.08	1.7	2.45	2.13	0.25	1.55	2.28	1.88	0.18
27698	2.17	3.03	2.56	0.2	1.75	2.3	2.09	0.16	1.67	2.2	2.02	0.12	1.73	2.5	2.11	0.2	1.43	2.8	2.23	0.34
29035	1.77	2.07	1.87	0.09	1.63	2.17	1.9	0.14	1.6	1.93	1.79	0.08	1.5	2	1.8	0.12	1.5	2.38	1.87	0.3
29040	2	2.4	2.26	0.11	1.83	2.93	2.43	0.36	1.5	2.37	2.13	0.2	1.73	2.4	2.18	0.15	1.7	2.3	1.96	0.21
13202	1.33	1.68	1.48	0.12	0.97	1.4	1.24	0.11	0.93	1.23	1.09	0.08	1	2.1	1.5	0.39	0.8	1.5	1.09	0.18
15294	2.53	2.9	2.67	0.11	2.33	3.23	2.78	0.27	1.43	2.17	1.89	0.19	1.43	2.17	1.89	0.19	1.53	3	2.1	0.41
15295	1.63	2.3	1.92	0.18	1.23	2.2	1.76	0.27	1.58	2.05	1.82	0.15	1.2	2.13	1.81	0.23	1.43	2.33	1.77	0.28
29044	2.27	2.87	2.63	0.18	1.9	2.57	2.3	0.16	2.03	2.5	2.18	0.13	1.78	2.28	2.02	0.12	1.53	2.23	2.02	0.16
29052	2.03	3.1	2.49	0.25	1.6	2.45	2.05	0.24	1.58	2.08	1.88	0.14	1.67	2.37	1.98	0.19	1.4	2.67	2.07	0.3
20881	2.09	2.5	2.34	0.11	1.94	2.42	2.16	0.16	1.7	2.24	1.9	0.12	1.71	2.39	2.09	0.22	1.71	2.53	2.27	0.27
29042	2.13	3.3	2.65	0.38	1.8	6.7	2.47	0.98	1.69	2.18	1.91	0.12	1.69	2.3	2	0.18	0	2.6	1.86	0.47
29045	1.92	2.51	2.17	0.18	1.99	2.52	2.2	0.16	1.59	2.53	2.23	0.23	1.68	2.4	1.94	0.23	1.37	2.43	1.68	0.3
29060	2.11	2.71	2.35	0.16	1.47	2.22	1.78	0.25	1.5	1.94	1.66	0.13	1.42	1.93	1.71	0.17	1.29	2.81	1.87	0.39
27696	1.57	2.82	2.16	0.37	1.46	2.09	1.66	0.19	1.31	1.79	1.54	0.13	1.59	1.94	1.76	0.12	1.39	3.28	1.88	0.45

Interspecific variability table showing minimum, maximum, mean and standard deviation in mm for curvature values in *P. paniscus* .																				
	MT1				MT2				MT3				MT4				MT5			
Specimen	Min	Max	Mean	SD	Min	Max	Mean	SD	Min	Max	Mean	SD	Min	Max	Mean	SD	Min	Max	Mean	SD
15296	-2.28	-0.97	-1.41	0.41	0.59	3.69	2.85	0.91	-0.83	1.6	0.88	0.73	-0.86	1.75	1	0.71	0.08	1.36	0.83	0.42
20882	-1.88	-0.77	-1.15	0.39	-1.49	1.12	0.34	0.8	-0.86	0.45	0.11	0.4	-2.23	-0.54	-0.88	0.46	-1.16	0.19	-0.19	0.39
27698	-1.6	-0.3	-0.73	0.41	-2.4	0.73	-0.12	0.95	-0.99	1.16	0.55	0.69	-0.91	0.74	0.25	0.53	0.24	3.18	2.39	0.85
29035	-2.6	-0.91	-1.39	0.47	-1.36	1.27	0.62	0.74	-0.41	1.98	1.25	0.75	-1.87	1.27	-0.13	0.64	-0.25	1.25	0.78	0.49
29040	-2.65	-1.26	-1.77	0.41	-0.39	1.8	1.12	0.67	-0.41	2.32	0.62	0.57	-2	0.2	-0.42	0.63	-0.63	1.63	1	0.64
13202	-2.25	-0.97	-1.27	0.36	-1.44	2.44	1.3	1.18	-1.26	0.9	0.23	0.67	-2.32	-0.52	-1.11	0.56	-2.12	0.3	-0.22	0.67
15294	-2.61	-1.21	-1.71	0.44	0.09	2.21	1.52	0.65	-1.05	0.44	0.09	0.48	-1.2	0.98	0.45	0.65	-0.67	1.84	1.08	0.71
15295	-2.72	-1.24	-1.63	0.47	-1.47	1.03	0.41	0.72	-1.8	0.43	-0.12	0.61	-1.02	0.99	0.45	0.58	-0.11	1.71	1.22	0.53
29044	-1.37	0.81	0.25	0.63	-0.72	3.76	2.5	1.34	-0.02	2.34	1.56	0.77	-0.37	1.98	1.2	0.74	0.13	2.01	1.49	0.57
29052	-2.96	-1.28	-1.7	0.5	-0.98	2.11	1.09	0.91	-1.47	0.34	-0.25	0.57	-1.53	0.47	-0.17	0.67	-1.55	0.97	0.25	0.69
20881	-1.3	0.8	0.18	0.62	-1.13	1.66	0.76	0.82	-1.01	1.59	0.84	0.75	-1.33	1.15	0.42	0.69	-0.31	1.91	1.27	0.64
29042	-2.93	-1.63	-2.12	0.43	-1.63	0.1	-0.51	0.55	-1.34	0.38	-0.09	0.49	-2.39	-0.29	-0.81	0.58	-0.85	1.32	0.71	0.64
29045	-1.68	-0.48	-0.91	0.42	-1.4	1.47	0.78	0.83	-2.01	1.2	0.29	0.91	-1.2	0.9	0.23	0.67	-1.05	1.34	0.73	0.71
29060	-3.62	-2.23	-2.6	0.4	-1.19	1.6	0.89	0.81	-1.37	0.61	0.07	0.63	-1.16	0.83	0.3	0.59	-0.66	1.14	0.64	0.53
27696	-4.06	-1.28	-2.14	0.89	-2.03	0.76	0.09	0.84	-1.78	0.32	-0.19	0.61	-1.3	0.37	-0.15	0.45	-1.58	0.29	-0.26	0.5

Interspecific variability table: minimum, maximum, mean & standard deviation in mm for plantar thickness in *H. sapiens*																				
	MT1				MT2				MT3				MT4				MT5			
Specimen	Min	Max	Mean	SD	Min	Max	Mean	SD	Min	Max	Mean	SD	Min	Max	Mean	SD	Min	Max	Mean	SD
Mixe	1.13	1.8	1.39	0.18	0.95	1.95	1.41	0.27	0.85	1.75	1.51	0.24	1.03	1.7	1.39	0.17	0.98	1.68	1.35	0.15
A5_Euro	1.53	1.95	1.73	0.11	1.58	2.55	1.98	0.22	0.93	1.65	1.4	0.25	0.93	1.65	1.4	0.25	0.93	1.78	1.45	0.29
A8_Soto	1	1.4	1.19	0.11	1.1	1.77	1.46	0.22	1	1.63	1.34	0.15	0.33	1.7	1.31	0.35	0.9	1.73	1.34	0.28
A9_Vend	1.33	1.7	1.53	0.09	1.73	3.4	2.24	0.44	1.7	3.4	2.28	0.46	1.38	1.9	1.65	0.13	1.15	1.75	1.43	0.15
A10_Xosa	0.87	2.2	1.27	0.28	1.43	2.07	1.79	0.19	0.97	1.63	1.45	0.17	0.7	1.53	1.14	0.2	0.55	1.8	1.3	0.38
A22_Xosa	0.93	1.6	1.33	0.22	0.95	1.55	1.26	0.17	0.93	1.6	1.36	0.13	0.93	2.1	1.56	0.32	0.73	1.37	1.17	0.2
A184_Soto	1.27	2.6	1.53	0.31	1.6	2.08	1.86	0.13	1.25	1.88	1.42	0.13	1.03	1.68	1.4	0.16	1.07	1.8	1.4	0.24
A209_Soto	0.73	2	1.43	0.34	1.15	1.48	1.31	0.07	0.85	1.48	1.15	0.15	0.83	1.43	1.06	0.12	0.17	1.73	1.09	0.28
A458_Soto	1.1	1.73	1.4	0.18	1.28	1.53	1.4	0.07	1	1.68	1.31	0.21	0.9	1.48	1.16	0.14	0.85	1.7	1.2	0.26
A741_Soto	1.03	1.93	1.4	0.23	1.3	2	1.67	0.19	1.15	1.88	1.54	0.19	1.18	1.93	1.54	0.19	1.1	1.6	1.35	0.13
A13_Pondo	1.36	1.96	1.59	0.17	2.2	4.03	3.12	0.56	1.16	1.68	1.41	0.16	1.07	1.74	1.43	0.21	1.03	1.52	1.34	0.14
A14_Zulu	1.28	1.93	1.56	0.16	1.13	1.88	1.63	0.19	0.88	1.78	1.52	0.21	0.63	1.56	1.26	0.26	0.65	1.75	1.25	0.31
A17_Soto	1.08	1.98	1.34	0.22	1.22	3.21	1.65	0.45	1.04	1.73	1.47	0.16	0.84	1.64	1.27	0.19	1.02	1.82	1.34	0.21
A21_Fing	0.78	1.03	0.9	0.07	1	2.02	1.46	0.28	0.82	1.22	1.02	0.11	0.71	1.08	0.87	0.09	0.54	1.32	0.89	0.18
A24_indi	0.89	1.92	1.44	0.33	1.8	2.54	2.18	0.22	1.49	2.44	1.77	0.21	1.05	1.66	1.28	0.16	1.05	1.66	1.28	0.16
A25_Shan	1.58	2.3	1.86	0.18	1.7	2.71	2.25	0.31	1.12	2.2	1.63	0.3	1.18	2.18	1.64	0.21	1.58	2.08	1.9	0.12
A98_Soto	1.27	1.9	1.56	0.15	1.71	3.2	2.2	0.36	1.39	2.86	2.18	0.36	1.33	1.78	1.63	0.12	0.99	1.67	1.33	0.2
A144_Soto	1.57	2.04	1.84	0.1	1.57	2.23	1.88	0.14	1.51	2.73	1.81	0.29	1.22	2.03	1.64	0.2	1.4	2.14	1.69	0.22
A163_Soto	0.86	1.57	1.02	0.17	1.32	2.16	1.8	0.22	0.88	1.59	1.31	0.21	0.88	2.67	1.2	0.36	1.03	1.98	1.53	0.21
A170_Soto	1.07	1.71	1.39	0.19	1.17	1.96	1.5	0.2	1.13	1.86	1.5	0.21	0.99	1.78	1.34	0.26	0.97	2.53	1.4	0.35
A218_Soto	0.8	1.36	1.12	0.15	1.25	1.54	1.45	0.09	1.46	2.87	1.77	0.3	1.31	1.71	1.5	0.11	1.16	1.74	1.53	0.18
A883_Soto	1.23	2.16	1.77	0.22	1.68	2.16	1.96	0.14	1.62	1.93	1.75	0.08	1.4	1.94	1.57	0.13	1.41	2.37	1.69	0.24

Interspecific variability table: minimum, maximum, mean & standard deviation in mm for dorsal thickness in *H. sapiens*																				
	MT1				MT2				MT3				MT4				MT5			
Specimen	Min	Max	Mean	SD	Min	Max	Mean	SD	Min	Max	Mean	SD	Min	Max	Mean	SD	Min	Max	Mean	SD
Mixe	1.03	2	1.61	0.34	0.55	2.08	1.52	0.5	0.8	1.73	1.35	0.29	0.9	1.85	1.39	0.27	0.8	1.63	1.29	0.29
A5_Euro	1.28	2.28	1.85	0.31	0.8	2.55	1.95	0.56	0.75	1.8	1.42	0.29	0.75	1.8	1.42	0.29	0.93	1.83	1.39	0.26
A8_Soto	1.57	2.43	1.95	0.2	0.77	2.17	1.51	0.45	0.78	1.68	1.31	0.3	0.83	1.87	1.29	0.23	0.73	1.8	1.16	0.25
A9_Vend	1.37	2.3	1.76	0.23	0.93	2.83	2.15	0.67	0.88	2.85	2.13	0.7	0.98	2.48	1.8	0.44	0.75	1.7	1.25	0.29
A10_Xosa	1.2	1.63	1.43	0.14	0.9	2.03	1.62	0.4	0.63	1.9	1.43	0.41	0.73	1.5	1.21	0.23	0.8	1.8	1.34	0.34
A22_Xosa	1.03	1.23	1.13	0.06	0.8	1.9	1.51	0.35	0.8	1.63	1.25	0.24	0.93	2.3	1.71	0.46	0.73	1.83	1.31	0.32
A184_Soto	1.27	1.7	1.55	0.12	0.88	2.68	1.89	0.67	0.75	1.75	1.39	0.31	0.8	1.63	1.34	0.24	0.7	1.63	1.22	0.33
A209_Soto	1.1	1.83	1.56	0.23	0.75	2.38	1.67	0.52	0.58	1.63	1.25	0.29	1.17	2	1.56	0.27	0.63	1.37	1.01	0.22
A458_Soto	0.97	1.67	1.15	0.18	1.23	1.75	1.46	0.15	0.53	1.1	0.85	0.16	0.75	1.6	1.13	0.23	0.68	1.4	1.07	0.21
A741_Soto	1	1.7	1.41	0.19	0.88	2.73	1.58	0.51	1.23	2	1.63	0.23	1.13	2.08	1.6	0.24	0.87	2.53	1.32	0.33
A13_Pondo	1.47	2.35	1.84	0.3	1.37	2.68	2.06	0.45	0.8	2.16	1.57	0.46	0.88	2.41	1.72	0.51	0.7	1.71	1.18	0.33
A14_Zulu	1.28	1.62	1.48	0.09	1.1	2.16	1.77	0.3	1	1.71	1.46	0.2	1.1	1.93	1.56	0.28	0.83	1.85	1.35	0.32
A17_Soto	1.18	1.69	1.46	0.16	0.68	2.62	1.77	0.67	0.87	1.92	1.42	0.33	0.31	1.83	1.29	0.51	0.6	1.65	1.15	0.27
A21_Fing	1.46	2.07	1.7	0.2	1.06	2.19	1.72	0.38	0.57	1.53	0.98	0.24	0.64	1.16	0.92	0.18	0.65	1.01	0.82	0.1
A24_indi	1.36	2.41	1.99	0.34	0.89	2.71	2.02	0.5	0.58	1.97	1.32	0.43	0.84	1.9	1.36	0.33	0.84	1.9	1.36	0.33
A25_Shan	1.42	2.42	1.98	0.26	1.2	2.39	2.04	0.31	0.93	2.02	1.68	0.35	1.49	2.54	2.04	0.3	0.99	1.97	1.49	0.29
A98_Soto	1.86	2.45	2.1	0.17	1.62	2.99	2.6	0.43	1.96	4.54	3.59	0.85	1.46	2.4	2.05	0.29	1.04	1.53	1.27	0.14
A144_Soto	1.5	2.55	1.91	0.36	1.09	2.9	2.28	0.61	1.09	2.63	2.03	0.54	1.2	2.3	1.83	0.33	0.68	2.17	1.34	0.45
A163_Soto	1.04	1.8	1.32	0.2	0.98	2.39	1.93	0.39	0.42	2.25	1.3	0.5	0.86	2.34	1.48	0.49	0.79	2.44	1.36	0.5
A170_Soto	1.25	2.22	1.8	0.25	0.81	3.15	2.02	0.74	0.99	2.13	1.58	0.36	0.99	2.02	1.58	0.33	0.79	1.65	1.29	0.25
A218_Soto	1.34	2.7	1.93	0.29	0.74	2.25	1.64	0.44	0.85	2.22	1.8	0.36	1.07	2.35	1.89	0.34	0.76	1.82	1.41	0.25
A883_Soto	1.65	2.22	1.97	0.19	1.01	2.73	2.09	0.51	1.22	2.27	1.82	0.3	1.12	2.06	1.73	0.3	1.2	2.23	1.72	0.28

Interspecific variability table: minimum, maximum, mean & standard deviation in mm for medial thickness in *H. sapiens*																				
	MT1				MT2				MT3				MT4				MT5			
Specimen	Min	Max	Mean	SD	Min	Max	Mean	SD	Min	Max	Mean	SD	Min	Max	Mean	SD	Min	Max	Mean	SD
Mixe	1.1	1.77	1.5	0.23	1.43	2.5	2.07	0.33	1.38	3	2.16	0.51	1.33	2.3	1.93	0.3	1.58	2.33	1.92	0.24
A5_Euro	1.1	2.5	1.87	0.44	1.05	2.83	2.19	0.56	1.25	2.85	2.23	0.52	1.25	2.85	2.23	0.52	1.43	3.33	2.36	0.62
A8_Soto	1.43	1.83	1.65	0.11	1.8	2.3	2.1	0.14	1.6	2.45	1.99	0.26	1.57	2.57	2.07	0.27	1.57	2.93	2.05	0.36
A9_Vend	1.27	3	1.73	0.49	1.75	3.7	2.8	0.65	1.73	3.75	2.8	0.65	1.53	3.18	2.39	0.45	1.18	2.7	2.06	0.44
A10_Xosa	1.17	2.67	1.75	0.45	1.37	3	2.41	0.55	1.47	2.83	2.13	0.48	1.5	3.37	2.39	0.55	1.2	3.25	2.28	0.65
A22_Xosa	1.1	2.1	1.76	0.31	1.1	2.45	1.88	0.38	1.2	2.7	2.05	0.49	1.37	2.77	2.09	0.46	1.03	3	2.04	0.58
A184_Soto	1.03	1.83	1.53	0.21	1.3	2.78	2.11	0.54	0.13	16.5	2.74	3.22	1.38	2.48	2.15	0.36	1	2.03	1.5	0.31
A209_Soto	0.87	2.07	1.55	0.37	1.15	2	1.58	0.26	1.23	2.98	2.05	0.5	0.97	1.9	1.56	0.3	1.2	2.43	1.7	0.39
A458_Soto	0.9	2.3	1.46	0.42	1.55	2.88	2.23	0.38	1.28	2.08	1.72	0.25	1.2	2.13	1.71	0.24	1.08	2.15	1.65	0.31
A741_Soto	1	1.6	1.25	0.2	1.38	1.93	1.73	0.15	1.03	1.85	1.63	0.2	1.05	1.83	1.61	0.21	1.33	1.87	1.67	0.15
A13_Pondo	1.23	3.41	2.06	0.6	1.41	2.32	1.91	0.24	1.21	2.71	2.14	0.47	1.22	2.6	2.03	0.48	1.29	2.45	1.87	0.33
A14_Zulu	1.23	2.6	1.84	0.39	1.52	3.21	2.48	0.45	1.8	3.09	2.39	0.43	1.51	2.46	2.03	0.26	1.22	2.63	1.93	0.38
A17_Soto	0.87	2.44	1.44	0.5	1.2	2.79	1.92	0.49	1.51	2.61	2.18	0.36	1.35	2.52	1.97	0.38	1.2	2.63	1.93	0.41
A21_Fing	0.71	1.53	1.13	0.25	1.27	2.81	2.02	0.6	1.16	2.61	2.04	0.51	0.91	1.93	1.69	0.23	1.13	2.91	1.94	0.44
A24_indi	1.19	2.3	1.83	0.31	1.63	3.22	2.56	0.51	1.12	3.08	2.34	0.58	1.37	3.28	2.59	0.53	1.37	3.28	2.59	0.53
A25_Shan	1.42	2.89	1.9	0.37	1.6	2.89	2.51	0.34	1.64	3.57	2.88	0.56	1.61	2.61	2.28	0.23	1.91	2.57	2.25	0.2
A98_Soto	1.2	2.89	1.82	0.47	1.6	2.4	2.09	0.25	1.29	2.13	1.81	0.21	1.41	2.01	1.75	0.19	1.38	2.22	1.83	0.21
A144_Soto	1.52	2.58	2.12	0.35	1.42	3.67	2.51	0.67	1.34	2.11	1.86	0.23	1.35	2.58	1.9	0.31	1.2	3.15	1.97	0.52
A163_Soto	0.76	1.62	1.14	0.28	1.41	2.5	2.07	0.34	1.13	2.56	2.04	0.43	0.92	2.65	1.96	0.47	0.97	2.15	1.81	0.42
A170_Soto	1.12	2.42	1.73	0.43	1.11	2.42	1.97	0.42	1.32	2.64	2.1	0.43	1.44	2.64	2.21	0.38	1.4	3.38	2.25	0.53
A218_Soto	1.51	3.08	2.06	0.4	1.48	3.2	2.46	0.54	1.36	2.71	2.16	0.41	1.54	2.63	2.18	0.28	1.49	3.9	2.73	0.73
A883_Soto	1.54	2.18	1.82	0.16	1.89	2.79	2.47	0.26	1.67	2.81	2.35	0.36	1.73	2.72	2.34	0.31	1.56	2.85	2.32	0.37

Interspecific variability table: minimum, maximum, mean & standard deviation in mm for lateral thickness in *H. sapiens*																				
	MT1				MT2				MT3				MT4				MT5			
Specimen	Min	Max	Mean	SD	Min	Max	Mean	SD	Min	Max	Mean	SD	Min	Max	Mean	SD	Min	Max	Mean	SD
Mixe	1.13	2.27	1.68	0.35	0.88	1.88	1.45	0.27	1.03	2.63	1.89	0.52	0.98	2.55	1.81	0.58	0.98	3	2.1	0.68
A5_Euro	0.98	2.68	1.83	0.56	0.88	1.88	1.42	0.26	0.93	1.93	1.51	0.32	0.93	1.93	1.51	0.32	0.8	4.38	2.93	1.09
A8_Soto	0.9	2.13	1.69	0.29	0.9	2.1	1.47	0.29	1.13	2.15	1.76	0.26	1.03	2.7	2.02	0.51	1.2	3.5	2.39	0.72
A9_Vend	1.5	3	1.91	0.45	1.35	2.33	1.81	0.37	1.28	2.4	1.8	0.41	1.13	2.8	1.92	0.63	0.98	2.83	1.9	0.57
A10_Xosa	0.9	1.6	1.27	0.23	0.97	2.43	1.73	0.46	1.13	2.8	1.96	0.56	1.23	3.07	2.18	0.7	1.05	4.85	2.88	1.2
A22_Xosa	0.9	2.3	1.5	0.46	0.85	2.03	1.37	0.38	0.87	2.17	1.59	0.42	0.97	3	2.07	0.69	0.87	3.13	2.22	0.78
A184_Soto	1.5	4.37	2.17	0.76	0.53	1.98	1.62	0.33	0.9	2.38	1.59	0.47	1.13	2.93	2.11	0.58	0.9	2.53	1.79	0.53
A209_Soto	0.77	2.7	1.71	0.61	0.83	1.4	1.06	0.15	0.6	2.8	1.49	0.67	0.83	2.63	1.54	0.46	0.97	2.33	1.62	0.43
A458_Soto	1.23	1.93	1.5	0.17	0.83	1.73	1.23	0.22	0.45	1.9	1.1	0.34	0.63	1.55	1.14	0.3	0.88	2.35	1.47	0.48
A741_Soto	1.17	1.77	1.42	0.18	1.35	1.78	1.58	0.12	1.15	1.7	1.46	0.17	1.13	1.68	1.43	0.18	1.23	2.03	1.55	0.19
A13_Pondo	1.3	3.05	1.85	0.41	1.03	2.5	1.81	0.44	0.93	2.73	1.89	0.52	0.84	2.5	1.8	0.59	0.89	2.83	1.78	0.62
A14_Zulu	1.49	2.76	1.88	0.34	0.75	2.62	1.65	0.47	1.36	2.22	1.82	0.26	0.9	2.41	1.74	0.46	0.91	3.09	2.11	0.76
A17_Soto	0.92	2.64	1.72	0.55	1.07	1.69	1.38	0.24	0.88	2.5	1.63	0.47	0.78	2.26	1.48	0.51	1.22	3.48	2.37	0.76
A21_Fing	0.64	3.34	1.29	0.69	0.8	2.02	1.33	0.36	0.76	3.01	1.71	0.76	0.82	3.93	2.24	1.12	1.09	2.85	2.11	0.63
A24_indi	1.03	3.47	1.77	0.64	1.01	1.68	1.34	0.18	0.78	2.2	1.4	0.48	0.79	2.5	1.79	0.57	0.79	2.5	1.79	0.57
A25_Shan	1.49	3.25	1.91	0.46	1.42	2.27	2.03	0.2	1.51	2.74	2.18	0.39	1.2	3.09	2.34	0.57	1.07	2.81	1.73	0.47
A98_Soto	1.2	3.29	1.82	0.63	1.57	2.22	1.9	0.2	1.42	2.09	1.82	0.2	1.36	2.16	1.7	0.15	1.42	2.16	1.74	0.19
A144_Soto	1.38	2.43	1.72	0.26	1.31	2.19	1.79	0.29	1.31	2.91	2.16	0.55	1.2	2.73	1.79	0.39	1.12	4.41	2.82	0.98
A163_Soto	1.04	2.11	1.46	0.31	1.04	2.05	1.48	0.26	0.93	1.85	1.37	0.26	0.88	2.44	1.53	0.37	0.86	2.24	1.62	0.37
A170_Soto	1.12	2.6	1.76	0.46	1.09	2.11	1.61	0.3	1.06	2.5	1.68	0.35	1.11	3.17	2.13	0.6	1.23	2.89	2.17	0.5
A218_Soto	1.4	3.6	2	0.56	1.08	1.5	1.37	0.11	1.22	3.32	1.76	0.46	1.23	2.35	1.81	0.35	0.88	3.39	2.26	0.8
A883_Soto	1.54	2.41	1.98	0.29	1.51	2.08	1.8	0.17	1.29	3.05	2.22	0.6	1.48	3.11	2.24	0.52	1.06	4.22	2.98	1.09

Interspecific Variability Table showing minimum, maximum, mean and standard deviation in mm for curvature values in *H. sapiens* .																				
	MT1				MT2				MT3				MT4				MT5			
Specimen	Min	Max	Mean	SD	Min	Max	Mean	SD	Min	Max	Mean	SD	Min	Max	Mean	SD	Min	Max	Mean	SD
Mixe	-7.2	-5.4	-5.95	0.54	-4.51	-2.93	-3.4	0.46	-4.42	-3.02	-3.37	0.41	-3.69	-2.09	-2.51	0.42	-3.39	-2.48	-2.73	0.28
A5_Euro	-6.94	-3.27	-4.27	1.17	-4.38	-0.58	-1.7	1.11	-3.2	-0.29	-1.05	0.81	-4.45	-0.63	-1.45	1.05	-3.32	-1.59	-2.13	0.52
A8_Soto	-6.68	-5.65	-5.98	0.36	-5.87	-2.59	-3.84	1.09	-4.64	-1.62	-2.6	0.92	-4.98	-2.67	-3.05	0.62	-5.78	-3.29	-4.05	0.73
A9_Vend	-5.63	-3.63	-4.16	0.58	-3.16	-0.57	-1.19	0.76	-3.1	-0.59	-1.24	0.73	-3.37	-1.1	-1.49	0.57	-3.59	-2.3	-2.84	0.46
A10_Xosa	-7.29	5.62	-5.47	2.9	-3.47	-1.54	-2.09	0.53	-3.55	-1.77	-2.21	0.5	-4.72	-3.21	-3.55	0.4	-2.65	-1.22	-1.69	0.42
A22_Xosa	-5.1	-2.83	-3.33	0.7	-3.69	-1.73	-2.18	0.53	-3.34	1.64	-1.79	1.05	-3.41	-1.62	-2.32	0.6	-3.48	-2.38	-2.76	0.35
A184_Soto	-5.93	-3.03	-3.74	0.88	-2.84	-0.54	-1.22	0.67	-2.45	-0.84	-1.15	0.41	-3.35	-0.53	-1.08	0.74	-4.2	-3.29	-3.68	0.26
A209_Soto	-6.52	-3.84	-4.54	0.84	-3.9	-2.43	-2.83	0.44	-2.14	-0.36	-0.86	0.5	-3.72	-0.59	-1.35	0.89	-3.11	-1.52	-1.96	0.45
A458_Soto	-5.38	-3.69	-4.06	0.51	-3.3	-1.28	-1.66	0.53	-3.63	-1.72	-2.08	0.54	-3.2	-0.69	-1.47	0.78	-3.25	-2.24	-2.67	0.3
A741_Soto	-7.43	-4.25	-5.27	1.16	-4.73	-1.74	-2.59	0.87	-4.37	-1.95	-2.53	0.65	-4.42	2.19	-2.51	1.25	-3.69	-2.15	-2.54	0.41
A13_Pondo	-5.88	-3.92	-4.48	0.62	-6.04	-4.69	-5.41	0.53	-2.82	-0.23	-1.11	0.82	-4.62	-2.31	-3.07	0.75	-3.87	-1.97	-2.49	0.57
A14_Zulu	-6.57	-4.26	-4.87	0.7	-4.36	-1.86	-2.48	0.7	-5.01	-1.72	-2.45	0.9	-5.81	3.5	-3.06	1.74	-6.1	-3.1	-4.08	0.84
A17_Soto	-5.82	-4.1	-4.57	0.51	-5.26	-1.53	-2.51	1.02	-4.13	1.92	-2.09	1.13	-5.32	-1.61	-2.42	1.1	-4.07	-2.78	-3.32	0.36
A21_Fing	-6.71	-4.52	-5.15	0.66	-3.73	-2.44	-2.96	0.43	-3.29	-1.55	-2.12	0.52	-5.45	-3.16	-3.57	0.56	-4.13	-2.92	-3.2	0.36
A24_indi	-7.5	-5.39	-5.91	0.62	-4.27	-2.07	-2.62	0.64	-4.08	-1.6	-2.19	0.71	-3.78	-1.74	-2.44	0.68	-4.07	-1.87	-2.4	0.55
A25_Shan	-5.9	-4.12	-4.54	0.53	-2.55	-0.8	-1.3	0.52	-2.13	-0.23	-0.81	0.55	-3	-1.11	-1.74	0.58	-3.9	-0.98	-1.98	0.89
A98_Soto	-5.69	-4.03	-4.48	0.48	-4.26	-1.77	-2.26	0.68	-5.95	-4.05	-4.42	0.54	-4.94	3.45	-3.06	1.6	-2.84	-1.43	-1.78	0.38
A144_Soto	-6.88	-5.41	-5.93	0.48	-4.09	-1.68	-2.42	0.71	-3.68	-1.39	-1.98	0.7	-4.65	-2.36	-2.89	0.66	-4.9	-4.19	-4.47	0.2
A163_Soto	-7.25	-5.04	-5.58	0.65	-4.72	-2.72	-3.26	0.56	-5.96	-2.45	-3.26	0.97	-5.59	-2.5	-3.26	0.88	-6.62	-2.98	-4.1	1.15
A170_Soto	-6.78	-3.96	-4.66	0.85	-5.78	-3.59	-4.2	0.62	-4.58	-1.76	-2.41	0.8	-5.06	-2.54	-3.04	0.71	-4.61	-2.42	-3.39	0.8
A218_Soto	-5.64	-2.36	-4.85	0.71	-3.85	-2.47	-2.8	0.42	-4.2	-2.72	-3.06	0.44	-4.19	-1.89	-2.37	0.6	-3.25	-1.65	-2.18	0.48
A883_Soto	-5.66	-3.57	-4.1	0.63	-3.82	-1.92	-2.53	0.55	-3.47	-0.98	-1.69	0.71	-3.26	-1.33	-1.98	0.58	-4.85	-3.45	-3.94	0.45

Interspecific variability table: minimum, maximum, mean & standard deviation in mm for plantar thickness in *P. t. schweinfurthii*																				
	MT1				MT2				MT3				MT4				MT5			
Specimen	Min	Max	Mean	SD	Min	Max	Mean	SD	Min	Max	Mean	SD	Min	Max	Mean	SD	Min	Max	Mean	SD
Charlie	1.81	2.55	2.19	0.19	2.22	2.92	2.56	0.22	2.45	3.5	2.99	0.32	1.6	2.78	2.24	0.27	1.72	2.32	2.05	0.15
7426	1.74	2.2	1.9	0.12	1.83	2.6	2.16	0.21	1.73	2.23	2.01	0.11	1.5	2.1	1.87	0.16	1.55	1.95	1.76	0.15
8341	1.65	2.35	1.99	0.19	1.77	2.66	2.26	0.26	1.91	2.43	2.18	0.17	1.7	2.22	2.03	0.15	1.43	2.03	1.74	0.16
14579	2	3.11	2.53	0.33	2.13	3.79	3.05	0.5	2.28	3.08	2.72	0.19	2.34	2.95	2.71	0.14	2.17	2.73	2.39	0.17
29074	1.91	2.72	2.45	0.23	2.16	3.06	2.49	0.25	1.88	3.08	2.48	0.24	1.07	2.99	2.59	0.44	1.63	2.7	2.12	0.35
30845	1.82	2.68	2.12	0.24	2.33	3.9	3.04	0.49	1.61	3.32	2.59	0.4	2.07	2.73	2.5	0.17	2.07	2.73	2.38	0.18
Flo	1.27	1.8	1.56	0.13	1.23	1.73	1.49	0.14	1.57	2.17	1.81	0.18	1.03	2.03	1.61	0.25	1.28	1.8	1.58	0.13
Gilka	1.53	1.83	1.65	0.08	1.1	2.68	1.79	0.45	0.98	2.4	1.55	0.42	0.95	2.57	1.65	0.4	1.02	1.88	1.38	0.2
8369	2.28	3.6	2.86	0.45	2.28	2.93	2.59	0.19	2.43	3.35	2.78	0.23	2.58	3.51	3.05	0.25	1.5	2.13	1.89	0.16
11362	1.98	3.03	2.52	0.28	2.65	4.4	3.21	0.55	3.1	4.15	3.55	0.3	2.43	2.9	2.67	0.12	1.93	2.57	2.27	0.18
Bee Madam	1.29	1.84	1.57	0.14	1.18	1.73	1.53	0.14	1.31	1.75	1.64	0.1	1.21	1.92	1.64	0.18	0.99	1.73	1.36	0.21
Jomeo	1.45	2.26	1.74	0.28	1.41	1.71	1.56	0.08	1.3	1.92	1.67	0.17	1.36	2.03	1.68	0.18	1.32	2.53	1.66	0.29
2916	2.33	3.12	2.86	0.19	2.52	4.32	3.33	0.5	2.62	3.34	2.94	0.18	2.34	3.12	2.67	0.19	2.04	2.74	2.39	0.19
15235	1.79	3.24	2.29	0.38	1.82	2.64	2.05	0.24	2.1	2.64	2.26	0.17	1.78	2.27	2.09	0.13	1.6	2.1	1.88	0.13
15350	1.63	2.66	1.98	0.25	2.32	3.29	2.82	0.3	1.9	3.2	2.43	0.28	1.56	2.41	1.99	0.26	1.41	1.97	1.67	0.12
29073	2.29	3.44	2.65	0.37	1.82	3.01	2.51	0.41	1.91	2.5	2.12	0.16	1.73	2.28	2.02	0.12	1.65	2.33	2.02	0.23
37663	2.55	3.04	2.85	0.16	2.53	4.13	3.28	0.48	2.79	6.65	3.67	1.13	1.89	3.08	2.45	0.24	1.97	5.09	2.78	0.83
McBee	1.71	2.68	2.03	0.27	2.04	2.91	2.42	0.26	1.86	2.51	2.27	0.2	1.8	2.2	2.02	0.11	1.53	2.02	1.8	0.12
Melissa	1.73	2.21	1.97	0.11	1.5	2.19	1.79	0.19	1.48	2.36	1.79	0.23	1.4	2.02	1.73	0.19	1.19	1.54	1.34	0.1
OldFemale	1.48	2.68	1.74	0.3	1.79	3.72	2.37	0.56	1.63	3.55	2.44	0.55	1.48	2.13	1.96	0.14	1.22	2.02	1.62	0.23
Palias	1.48	2.32	2.03	0.24	1.62	2.31	1.92	0.21	1.7	2.5	2	0.23	1.31	2.13	1.7	0.23	1.32	1.66	1.44	0.08
Passion	1.44	1.9	1.7	0.14	1.53	2.49	2.09	0.33	1.64	2.24	2.02	0.17	1.71	2.32	1.88	0.14	1.25	3.37	1.82	0.48

Interspecific variability table: minimum, maximum, mean & standard deviation in mm for dorsal thickness in *P. t. schweinfurthii*																				
	MT1				MT2				MT3				MT4				MT5			
Specimen	Min	Max	Mean	SD	Min	Max	Mean	SD	Min	Max	Mean	SD	Min	Max	Mean	SD	Min	Max	Mean	SD
Charlie	2.5	3.5	2.89	0.27	1.97	3.2	2.83	0.4	1.6	3.38	2.63	0.53	1.83	2.58	2.19	0.19	2	2.43	2.25	0.11
7426	1.7	2.43	1.98	0.19	1.67	3.27	2.49	0.39	1.47	2.43	1.9	0.25	1.43	2.08	1.8	0.17	1.43	2.18	1.8	0.25
8341	2	2.65	2.34	0.22	1.68	3.06	2.4	0.41	1.94	2.6	2.27	0.18	1.98	2.55	2.2	0.14	1.57	2.07	1.87	0.13
14579	2.19	3.17	2.66	0.35	2.16	3.76	3.19	0.53	1.99	3.65	2.91	0.52	1.99	2.95	2.76	0.23	1.76	2.73	2.43	0.23
29074	2.58	3.28	2.94	0.24	1.92	3.9	2.98	0.62	1.49	3.77	3.05	0.64	2	3.56	2.94	0.5	2.06	2.93	2.49	0.25
30845	2.18	2.47	2.31	0.1	1.8	3.47	2.69	0.51	1.76	3.29	2.53	0.49	2.1	2.8	2.51	0.19	1.47	3.17	2.44	0.44
Flo	1.47	1.9	1.69	0.14	1.3	2.79	1.99	0.53	1.17	2.5	1.74	0.34	1.28	1.88	1.67	0.15	1.23	2	1.62	0.23
Gilka	1.08	1.98	1.56	0.29	1.3	2.15	1.67	0.19	1.38	1.9	1.71	0.14	1.37	2.12	1.72	0.22	1.05	1.5	1.27	0.12
8369	2.3	3.25	2.69	0.27	2.35	3.33	2.89	0.3	2.1	3.38	2.6	0.34	2.28	3.49	2.78	0.33	1.65	2.5	2.15	0.23
11362	2.15	2.75	2.5	0.16	1.9	3.93	3	0.62	2.28	3.7	2.99	0.32	1.68	2.95	2.6	0.37	1.47	2.62	2.12	0.25
Bee Madam	1.29	1.88	1.5	0.15	1.12	2.3	1.83	0.36	1.12	1.8	1.42	0.22	1.19	1.91	1.53	0.19	1.18	1.43	1.28	0.07
Jomeo	1.4	2.63	1.91	0.39	1.11	2.67	1.81	0.37	1.3	2.38	1.68	0.33	1.36	1.76	1.55	0.12	1.28	1.79	1.64	0.12
2916	2.9	3.79	3.19	0.21	2.56	5.2	3.71	0.87	2.4	3.85	3.3	0.35	2.43	3.29	3.04	0.23	1.96	2.76	2.54	0.18
15235	2.11	2.58	2.35	0.15	1.82	3.3	2.47	0.52	1.8	2.9	2.31	0.33	1.6	2.49	2.06	0.25	1.42	2.21	1.79	0.26
15350	2.17	2.46	2.32	0.09	2.16	3.59	2.89	0.48	1.74	2.83	2.43	0.29	1.66	2.45	2.16	0.18	1.45	2.05	1.72	0.17
29073	2.73	3.23	2.96	0.14	1.62	3.52	2.9	0.6	2.03	2.95	2.47	0.24	1.89	2.49	2.23	0.13	1.7	2.48	2.18	0.21
37663	3.1	4.17	3.49	0.3	2.46	4.32	3.38	0.59	2.42	3.28	2.94	0.21	2.01	3.39	2.86	0.31	1.75	3.45	2.5	0.47
McBee	1.44	2.22	1.95	0.23	1.65	3.07	2.58	0.4	1.47	2.55	2.15	0.36	1.41	2.31	2.06	0.24	1.41	2.12	1.79	0.17
Melissa	1.69	2.21	1.93	0.13	1.38	2.48	1.9	0.42	1.3	2.5	1.82	0.38	1.16	1.91	1.65	0.19	1.19	1.82	1.52	0.18
OldFemale	1.49	2.14	1.96	0.16	1.29	3.46	2.35	0.58	1.79	3.07	2.43	0.35	1.38	2.17	1.84	0.17	1.22	1.97	1.7	0.23
Palias	1.79	2.23	2.06	0.13	1.62	2.79	2.41	0.34	1.18	3.13	2.27	0.62	1.31	1.93	1.74	0.13	1.12	1.73	1.52	0.17
Passion	1.48	2.36	1.86	0.21	1.59	2.63	2.23	0.39	1.31	2.61	2.02	0.37	1.44	2.06	1.84	0.17	1.11	2.83	1.72	0.46

Interspecific variability table: minimum, maximum, mean & standard deviation in mm for medial thickness in *P. t. schweinfurthii*																				
	MT1				MT2				MT3				MT4				MT5			
Specimen	Min	Max	Mean	SD	Min	Max	Mean	SD	Min	Max	Mean	SD	Min	Max	Mean	SD	Min	Max	Mean	SD
Charlie	1.95	3.1	2.38	0.32	2.22	2.93	2.63	0.24	1.73	2.13	2.03	0.1	1.75	2.5	2.27	0.21	2	2.7	2.4	0.24
7426	1.7	2.7	2.37	0.26	1.5	2.73	2.16	0.36	1.33	2	1.76	0.16	1.2	2.85	2.17	0.49	1.35	2.05	1.73	0.21
8341	1.9	2.6	2.25	0.21	1.84	2.56	2.34	0.18	1.64	2.37	2.1	0.21	1.59	2.31	2.09	0.18	1.7	2.17	1.99	0.14
14579	2.18	3.7	2.77	0.49	2.37	3.64	2.97	0.44	1.57	2.76	2.39	0.35	1.73	2.92	2.48	0.36	1.87	2.67	2.42	0.21
29074	2.23	2.96	2.66	0.23	2.28	3.3	2.81	0.34	1.65	2.48	2.17	0.25	1.54	3.25	2.52	0.51	1.72	2.76	2.31	0.26
30845	2.07	2.99	2.44	0.26	1.97	3.3	2.69	0.49	1.64	3.85	2.63	0.67	1.43	2.53	2.23	0.31	1.7	2.6	2.34	0.29
Flo	1.33	1.8	1.59	0.13	1.3	2.27	1.87	0.33	1.1	1.7	1.39	0.18	1.2	1.85	1.61	0.18	1.4	1.98	1.72	0.18
Gilka	1.2	1.58	1.45	0.11	1.23	1.93	1.57	0.22	1.13	1.97	1.48	0.18	1.13	2	1.73	0.21	1.27	2	1.55	0.22
8369	1.83	3.83	2.23	0.49	2.4	3.5	2.93	0.27	1.65	2.6	2.23	0.22	1.79	2.69	2.34	0.2	1.73	2.55	2.2	0.25
11362	2.05	2.88	2.47	0.25	2	3.23	2.64	0.34	1.7	2.48	2.18	0.19	1.73	3.4	2.59	0.43	1.8	2.9	2.37	0.24
Bee Madam	1.31	1.92	1.56	0.18	1.18	1.8	1.59	0.17	1.22	1.51	1.37	0.08	1.02	1.81	1.5	0.18	1.19	1.51	1.38	0.09
Jomeo	1.47	2.47	1.95	0.29	1.58	2.2	1.96	0.19	1.37	1.85	1.69	0.13	1.22	2.16	1.76	0.31	1.41	1.91	1.77	0.13
2916	2.44	3.17	2.84	0.23	2.64	3.68	3.16	0.33	2.08	3.22	2.73	0.3	1.92	3.14	2.78	0.35	2.02	2.81	2.59	0.2
15235	1.78	2.28	2.03	0.17	1.76	2.6	2.14	0.28	1.58	1.99	1.78	0.12	1.52	2.72	2.09	0.38	1.48	2.5	2.01	0.29
15350	1.75	3.06	2.14	0.32	2.31	3.31	2.77	0.38	1.44	2.13	1.85	0.2	1.43	2.32	2.04	0.25	1.43	2.51	1.92	0.33
29073	2.69	3.1	2.84	0.14	2.18	3.22	2.62	0.3	1.61	2.5	2.12	0.27	1.7	2.68	2.23	0.32	1.54	2.58	2.23	0.26
37663	2.66	3.66	3.2	0.33	2.36	3.49	3.01	0.34	1.89	2.58	2.24	0.21	1.98	2.99	2.58	0.28	1.94	3.57	2.63	0.49
McBee	1.31	2.51	1.88	0.31	1.65	2.59	2.24	0.25	1.4	2.12	1.91	0.23	1.42	2.5	2.06	0.32	1.58	2.4	2.06	0.21
Melissa	1.59	2.03	1.83	0.12	1.49	2.5	1.92	0.34	1.22	1.79	1.45	0.13	1.3	1.98	1.71	0.18	1.12	1.92	1.53	0.22
OldFemale	1.6	2.2	1.87	0.22	1.49	3.42	2.33	0.63	1.08	1.81	1.6	0.2	1.09	2.72	2.05	0.49	1.1	2.23	1.84	0.3
Palias	1.6	2.1	1.97	0.13	1.59	2.3	1.97	0.2	1.21	1.77	1.59	0.12	1.12	2.24	1.79	0.3	1.3	2.02	1.77	0.2
Passion	1.41	2.2	1.8	0.19	1.29	2.3	1.89	0.3	1.04	1.62	1.46	0.15	1.06	2.61	1.84	0.49	1.2	2.16	1.74	0.28

Interspecific variability table: minimum, maximum, mean & standard deviation in mm for lateral thickness in *P. t. schweinfurthii*																				
	MT1				MT2				MT3				MT4				MT5			
Specimen	Min	Max	Mean	SD	Min	Max	Mean	SD	Min	Max	Mean	SD	Min	Max	Mean	SD	Min	Max	Mean	SD
Charlie	1.87	2.6	2.43	0.22	2.1	2.65	2.42	0.18	1.83	2.35	2.18	0.13	1.83	2.7	2.22	0.27	1.8	3.28	2.53	0.43
7426	1.43	2.1	1.88	0.15	1.5	2.53	2.03	0.29	1.27	2.53	1.95	0.35	1.25	2.2	1.82	0.26	1.18	2.7	1.92	0.43
8341	1.9	2.5	2.19	0.18	1.58	2.37	2.06	0.25	1.74	2.4	2.13	0.19	1.47	2.4	2.07	0.23	1.7	3.3	2.15	0.48
14579	2.33	2.98	2.57	0.19	2.01	3.97	3.02	0.54	1.57	2.85	2.42	0.38	1.99	3.01	2.51	0.32	1.95	3.07	2.5	0.34
29074	2.23	4.06	2.71	0.49	2.1	2.97	2.59	0.27	1.72	2.38	2.08	0.22	1.48	2.49	2.11	0.31	1.72	3.01	2.48	0.43
30845	2	2.4	2.26	0.11	1.9	3.13	2.58	0.37	1.38	2.88	2.28	0.42	1.7	2.63	2.22	0.3	1.7	4.03	2.57	0.64
Flo	1.43	2.4	1.84	0.31	1.4	2	1.68	0.19	1.13	1.7	1.47	0.17	1.13	1.93	1.59	0.22	1.2	2.2	1.75	0.28
Gilka	1.48	1.98	1.76	0.14	1.15	1.48	1.34	0.09	1.03	1.57	1.19	0.11	1.1	1.78	1.49	0.15	1.2	1.5	1.36	0.08
8369	1.95	2.9	2.41	0.32	2.23	2.68	2.47	0.11	1.78	2.28	2.04	0.13	1.83	2.39	2.15	0.14	1.8	3.75	2.55	0.47
11362	2.15	2.83	2.47	0.16	2.23	2.68	2.41	0.12	1.8	2.73	2.36	0.23	1.8	2.73	2.34	0.26	1.67	3.85	2.94	0.65
Bee Madam	1.4	2.01	1.73	0.16	1.33	1.8	1.54	0.15	1.09	1.75	1.46	0.17	1.26	1.73	1.54	0.14	1.11	1.61	1.4	0.13
Jomeo	1.4	2.37	1.88	0.24	1.41	1.91	1.72	0.13	1.21	2.03	1.67	0.26	1.28	2.27	1.89	0.32	1.38	2.24	1.92	0.29
2916	2.73	3.43	3.1	0.23	2.37	3.51	3.06	0.34	1.92	3.07	2.4	0.28	2	3.67	2.78	0.51	2.01	4.03	2.87	0.62
15235	1.72	1.93	1.83	0.06	1.61	2.19	1.92	0.15	1.53	2.02	1.79	0.14	1.35	2.51	1.93	0.33	1.51	2.51	1.98	0.39
15350	2.29	2.59	2.42	0.09	2.49	3.97	2.85	0.34	1.61	2.09	1.93	0.11	1.57	2.22	1.95	0.18	1.65	2.83	2.03	0.33
29073	2.42	3.06	2.8	0.19	1.79	2.89	2.29	0.34	1.58	2.5	2.13	0.26	1.76	2.4	1.95	0.17	1.75	2.81	2.45	0.34
37663	2.52	3.17	2.87	0.21	2.13	2.96	2.65	0.23	1.68	2.58	2.26	0.2	2.11	2.92	2.59	0.23	1.82	3.61	3	0.51
McBee	2.09	2.4	2.23	0.09	1.74	2.4	2.08	0.2	1.16	2.74	2.1	0.42	1.41	2.61	2.01	0.37	1.2	2.89	2.02	0.48
Melissa	1.49	2.39	1.96	0.26	1.3	1.77	1.57	0.13	1.09	1.83	1.55	0.2	1.29	2.18	1.71	0.29	1.12	2.19	1.62	0.31
OldFemale	1.71	2.48	1.97	0.21	1.49	2.03	1.78	0.15	1.08	2.04	1.68	0.24	1.3	2.62	2.05	0.44	1.18	2.53	2.03	0.44
Palias	1.79	2.22	2.02	0.13	1.62	2.13	1.93	0.14	1.24	2.11	1.63	0.26	1.11	1.91	1.59	0.23	1.12	2.42	1.7	0.29
Passion	1.81	2.21	2.01	0.13	1.29	2.32	1.87	0.3	1.01	1.91	1.72	0.23	1.01	2.2	1.69	0.36	1	3.25	1.84	0.64

Interspecific Variability Table showing minimum, maximum, mean and standard deviation in mm for curvature values in *P. t. schweinfurthii* .																				
	MT1				MT2				MT3				MT4				MT5			
Specimen	Min	Max	Mean	SD	Min	Max	Mean	SD	Min	Max	Mean	SD	Min	Max	Mean	SD	Min	Max	Mean	SD
Charlie	-0.76	0.84	0.37	0.49	-1.55	0.85	0.18	0.71	-2.02	-0.11	-0.67	0.64	-2.13	0.35	-0.26	0.69	-1.54	-0.13	-0.63	0.42
7426	-1.91	-0.73	-1.08	0.39	-1.89	3.94	2.75	1.38	-2.09	2.2	0.94	1.31	-1.44	1.91	1.01	0.85	-0.79	1.02	0.35	0.61
8341	-2.65	-0.62	-1.29	0.61	-1.5	1.71	0.78	0.89	-2.9	0.24	-0.48	0.79	-3.35	-1.47	-1.96	0.49	-2.3	-1.09	-1.51	0.33
14579	-2.38	-1.37	-1.74	0.35	-0.26	2.13	1.35	0.78	-4.35	-0.95	-1.83	0.95	-2.78	0.83	-0.13	1.04	-1.73	0.87	0.13	0.74
29074	-1.34	0.27	-0.19	0.46	-1.06	2.56	1.61	1.09	-2.92	0.52	-0.32	0.88	-2.56	0.16	-0.43	0.72	-5.42	-2.25	-3.09	0.95
30845	-2.82	-0.52	-1.09	0.69	-0.55	2.28	1.21	1	-3.3	0.84	-0.28	1.17	-2.13	1.15	0.17	0.99	-2.62	-0.47	-1.15	0.64
Flo	-0.98	0.23	-0.14	0.36	-0.12	1.85	1.2	0.66	-3.53	-0.82	-1.5	0.78	-2.74	0.94	0.13	0.95	-1.68	-0.06	-0.52	0.45
Gilka	-0.67	1.72	1.08	0.74	-2.99	0.29	-0.48	0.88	-2.36	0.45	-0.23	0.76	-2.08	0.92	0.23	0.78	-2.02	-0.31	-0.81	0.52
8369	-4.66	-2.95	-3.45	0.5	-0.67	1.87	0.96	0.81	-1.83	0.71	-0.08	0.76	-2.85	0.14	-0.65	0.83	-2.48	-0.14	-0.94	0.59
11362	-2.2	-0.72	-1.16	0.46	0.15	2.92	2.04	0.85	0	2.28	1.04	0.54	-1.71	2	1.14	1.04	-1.45	1.09	0.38	0.66
Bee Madam	-1.84	1.08	0.28	0.93	-2.14	-0.33	-0.77	0.54	-3.04	-1.03	-1.56	0.54	-2.39	-0.78	-1.28	0.47	-2.08	-0.99	-1.31	0.3
Jomeo	-2.57	-0.27	-0.86	0.69	-1.19	0.79	0.16	0.66	-4.17	-1.29	-1.99	0.77	-4.7	-1	-1.86	1.01	-3.74	-1.14	-1.76	0.7
2916	-1.57	-0.19	-0.62	0.41	-0.14	3.29	2.31	1.04	-2.7	1.21	0.34	1.07	-2.46	0.64	-0.05	0.84	-2.89	-0.11	-0.82	0.7
15235	-2.8	-1.94	-2.22	0.22	-1.81	0.81	0.2	0.76	-2.39	-0.02	-0.62	0.64	-0.49	1.22	0.69	0.48	-0.91	0.82	0.3	0.48
15350	-2.35	-0.83	-1.42	0.5	0.11	2.58	1.8	0.73	-2.45	1.63	0.72	1.12	-2.56	-0.66	-1.24	0.64	-2.12	0.48	-0.31	0.78
29073	-2.62	-1.23	-1.7	0.43	-1.36	1.05	0.36	0.73	-1.3	2.12	1.15	0.95	-1.94	0.81	0.08	0.77	-0.63	0.87	0.44	0.47
37663	-1.85	0.18	-0.51	0.63	-0.89	1.97	1.14	0.86	-5.24	0.92	-0.53	1.88	-3.43	-0.36	-1.09	0.82	-1.9	1.92	1.08	1.07
McBee	-3.18	-1.07	-1.84	0.68	-0.5	1.59	0.91	0.68	-3.99	0.71	-0.38	1.27	-2.83	0.45	-0.4	0.91	-1.86	-0.44	-0.89	0.46
Melissa	-2.83	-0.21	-0.84	0.76	-0.06	2.66	1.83	0.8	-1.45	1.35	0.52	0.8	-2.03	1.15	0.23	0.97	-1.34	0.54	0.05	0.53
OldFemale	-1.9	-0.41	-0.88	0.46	-2.35	1.37	0.29	1.11	-4.12	0.02	-1.03	1.22	-2.01	0.29	-0.42	0.7	-1.72	0.89	0.22	0.72
Palias	-2.64	-1.67	-1.99	0.33	-1.18	0.84	0.28	0.62	-3.27	-0.45	-1.16	0.78	-3.22	-0.31	-1.01	0.81	-2.14	-0.47	-0.91	0.48
Passion	-2.06	-0.78	-1.13	0.41	-0.66	1.13	0.6	0.56	-4.09	-0.56	-1.28	0.91	-2.14	0.95	0.16	0.85	-1.14	2.87	1.21	1.24

APPENDIX B: Intraobserver error values table

Intraobserver error study: *Pan schweinfurthii*																										
Specimen	CS	MT1					MT2					MT3					MT4					MT5				
Charlie	0	1.812	3.12	2.465	1.87	-0.75	2.567	3.11	2.715	2.483	-1.54	3.45	3.274	2.075	2.176	-2	1.6	1.823	2.4	2.423	-1.04	1.718	2.2	2.082	3.282	-1.26
Charlie	1	2.132	3	2.767	2.35	-0.36	2.6332	3.1166	2.8168	2.484	-1.265	3.476	3.36	2.05	2.1	-1.72	1.8	1.87	2.475	2.6	-0.75	1.818	2.3	2.265	3.116	-1.15
Charlie	2	2.033	2.94	2.6	2.55	-0.2	2.52	3.116	2.717	2.617	-0.831	3.5	3.374	2.1	2.25	-1.3	2.1	2	2.475	2.7	-0.45	1.982	2.216	2.332	3.034	-0.95
Charlie	3	2.2	2.79	2.48	2.579	-0.07	2.617	3.117	2.8167	2.633	-0.541	3.4	3.326	2.126	2.35	-1.02	2.1	1.977	2.5	2.523	-0.25	1.9	2.434	2.532	3.083	-0.86
Charlie	4	2.48	2.83	2.36	2.39	0.03	2.617	3	2.81	2.6333	-0.25	3.324	3.224	2.126	2.326	-0.74	1.95	2	2.45	2.525	-0.08	1.982	2.25	2.582	2.9	-0.65
Charlie	5	2.54	3.04	2.26	2.4	0.23	2.917	3.11	2.9333	2.66	-0.045	3.15	2.924	2.025	2.275	-0.51	1.975	2.077	2.5	2.5	0.13	2.084	2.3	2.651	2.85	-0.55
Charlie	6	2.457	3.32	2.27	2.657	0.42	2.92	3.12	2.8833	2.4844	0.134	3.2	2.85	2.124	2.125	-0.41	2.13	2.16	2.5	2.4	0.23	2.05	2.316	2.618	2.7	-0.45
Charlie	7	2.21	3.4	2.35	2.49	0.57	2.92	3.11	2.91	2.6167	0.355	3.1	2.825	2.05	2.226	-0.22	2.15	2.2	2.4	2.4	0.347	1.982	2.3	2.666	2.682	-0.34
Charlie	8	2.22	2.81	2.31	2.62	0.66	2.8	3.21	2.89	2.4833	0.543	3.075	2.8	2.075	2.176	-0.22	2.225	2.25	2.37	2.3	0.34	2.034	2.35	2.6	2.682	-0.35
Charlie	9	2.21	3.156	2.15	2.67	0.83	2.72	3.12	2.8	2.61	0.67	3.074	2.725	2.05	2.225	-0.12	2.27	2.37	2.425	2.3	0.34	2	2.316	2.7	2.584	-0.24
Charlie	10	2.24	2.91	2.1	2.57	0.85	2.74	3.22	2.87	2.54	0.78	2.924	2.726	2.1	2.226	-0.12	2.325	2.275	2.31	2.2	0.35	2.017	2.282	2.6	2.6	-0.15
Charlie	11	2.17	2.67	1.97	2.68	0.87	2.63	3.135	2.67	2.41	0.86	2.85	2.576	1.95	2.2	-0.11	2.3	2.325	2.3	2.17	0.34	2.015	2.282	2.618	2.5	-0.15
Charlie	12	2.2	2.56	2	2.61	0.84	2.44	2.98	2.64	2.32	0.87	2.974	2.6	2.05	2.326	-0.12	2.475	2.225	2.2	2	0.25	2.032	2.3	2.484	2.482	-0.13
Charlie	13	2.1	2.66	2.16	2.46	0.85	2.55	2.84	2.6	2.38	0.86	2.95	2.475	2.1	2.25	-0.11	2.375	2.2	2.125	2	0.15	2.016	2.316	2.5	2.382	-0.25
Charlie	14	1.95	2.55	2.41	2.34	0.76	2.55	2.73	2.5167	2.28	0.85	2.674	2.3	2.125	2.225	-0.11	2.325	2.25	2.125	1.926	0.15	2.116	2.366	2.416	2.316	-0.32
Charlie	15	2.12	2.51	2.94	2	0.51	2.4	2.6	2.4	2.1	0.756	2.7	2.326	2	2.25	-0.22	2.375	2.2	2.2	1.929	-0.06	2.232	2.332	2.234	2.1	-0.45
Charlie	16	2.1	3.05	3.1	2.17	0.35	2.2833	2.533	2.3	2.2	0.64	2.775	2.175	2.075	2.174	-0.32	2.627	2.375	2.126	2.025	-0.25	2.316	2.216	2.182	2.1	-0.54
Charlie	17						2.216	2.3	2.3	2.183	0.53	2.6	2	1.95	2.15	-0.52	2.4	2.4	2.1	2.027	-0.54	2.3	2.182	2.116	1.982	-0.74
Charlie	18						2.316	2.216	2.4	2.183	0.25	2.55	1.876	1.924	2.076	-0.82	2.425	2.577	2.025	2.025	-0.94	2.215	2.032	2.1	1.982	-0.92
Charlie	19						2.283	2.05	2.266	2.3	0.04	2.65	1.85	1.85	1.876	-1.29	2.476	2.325	1.9	1.825	-1.56	2.232	2	2	2	-1.27
Charlie	20						2.266	1.966	2.22	2.2	0.27	2.45	1.6	1.725	1.824	-2.02	2.775	2.075	1.75	1.826	-2.13	2.084	2.018	2.017	1.8	-1.54

Intraobserver error study: *Pan schweinfurthii*																										
Specimen	CS	MT1					MT2					MT3					MT4					MT5				
7426_#27	0	1.744	1.82	1.71	1.432	-1.911	2.6	2.867	2.367	2.233	1.62	2.066	1.966	1.934	2.534	0.9	1.5	1.927	2.65	2.2	0.42	1.6	1.9	1.874	2.7	-0.6
7426_#28	1	1.766	2.01	1.92	1.668	-1.65	2.533	2.8	2.367	2.233	2.13	1.967	1.866	1.9	2.4	1.19	1.6	2	2.8	2.2	0.61	1.725	1.95	1.95	2.55	-0.38
7426_#29	2	1.832	2.03	2.233	1.766	-1.25	2.4	2.933	2.433	2.233	2.53	1.867	1.93	1.9	2.233	1.49	1.65	2.077	2.8	2.176	0.91	1.8	2.074	1.925	2.425	-0.19
7426_#30	3	1.866	2.13	2.12	1.932	-1.021	2.3	3.267	2.5	2.367	2.94	2.066	2.066	2	2.234	1.79	1.85	2.024	2.8	2.075	1.13	1.724	2.076	2	2.075	0.11
7426_#31	4	1.868	2.07	2.266	1.867	-0.931	2.3	2.467	2.5	2.433	3.22	2.033	2.233	1.9	2.166	1.99	1.876	2.077	2.85	2.05	1.33	1.9	1.95	2.052	1.95	0.22
7426_#32	5	1.866	1.87	2.434	2.034	-0.732	2.3	2.5	2.733	2.533	3.43	1.966	2.434	1.866	2.168	2.1	1.975	1.925	2.674	1.86	1.51	1.925	2.175	1.876	2.1	0.42
7426_#33	6	1.81	2.23	2.566	1.91	-0.743	2.333	2.467	2.667	2.233	3.73	2.033	2.333	1.9	2.232	2.1	2	1.85	2.475	1.85	1.62	1.925	2.1	1.85	2.6	0.61
7426_#34	7	1.832	2.43	2.61	1.867	-0.74	2.267	2.333	2.533	2.2	3.82	2.066	2.1	1.833	2.232	2.2	1.925	1.85	2.425	2.04	1.71	1.925	1.926	1.856	2.324	0.7
7426_#35	8	1.8	2.03	2.467	1.867	-0.74	2.167	2.967	2.367	2.1	3.94	2.067	2	1.832	2.132	2.1	2.05	1.827	2.325	1.9	1.8	1.95	1.974	1.75	2.075	0.8
7426_#36	9	1.9	1.87	2.332	1.933	-0.73	2.2	2.5	2.333	2.133	3.94	1.967	1.967	1.8	2.066	1.98	2.1	1.85	2.25	1.925	1.91	1.9	1.974	1.824	1.974	0.91
7426_#37	10	1.933	1.87	2.6	1.933	-0.74	2.167	2.6	2.133	2.133	3.94	2	1.9	1.732	2.066	1.887	2.05	1.775	2.176	1.85	1.8	1.924	1.925	1.85	1.8	0.91
7426_#38	11	1.933	2	2.7	1.933	-0.84	2.033	2.533	2.1	1.967	3.82	1.932	1.967	1.766	1.932	1.68	2.026	1.8	2.125	1.75	1.71	1.85	1.825	1.75	1.876	1.02
7426_#39	12	1.966	2.1	2.51	1.91	-0.93	1.9	2.467	2.033	1.967	3.63	1.732	1.8	1.766	2	1.49	2	1.75	2.026	1.75	1.6	1.674	1.7	1.7	1.85	1
7426_#40	13	1.933	2	2.5	1.933	-1.021	2.033	2.533	1.967	1.9	3.4	1.832	1.732	1.733	1.766	1.2	1.975	1.6	1.876	1.75	1.52	1.65	1.676	1.7	1.8	1
7426_#41	14	2.167	1.8	2.467	1.867	-1.24	2.1	2.633	1.933	1.9	3.24	2	1.8	1.7	1.7	0.87	1.876	1.725	1.775	1.725	1.33	1.7	1.626	1.65	1.85	0.9
7426_#42	15	1.967	1.7	2.433	2.033	-1.42	2	2.433	1.933	1.8	2.91	2.03	1.7	1.566	1.7	0.38	1.75	1.825	1.725	1.725	1.02	1.55	1.675	1.55	1.626	0.71
7426_#43	16	2.2	1.77	2.532	2.1	-1.73	2.067	2.4	1.8	1.833	2.64	2.2	1.733	1.7	1.632	-0.14	1.827	1.7	1.7	1.6	0.71	1.6	1.5	1.576	1.525	0.61
7426_#44	17						1.967	2.167	1.767	1.633	2.23	2.1	1.7	1.566	1.633	-0.84	1.95	1.625	1.677	1.57	0.52	1.55	1.45	1.5	1.4	0.234
7426_#45	18						1.867	1.967	1.733	1.667	1.6	2.232	1.532	1.632	1.467	-1.47	1.875	1.7	1.67	1.5	0.01	1.555	1.426	1.4	1.31	-0.19
7426_#46	19						1.833	1.733	1.567	1.567	0.91	2.1	1.667	1.5	1.3	-2.09	1.75	1.56	1.554	1.4	-0.48	1.574	1.425	1.35	1.376	-0.79
7426_#47	20						2.067	1.667	1.5	1.5	-1.89	2	1.466	1.332	1.266	-0.99	1.75	1.425	1.2	1.257	-1.44	1.95	1.456	1.35	1.174	-0.7

Intraobserver error study: *Pan paniscus*																										
Specimen	CS	MT1					MT2					MT3					MT4					MT5				
15296_P58	0	1.526	1.575	1.8	1.675	-2.14	1.71	2.433	2.067	1.817	0.59	1.871	2.11	1.6	1.571	-0.11	1.151	1.667	1.6	1.582	-0.05	1.182	1.317	1.282	1.783	0.08
15296_P59	1	1.626	1.675	1.9	1.75	-1.732	1.783	2.332	2.082	1.817	1.08	1.9	2.2	1.632	1.582	0.291	1.517	1.481	1.7	1.717	0.461	1.216	1.31	1.62	1.551	0.34
15296_P60	2	1.95	1.51	1.31	1.65	-1.55	0.024	2.367	2.1	1.834	1.59	1.816	2.382	1.532	1.633	0.68	1.433	1.532	1.9	1.751	0.79	1.152	1.167	1.682	1.6	0.64
15296_P61	3	1.9	1.4	1.325	1.776	-1.36	1.583	2.317	2.117	1.767	1.981	1.75	2.167	1.55	1.51	0.98	1.483	1.633	1.933	1.717	1.081	1.216	1.35	1.716	1.5	0.96
15296_P62	4	1.7	1.375	1.576	1.8	-1.16	1.61	2.4	2.3	1.783	2.4	1.75	2.134	1.483	1.617	1.17	1.553	1.6	1.882	1.683	1.2	1.266	1.517	1.782	1.91	1.05
15296_P63	5	1.424	1.41	1.925	2.075	-1.06	1.767	2.367	2.3	1.7	2.81	1.683	2	1.432	1.651	1.3	1.55	1.62	1.884	1.6	1.33	1.316	1.382	1.616	1.833	1.24
15296_P64	6	1.41	1.276	1.65	1.8	-0.978	1.683	2.182	2.15	1.832	3.081	1.566	1.811	1.35	1.6	1.49	1.6	1.417	1.882	1.6	1.53	1.333	1.45	1.45	1.751	1.26
15296_P65	7	1.725	1.325	1.4	1.7	-0.97	1.633	2.133	2.217	1.682	3.3	1.9	1.717	1.366	1.517	1.6	1.55	1.4	1.767	1.533	1.66	1.3	1.4	1.582	1.583	1.36
15296_P66	8	1.95	1.25	1.325	1.525	-1.071	1.7	2.116	2.183	1.682	3.5	1.767	1.7	1.232	1.6	1.7	1.767	1.533	1.781	1.617	1.75	1.21	1.552	1.415	1.483	1.36
15296_P67	9	2.026	1.5	1.126	1.426	-1.07	1.6	2.1	2.116	1.5	3.6	1.882	1.618	1.183	1.582	1.6	1.633	1.584	1.717	1.517	1.75	1.267	1.567	1.367	1.467	1.26
15296_P68	10	1.625	1.4	1.475	1.8	-1.178	1.683	2	1.983	1.632	3.69	1.632	1.717	1.217	1.633	1.6	1.832	1.45	1.682	1.483	1.75	1.417	1.482	1.5	1.616	1.26
15296_P69	11	1.575	1.275	1.524	2.126	-1.17	1.683	2.217	1.9	1.632	3.69	1.55	1.768	1.531	1.6	1.45	2	1.4	1.717	1.483	1.632	1.582	1.433	1.516	1.568	1.15
15296_P70	12	1.6	1.376	1.75	1.75	-1.26	1.7	2.033	1.917	1.683	3.69	1.917	1.583	1.483	1.557	1.43	1.917	1.367	1.584	1.433	1.46	1.617	1.252	1.55	1.566	1.05
15296_P71	13	1.8	1.35	1.176	1.65	-1.44	1.6	2.017	2	1.783	3.69	2.033	1.6	1.416	1.567	1.28	1.968	1.317	1.466	1.5	1.38	1.666	1.267	1.484	1.266	0.94
15296_P72	14	1.775	1.45	1.175	1.576	-1.67	1.583	1.867	1.8	1.583	3.61	1.95	1.483	1.482	1.583	1.17	1.867	1.45	1.6	1.533	1.261	1.65	1.267	1.366	1.3	0.85
15296_P73	15	1.95	1.35	1.024	1.75	-1.97	1.583	1.617	1.767	1.516	3.49	2.1	1.332	1.45	1.517	0.97	1.95	1.384	1.417	1.516	1.05	1.71	1.383	1.3	1.233	0.75
15296_P74	16	2.174	1.05	0.95	1.75	-2.284	1.582	1.382	1.816	1.516	3.39	2.15	1.317	1.282	1.6	0.86	1.82	1.51	1.6	1.482	0.84	1.7	1.41	1.282	1.217	0.66
15296_P75	17						1.766	1.584	1.684	1.65	3.1	2.033	1.3	1.283	1.45	0.45	1.982	1.35	1.534	1.332	0.78	1.85	1.3	1.283	1.151	0.56
15296_P76	18						1.85	1.6	1.7	1.517	2.81	2.033	1.183	1.333	1.432	0	2.115	1.367	1.31	1.267	0.371	1.783	1.283	1.232	1.167	0.38
15296_P77	19						1.9	1.417	1.517	1.417	2.5	1.867	1.317	1.1	1.168	-0.49	2.4	1.432	1.3	1.217	-0.15	1.617	1.284	1	0.983	0.17
15296_P78	20						1.733	1.266	1.45	1.466	2.2	1.682	1.1	1.2	1.217	-0.83	2.216	1.251	1.21	1.132	-0.86	1.733	1.117	1.05	0.933	0.15

Intraobserver error study: *Pan paniscus*																										
Specimen	CS	MT1					MT2					MT3					MT4					MT5				
20882_P56	0	1.77	2.487	2.01	1.69	-1.8	2.35	2.95	2.2	1.817	-1.49	2.55	2.632	1.966	1.91	-0.7	1.75	2.025	2.425	2.25	-1.231	1.374	1.925	1.926	2.271	-0.25
20882_P57	1	1.8	2.483	2	1.716	-1.48	2.217	2.882	2.217	1.934	-1.18	2.85	2.516	1.966	1.818	-0.39	1.926	2.05	2.474	2.32	-0.94	1.425	1.826	2.05	2.276	-0.62
20882_P58	2	1.783	2.4	2.081	1.883	-1.2	2.166	3.018	2.31	1.8	-0.88	2.832	2.555	1.867	1.866	-0.19	1.9	2.05	2.526	2.351	-0.74	1.51	1.8	1.875	1.925	-0.52
20882_P59	3	1.985	2.317	2.22	2.066	-1.06	2.267	2.75	2.4	1.884	-0.59	2.81	2.61	1.868	1.91	0.05	1.851	2.024	2.475	2.324	-0.74	1.5	1.82	1.876	1.925	-0.33
20882_P60	4	2.067	2.45	2.083	1.983	-0.91	2.333	2.733	2.351	1.95	-0.28	2.31	2.366	1.882	1.81	0.132	2.05	1.974	2.475	2.45	-0.67	1.525	1.925	1.775	1.97	-0.25
20882_P61	5	2.183	2.367	2.067	2.083	-0.776	2.217	2.667	2.266	1.917	-0.08	2.383	2.25	1.817	1.8	0.24	2.123	2.31	2.354	2.376	-0.54	1.825	1.95	1.75	1.853	-0.80
20882_P62	6	2.2	2.34	2.13	2.11	-0.77	2.15	2.634	2.2	1.851	0.11	2.466	2.21	1.982	1.666	0.24	2.076	2.2	2.325	2.326	-0.541	1.8	1.926	1.776	1.85	0.00
20882_P63	7	2	2.317	2.917	2.13	-0.77	2.2	2.7	2.283	1.81	0.3	2.518	2.252	1.968	1.683	0.341	1.95	2.076	2.174	2.325	-0.54	1.91	1.826	1.775	1.776	0.12
20882_P64	8	2.05	2.133	2	2.082	-0.77	2.166	2.6	2.183	1.8	0.4	2.71	2.252	1.832	1.784	0.43	2.05	1.975	2.076	2.325	-0.54	1.951	2.027	1.876	1.93	0.14
20882_P65	9	2.1	2.133	2.282	2.183	-0.77	2.2	2.6	2.083	1.783	0.62	2	2.267	1.8	1.883	0.45	2.226	2.024	2.1	2.326	-0.54	2.051	2.051	1.857	2.025	0.14
20882_P66	10	2.1	2.168	2.083	2.117	-0.88	2.282	2.5	2.117	1.683	0.7	1.932	2.252	1.733	1.866	0.45	2.225	1.975	2.253	2.2	-0.54	2.125	1.8	1.95	2.024	0.14
20882_P67	11	2.083	1.983	1.932	1.983	-0.99	2.451	2.382	2.1	1.634	0.81	2.216	2.167	1.868	1.917	0.45	2.375	2.126	2.225	2.2	-0.54	1.91	1.725	1.726	1.926	0.14
20882_P68	12	2.1	1.85	1.983	2.116	-1.07	2.583	2.183	2.1	1.6	0.911	2.652	2.24	1.91	1.82	0.45	2.41	2.325	2.225	2.075	-0.64	1.94	1.826	1.6	1.851	0.01
20882_P69	13	2.083	1.933	1.9	2.1	-1.298	2.8	2.267	1.983	1.6	0.99	2.1	2.15	1.85	1.933	0.44	2.35	1.876	2.126	2.05	-0.64	2.174	1.7	1.753	1.91	0.19
20882_P70	14	2.167	1.933	1.783	2.082	-1.5	2.683	2.317	2.233	1.667	1	2.42	2.066	2	1.816	0.35	2.351	2.126	2.1	2.112	-0.741	2.352	1.926	1.826	1.82	0.16
20882_P71	15	2.417	1.816	1.9	2	-1.67	2.333	1.933	2.117	1.9	1.13	2.432	2.382	1.9	1.716	0.35	2.224	2	1.81	1.824	-0.84	2.4	1.875	1.8	1.8	0.14
20882_P72	16	2.35	1.717	1.832	1.9	-1.88	2.467	1.9	2.05	1.855	1.12	2.467	2.367	1.7	1.715	0.351	2.375	1.9	1.875	1.725	-1.041	2.4	2.024	1.89	1.856	0.00
20882_P73	17						2.466	1.85	1.967	1.7	1.12	2.416	2.282	1.651	1.732	0.151	2.475	2.176	1.875	1.81	-1.14	2.276	1.876	1.777	1.724	-0.16
20882_P74	18						2.333	1.91	1.682	1.8	1.01	2.352	2.082	1.817	1.733	-0.05	2.474	2.1	2	1.876	-1.441	2.276	2.176	1.834	1.754	-0.41
20882_P75	19						2.35	1.883	1.717	1.766	0.82	2.317	2.083	1.617	1.816	-0.48	2.4	1.874	1.753	1.752	-1.752	2.326	1.924	1.62	1.624	-0.74
20882_P76	20						2.2	1.918	1.7	1.751	0.62	2.617	1.81	1.517	1.733	-0.86	2.026	1.625	1.674	1.71	-2.23	2.474	1.95	1.625	1.553	-1.16

Intraobserver error study: *Homo sapiens*																										
Specimen	CS	MT1					MT2					MT3					MT4					MT5				
A5_Euro	0	1.575	1.275	1.123	0.976	-6.94	2.554	2.277	1.75	1.474	-4.38	0.951	1.624	2.41	1.451	-3.21	0.952	1.626	2.4	1.455	-4.455	0.974	1.326	2.81	3.025	-3.31
A5_Euro	1	1.776	1.274	1.112	0.974	-6.36	2.25	2.324	2.174	1.35	-3.798	0.924	1.625	2.424	1.3	-2.42	0.925	1.624	2.424	1.3	-3.46	0.925	1.21	3.25	3.033	-3.23
A5_Euro	2	1.524	1.45	1.31	1.074	-5.75	2.21	2.34	2.26	1.575	-3.3	0.924	1.83	2.676	1.726	-1.72	0.926	1.826	2.677	1.726	-2.63	1.076	1.376	2.95	3.076	-2.94
A5_Euro	3	1.674	1.55	1.474	1.225	-5.25	2.274	2.5	2.5	1.876	-2.778	1.126	1.75	2.776	1.85	-1.311	1.126	1.751	2.776	1.855	-2.12	1.012	1.5	3.324	3.476	-2.64
A5_Euro	4	1.71	1.675	1.5	1.425	-4.88	2.11	2.552	2.624	1.8	-2.29	1.21	1.576	2.85	1.927	-0.99	1.21	1.576	2.85	1.924	-1.71	1.154	1.476	3.1	3.96	-2.3
A5_Euro	5	1.764	1.825	1.624	1.55	-4.49	2.054	2.55	2.824	1.724	-1.9	1.276	1.624	2.7	1.84	-0.76	1.276	1.626	2.7	1.856	-1.32	1.4	1.4	3.076	4.175	-2.23
A5_Euro	6	1.774	1.924	1.73	1.65	-4.221	2.124	2.41	2.774	1.576	-1.57	1.356	1.526	2.777	1.824	-0.481	1.3	1.526	2.776	1.826	-1.13	1.676	1.776	2.95	4.326	-2
A5_Euro	7	1.95	1.751	1.91	1.85	-3.92	1.976	2.2	2.674	1.6	-1.278	1.424	1.554	2.825	1.826	-0.382	1.426	1.556	2.826	1.824	-0.95	1.776	1.826	2.9	4.376	-1.94
A5_Euro	8	1.875	2	2	1.824	-3.72	1.876	2.26	2.625	1.725	-0.965	1.624	1.575	2.635	1.826	-0.29	1.626	1.576	2.634	1.826	-0.82	1.776	1.676	2.65	4.326	-1.83
A5_Euro	9	1.851	2	2.124	1.975	-3.561	1.97	2.225	2.752	1.475	-0.8	1.6	1.45	2.375	1.75	-0.3	1.645	1.455	2.376	1.751	-0.71	1.71	1.7	2.327	4	-1.72
A5_Euro	10	1.774	2.25	2.051	1.951	-3.47	1.923	2.374	2.774	1.575	-0.68	1.576	1.53	2.5	1.81	-0.29	1.576	1.5	2.5	1.8	-0.72	1.676	1.8	2.1	3.526	-1.72
A5_Euro	11	1.75	2.174	2.174	2.175	-3.271	2	2.176	2.65	1.454	-0.68	1.653	1.524	2.35	1.654	-0.4	1.654	1.524	2.356	1.645	-0.63	1.674	1.464	2.025	3.025	-1.72
A5_Euro	12	1.651	2.1	2.25	2.35	-3.27	1.776	2.076	2.276	1.375	-0.58	1.65	1.474	2.225	1.375	-0.5	1.654	1.473	2.226	1.374	-0.64	1.726	1.174	2.1	2.89	-1.71
A5_Euro	13	1.65	2.276	2.3	2.512	-3.27	1.9	1.974	2.275	1.223	-0.7	1.64	1.5	2.263	1.453	-0.49	1.6	1.5	2.262	1.443	-0.64	1.7	1.3	2.176	2.676	-1.59
A5_Euro	14	1.625	2.075	2.251	2.425	-3.271	1.974	1.775	2.212	1.276	-0.77	1.454	1.44	1.926	1.376	-0.59	1.456	1.4	1.926	1.376	-0.63	1.474	1.525	1.926	2.376	-1.61
A5_Euro	15	1.733	1.851	2.351	2.425	-3.36	1.924	1.574	1.926	1.3	-0.877	1.574	1.375	1.824	1.455	-0.68	1.574	1.375	1.826	1.456	-0.72	1.557	1.224	1.754	2.356	-1.72
A5_Euro	16	1.75	1.95	2.5	2.674	-3.56	1.976	1.376	1.75	1.275	-1.08	1.54	1.276	1.656	1.155	-0.89	1.5	1.274	1.656	1.15	-0.82	1.6	1.24	1.756	1.9	-1.82
A5_Euro	17						1.75	1.225	1.526	1.254	-1.26	1.55	1.224	1.613	1.126	-1.08	1.554	1.224	1.61	1.124	-0.9	1.6	1.1	1.676	1.76	-1.921
A5_Euro	18						1.825	1.061	1.35	1.025	-1.52	1.524	0.924	1.474	1.15	-1.38	1.526	0.926	1.476	1.157	-1.22	1.5	1.1	1.626	1.456	-2.021
A5_Euro	19						1.652	0.91	1.172	1.025	-1.97	1.589	0.775	1.35	0.926	-1.8	1.59	0.777	1.34	0.925	-1.7	1.374	0.924	1.6	1.051	-2.211
A5_Euro	20						1.575	0.81	1.051	0.876	-2.67	1.325	0.75	1.252	0.95	-2.212	1.326	0.75	1.253	0.96	-2.61	1.2	1.026	1.424	0.8	-2.523

Intraobserver error study: *Homo sapiens*																										
Specimen	CS	MT1					MT2					MT3					MT4					MT5				
A8_Soto	0	1.166	1.567	1.432	0.91	-6.65	1.267	1	1.967	1.267	-5.876	1.051	0.975	1.974	1.55	-4.65	0.33	1.233	2.566	2.3	-4.989	0.9	1.21	2.666	2.868	-5.788
A8_Soto	1	1	1.833	1.533	1.212	-6.36	1.267	1.368	2.2	1.668	-5.46	1	1.026	1.71	1.976	-4.33	0.41	1.1	2.466	2.532	-4.36	0.934	1.066	2.932	2.932	-5.377
A8_Soto	2	1.166	1.933	1.566	1.466	-6.181	1.468	1.4	2.066	2.1	-5.27	1.424	1.126	2	1.954	-3.93	1.366	1.123	2.23	2.532	-3.77	1.21	1.2	2.534	2.6	-5.06
A8_Soto	3	1.265	1.932	1.81	1.566	-5.97	1.11	2.166	2.12	1.91	-5.18	1.31	1.523	2.456	1.977	-3.65	1.765	1.468	2.12	2.634	-3.489	1.5	1.266	2.132	3.168	-4.75
A8_Soto	4	1.233	1.932	1.733	1.866	-5.87	1.21	2.12	2.132	1.766	-4.99	1.2	1.524	2.226	2.155	-3.32	1.467	1.433	2.233	2.7	-3.19	1.466	1.668	2.166	3.368	-4.55
A8_Soto	5	1.21	2	1.81	1.832	-5.76	1.3	2.1	2.066	1.734	-4.776	1.224	1.625	2.154	2.025	-3.12	1.433	1.32	2.166	2.666	-3.092	1.732	1.432	2.01	3.512	-4.44
A8_Soto	6	1.067	2.433	1.767	1.667	-5.661	1.268	2	1.932	1.566	-4.599	1.375	1.525	2.3	1.876	-2.94	1.665	1.4	2.366	2.534	-2.89	1.7	1.132	1.934	3.166	-4.36
A8_Soto	7	1.21	1.932	1.6	1.766	-5.65	1.2	1.834	2	1.632	-4.289	1.55	1.626	2.374	1.8	-2.74	1.634	1.333	2.166	2.432	-2.78	1.666	1.2	2.132	2.832	-4.27
A8_Soto	8	1.166	1.71	1.666	1.733	-5.65	1.33	1.668	2.134	1.5	-4.076	1.476	1.624	2.3	1.86	-2.634	1.566	1.466	2.166	2.366	-2.76	1.666	1.21	2.066	2.832	-4.18
A8_Soto	9	1.2	1.9	1.667	1.7	-5.65	1.5	1.8	2.166	1.532	-3.798	1.474	1.55	2.124	1.825	-2.543	1.366	1.366	2.123	2.134	-2.76	1.656	1.212	2.034	2.734	-3.967
A8_Soto	10	1.166	1.91	1.567	1.766	-5.65	1.65	1.866	2.212	1.42	-3.598	1.424	1.526	2.22	1.84	-2.33	1.321	1.666	2.167	2.069	-2.69	1.566	1.2	2.032	2.3	-3.86
A8_Soto	11	1.21	1.868	1.5	1.867	-5.65	1.7	1.71	2.168	1.366	-3.388	1.376	1.524	2.1	1.854	-2.24	1.332	1.866	2.168	1.823	-2.68	1.4	1.066	2.032	2.432	-3.75
A8_Soto	12	1.4	1.8	1.6	1.966	-5.84	1.665	1.568	2.233	1.533	-3.17	1.376	1.5	1.9	1.824	-2.14	1.534	1.466	2.132	1.834	-2.69	1.412	1.81	2.566	2.4	-3.65
A8_Soto	13	1.4	1.867	1.633	2.132	-5.95	1.667	1.733	2.3	1.466	-3.08	1.326	1.675	1.777	1.825	-2.022	1.432	1.366	2.067	1.732	-2.68	1.3	0.966	1.866	2.4	-3.54
A8_Soto	14	1.266	2.133	1.832	1.733	-6.18	1.632	1.6	2.31	1.4	-2.87	1.276	1.276	1.654	1.726	-1.93	1.267	1.234	2.067	1.732	-2.67	1.465	1.232	1.7	2.032	-3.52
A8_Soto	15	1.066	2.21	1.632	1.8	-6.36	1.732	1.366	2.2	1.432	-2.78	1.476	1.126	1.7	1.7	-1.741	1.166	1.232	1.868	1.566	-2.76	1.332	1.166	1.734	1.612	-3.42
A8_Soto	16	1.089	2.2	1.688	1.71	-6.68	1.666	1.032	2.2	1.4	-2.67	1.474	1.124	1.652	1.676	-1.74	1.32	1.066	1.832	1.566	-2.77	1.1	1	1.732	1.766	-3.44
A8_Soto	17						1.767	0.968	2.068	1.2	-2.59	1.277	0.976	1.9	1.7	-1.63	1.45	1.12	1.766	1.432	-2.77	1.1	0.732	1.712	1.366	-3.33
A8_Soto	18						1.7	0.767	1.8	1.068	-2.59	1.624	0.876	1.9	1.477	-1.62	1.367	1.132	1.567	1.366	-2.76	0.966	0.834	1.566	1.232	-3.32
A8_Soto	19						1.532	0.8	1.92	1	-2.66	1.324	0.976	1.776	1.125	-1.63	1.267	0.965	1.7	1.366	-2.78	1.032	0.932	1.768	1.2	-3.28
A8_Soto	20						1.2	0.866	1.932	0.9	-2.89	1.2	0.776	1.6	1.155	-1.823	1.23	0.834	1.568	1.032	-2.78	1.002	0.832	1.733	1.366	-3.31

APPENDIX C: *P*-value SPSS outputs

5.2.1. P. paniscus maximum thickness comparisons

P. paniscus plantar dorsal thicknesses metatarsal 1

Hypothesis Test Summary

	Null Hypothesis	Test	Sig.	Decision
1	The median of differences between PanM1Pth and PanM1Dth equals 0.	Related-Samples Wilcoxon Signed Rank Test	.111	Retain the null hypothesis.

Asymptotic significances are displayed. The significance level is .05.

P. paniscus plantar medial thicknesses metatarsal 1

Hypothesis Test Summary

	Null Hypothesis	Test	Sig.	Decision
1	The median of differences between PanM1Pth and PanM1Mth equals 0.	Related-Samples Wilcoxon Signed Rank Test	.262	Retain the null hypothesis.

Asymptotic significances are displayed. The significance level is .05.

P. paniscus plantar lateral thicknesses metatarsal 1

Hypothesis Test Summary

	Null Hypothesis	Test	Sig.	Decision
1	The median of differences between PanM1Pth and PanM1Lth equals 0.	Related-Samples Wilcoxon Signed Rank Test	.420	Retain the null hypothesis.

Asymptotic significances are displayed. The significance level is .05.

P. paniscus dorsal medial thicknesses metatarsal 1

Hypothesis Test Summary

	Null Hypothesis	Test	Sig.	Decision
1	The median of differences between PanM1Dth and PanM1Mth equals 0.	Related-Samples Wilcoxon Signed Rank Test	.266	Retain the null hypothesis.

Asymptotic significances are displayed. The significance level is .05.

P. paniscus dorsal lateral thicknesses metatarsal 1

Hypothesis Test Summary

	Null Hypothesis	Test	Sig.	Decision
1	The median of differences between PanM1Dth and PanM1Lth equals 0.	Related-Samples Wilcoxon Signed Rank Test	.004	Reject the null hypothesis.

Asymptotic significances are displayed. The significance level is .05.

P. paniscus medio lateral thicknesses metatarsal 1

Hypothesis Test Summary

	Null Hypothesis	Test	Sig.	Decision
1	The median of differences between PanM1Mth and PanM1Lth equals 0.	Related-Samples Wilcoxon Signed Rank Test	.021	Reject the null hypothesis.

Asymptotic significances are displayed. The significance level is .05.

P. paniscus plantar dorsal thicknesses metatarsal 2

Hypothesis Test Summary

	Null Hypothesis	Test	Sig.	Decision
1	The median of differences between PanM2Pth and PanM2Dth equals 0.	Related-Samples Wilcoxon Signed Rank Test	.004	Reject the null hypothesis.

Asymptotic significances are displayed. The significance level is .05.

P. paniscus plantar medial thicknesses metatarsal 2

Hypothesis Test Summary

	Null Hypothesis	Test	Sig.	Decision
1	The median of differences between PanM2Pth and PanM2Mth equals 0.	Related-Samples Wilcoxon Signed Rank Test	.006	Reject the null hypothesis.

Asymptotic significances are displayed. The significance level is .05.

P. paniscus plantar lateral thicknesses metatarsal 2

Hypothesis Test Summary

	Null Hypothesis	Test	Sig.	Decision
1	The median of differences between PanM2Pth and PanM2Lth equals 0.	Related-Samples Wilcoxon Signed Rank Test	.010	Reject the null hypothesis.

Asymptotic significances are displayed. The significance level is .05.

P. paniscus dorsal medial thicknesses metatarsal 2

Hypothesis Test Summary

	Null Hypothesis	Test	Sig.	Decision
1	The median of differences between PanM2Dth and PanM2Mth equals 0.	Related-Samples Wilcoxon Signed Rank Test	.657	Retain the null hypothesis.

Asymptotic significances are displayed. The significance level is .05.

P. paniscus dorsal lateral thicknesses metatarsal 2

Hypothesis Test Summary

	Null Hypothesis	Test	Sig.	Decision
1	The median of differences between PanM2Dth and PanM2Lth equals 0.	Related-Samples Wilcoxon Signed Rank Test	.078	Retain the null hypothesis.

Asymptotic significances are displayed. The significance level is .05.

P. paniscus medial lateral thicknesses metatarsal 2

Hypothesis Test Summary

	Null Hypothesis	Test	Sig.	Decision
1	The median of differences between PanM2Lth and PanM2Mth equals 0.	Related-Samples Wilcoxon Signed Rank Test	.132	Retain the null hypothesis.

Asymptotic significances are displayed. The significance level is .05.

P. paniscus plantar dorsal thicknesses metatarsal 3

Hypothesis Test Summary

	Null Hypothesis	Test	Sig.	Decision
1	The median of differences between PANm3Pth and PanM3Dth equals 0.	Related-Samples Wilcoxon Signed Rank Test	.006	Reject the null hypothesis.

Asymptotic significances are displayed. The significance level is .05.

P. paniscus plantar medial thicknesses metatarsal 3

Hypothesis Test Summary

	Null Hypothesis	Test	Sig.	Decision
1	The median of differences between PANm3Pth and PanM3Mth equals 0.	Related-Samples Wilcoxon Signed Rank Test	.023	Reject the null hypothesis.

Asymptotic significances are displayed. The significance level is .05.

P. paniscus plantar lateral thicknesses metatarsal 3

Hypothesis Test Summary

	Null Hypothesis	Test	Sig.	Decision
1	The median of differences between PANm3Pth and PanM3Lth equals 0.	Related-Samples Wilcoxon Signed Rank Test	.024	Reject the null hypothesis.

Asymptotic significances are displayed. The significance level is .05.

P. paniscus dorsal medial thicknesses metatarsal 3

Hypothesis Test Summary

	Null Hypothesis	Test	Sig.	Decision
1	The median of differences between PanM3Dth and PanM3Mth equals 0.	Related-Samples Wilcoxon Signed Rank Test	.483	Retain the null hypothesis.

Asymptotic significances are displayed. The significance level is .05.

P. paniscus dorsal lateral thicknesses metatarsal 3

Hypothesis Test Summary

	Null Hypothesis	Test	Sig.	Decision
1	The median of differences between PanM3Dth and PanM3Lth equals 0.	Related-Samples Wilcoxon Signed Rank Test	.285	Retain the null hypothesis.

Asymptotic significances are displayed. The significance level is .05.

P. paniscus medial lateral thicknesses metatarsal 3

Hypothesis Test Summary

	Null Hypothesis	Test	Sig.	Decision
1	The median of differences between PanM3Lth and PanM3Mth equals 0.	Related-Samples Wilcoxon Signed Rank Test	.858	Retain the null hypothesis.

Asymptotic significances are displayed. The significance level is .05.

P. paniscus plantar dorsal thicknesses metatarsal 4

Hypothesis Test Summary

	Null Hypothesis	Test	Sig.	Decision
1	The median of differences between PanM4Pth and PanM4Dth equals 0.	Related-Samples Wilcoxon Signed Rank Test	.002	Reject the null hypothesis.

Asymptotic significances are displayed. The significance level is .05.

P. paniscus plantar medial thicknesses metatarsal 4

Hypothesis Test Summary

	Null Hypothesis	Test	Sig.	Decision
1	The median of differences between PanM4Pth and PanM4Mth equals 0.	Related-Samples Wilcoxon Signed Rank Test	.001	Reject the null hypothesis.

Asymptotic significances are displayed. The significance level is .05.

P. paniscus plantar lateral thicknesses metatarsal 4

Hypothesis Test Summary

	Null Hypothesis	Test	Sig.	Decision
1	The median of differences between PanM4Pth and PanM4Lth equals 0.	Related-Samples Wilcoxon Signed Rank Test	.003	Reject the null hypothesis.

Asymptotic significances are displayed. The significance level is .05.

P. paniscus dorsal medial thicknesses metatarsal 4

Hypothesis Test Summary

	Null Hypothesis	Test	Sig.	Decision
1	The median of differences between PanM4Dth and PanM4Mth equals 0.	Related-Samples Wilcoxon Signed Rank Test	.068	Retain the null hypothesis.

Asymptotic significances are displayed. The significance level is .05.

P. paniscus dorsal lateral thicknesses metatarsal 4

Hypothesis Test Summary

	Null Hypothesis	Test	Sig.	Decision
1	The median of differences between PanM4Dth and PanM4Lth equals 0.	Related-Samples Wilcoxon Signed Rank Test	.875	Retain the null hypothesis.

Asymptotic significances are displayed. The significance level is .05.

P. paniscus medial lateral thicknesses metatarsal 4

Hypothesis Test Summary

	Null Hypothesis	Test	Sig.	Decision
1	The median of differences between PanM4Lth and PanM4Mth equals 0.	Related-Samples Wilcoxon Signed Rank Test	.027	Reject the null hypothesis.

Asymptotic significances are displayed. The significance level is .05.

P. paniscus plantar dorsal thicknesses metatarsal 5

Hypothesis Test Summary

	Null Hypothesis	Test	Sig.	Decision
1	The median of differences between PanM4Pth and PanM4Lth equals 0.	Related-Samples Wilcoxon Signed Rank Test	.003	Reject the null hypothesis.

Asymptotic significances are displayed. The significance level is .05.

P. paniscus plantar medial thicknesses metatarsal 5

Hypothesis Test Summary

	Null Hypothesis	Test	Sig.	Decision
1	The median of differences between PanM4Pth and PanM4Lth equals 0.	Related-Samples Wilcoxon Signed Rank Test	.003	Reject the null hypothesis.

Asymptotic significances are displayed. The significance level is .05.

P. paniscus plantar lateral thicknesses metatarsal 5

Hypothesis Test Summary

	Null Hypothesis	Test	Sig.	Decision
1	The median of differences between PanM4Pth and PanM4Lth equals 0.	Related-Samples Wilcoxon Signed Rank Test	.003	Reject the null hypothesis.

Asymptotic significances are displayed. The significance level is .05.

P. paniscus dorsal medial thicknesses metatarsal 5

Hypothesis Test Summary

	Null Hypothesis	Test	Sig.	Decision
1	The median of differences between PanM5Dth and PanM5Mth equals 0.	Related-Samples Wilcoxon Signed Rank Test	.488	Retain the null hypothesis.

Asymptotic significances are displayed. The significance level is .05.

P. paniscus dorsal lateral thicknesses metatarsal 5

Hypothesis Test Summary

	Null Hypothesis	Test	Sig.	Decision
1	The median of differences between PanM5Dth and PanM5Lth equals 0.	Related-Samples Wilcoxon Signed Rank Test	.054	Retain the null hypothesis.

Asymptotic significances are displayed. The significance level is .05.

P. paniscus medial lateral thicknesses metatarsal 5

Hypothesis Test Summary

	Null Hypothesis	Test	Sig.	Decision
1	The median of differences between PanM5Mth and PanM5Lth equals 0.	Related-Samples Wilcoxon Signed Rank Test	.051	Retain the null hypothesis.

Asymptotic significances are displayed. The significance level is .05.

5.2.2. H. sapiens maximum thickness comparisons

H. sapiens plantar dorsal thicknesses metatarsal 1

Hypothesis Test Summary

	Null Hypothesis	Test	Sig.	Decision
1	The median of differences between HomM5Pth and HomM5Dth equals 0.	Related-Samples Wilcoxon Signed Rank Test	.512	Retain the null hypothesis.

Asymptotic significances are displayed. The significance level is .05.

H. sapiens plantar medial thicknesses metatarsal 1

Hypothesis Test Summary

	Null Hypothesis	Test	Sig.	Decision
1	The median of differences between HomM1Pth and HomM1Mth equals 0.	Related-Samples Wilcoxon Signed Rank Test	.065	Retain the null hypothesis.

Asymptotic significances are displayed. The significance level is .05.

H. sapiens plantar lateral thicknesses metatarsal 1

Hypothesis Test Summary

	Null Hypothesis	Test	Sig.	Decision
1	The median of differences between HomM1Pth and HomM1Lth equals 0.	Related-Samples Wilcoxon Signed Rank Test	.003	Reject the null hypothesis.

Asymptotic significances are displayed. The significance level is .05.

H. sapiens dorsal medial thicknesses metatarsal 1

Hypothesis Test Summary

	Null Hypothesis	Test	Sig.	Decision
1	The median of differences between HomM1Dth and HomM1Mth equals 0.	Related-Samples Wilcoxon Signed Rank Test	.000	Reject the null hypothesis.

Asymptotic significances are displayed. The significance level is .05.

H. sapiens dorsal lateral thicknesses metatarsal 1

Hypothesis Test Summary

	Null Hypothesis	Test	Sig.	Decision
1	The median of differences between HomM1Dth and HomM1Lth equals 0.	Related-Samples Wilcoxon Signed Rank Test	.000	Reject the null hypothesis.

Asymptotic significances are displayed. The significance level is .05.

H. sapiens medial lateral thicknesses metatarsal 1

Hypothesis Test Summary

	Null Hypothesis	Test	Sig.	Decision
1	The median of differences between HomM1Mth and HomM1Lth equals 0.	Related-Samples Wilcoxon Signed Rank Test	.110	Retain the null hypothesis.

Asymptotic significances are displayed. The significance level is .05.

H. sapiens plantar dorsal thicknesses metatarsal 2

Hypothesis Test Summary

	Null Hypothesis	Test	Sig.	Decision
1	The median of differences between HomM2Pth and HomM2Dth equals 0.	Related-Samples Wilcoxon Signed Rank Test	.520	Retain the null hypothesis.

Asymptotic significances are displayed. The significance level is .05.

H. sapiens plantar medial thicknesses metatarsal 2

Hypothesis Test Summary

	Null Hypothesis	Test	Sig.	Decision
1	The median of differences between HomM2Pth and HomM2Mth equals 0.	Related-Samples Wilcoxon Signed Rank Test	.394	Retain the null hypothesis.

Asymptotic significances are displayed. The significance level is .05.

H. sapiens plantar lateral thicknesses metatarsal 2

Hypothesis Test Summary

	Null Hypothesis	Test	Sig.	Decision
1	The median of differences between HomM2Pth and HomM2Lth equals 0.	Related-Samples Wilcoxon Signed Rank Test	.295	Retain the null hypothesis.

Asymptotic significances are displayed. The significance level is .05.

H. sapiens dorsalmedial thicknesses metatarsal 2

Hypothesis Test Summary

	Null Hypothesis	Test	Sig.	Decision
1	The median of differences between HomM2Dth and HomM2Mth equals 0.	Related-Samples Wilcoxon Signed Rank Test	.982	Retain the null hypothesis.

Asymptotic significances are displayed. The significance level is .05.

H. sapiens dorsal lateral thicknesses metatarsal 2

Hypothesis Test Summary

	Null Hypothesis	Test	Sig.	Decision
1	The median of differences between HomM2Dth and HomM2Lth equals 0.	Related-Samples Wilcoxon Signed Rank Test	.277	Retain the null hypothesis.

Asymptotic significances are displayed. The significance level is .05.

H. sapiens medial lateral thicknesses metatarsal 2

Hypothesis Test Summary

	Null Hypothesis	Test	Sig.	Decision
1	The median of differences between HomM2Mth and HomM2Lth equals 0.	Related-Samples Wilcoxon Signed Rank Test	.378	Retain the null hypothesis.

Asymptotic significances are displayed. The significance level is .05.

H. sapiens plantar dorsal thicknesses metatarsal 3

Hypothesis Test Summary

	Null Hypothesis	Test	Sig.	Decision
1	The median of differences between HomM3Pth and HomM3Dth equals 0.	Related-Samples Wilcoxon Signed Rank Test	.134	Retain the null hypothesis.

Asymptotic significances are displayed. The significance level is .05.

H. sapiens plantar medial thicknesses metatarsal 3

Hypothesis Test Summary

	Null Hypothesis	Test	Sig.	Decision
1	The median of differences between HomM3Pth and HomM3Mth equals 0.	Related-Samples Wilcoxon Signed Rank Test	.097	Retain the null hypothesis.

Asymptotic significances are displayed. The significance level is .05.

H. sapiens plantar lateral thicknesses metatarsal 3

Hypothesis Test Summary

	Null Hypothesis	Test	Sig.	Decision
1	The median of differences between HomM3Pth and HomM3Lth equals 0.	Related-Samples Wilcoxon Signed Rank Test	.005	Reject the null hypothesis.

Asymptotic significances are displayed. The significance level is .05.

H. sapiens dorsal medial thicknesses metatarsal 3

Hypothesis Test Summary

	Null Hypothesis	Test	Sig.	Decision
1	The median of differences between HomM3Dth and HomM3Mth equals 0.	Related-Samples Wilcoxon Signed Rank Test	.936	Retain the null hypothesis.

Asymptotic significances are displayed. The significance level is .05.

H. sapiens dorsal lateral thicknesses metatarsal 3

Hypothesis Test Summary

	Null Hypothesis	Test	Sig.	Decision
1	The median of differences between HomM3Dth and HomM3Lth equals 0.	Related-Samples Wilcoxon Signed Rank Test	.007	Reject the null hypothesis.

Asymptotic significances are displayed. The significance level is .05.

H. sapiens medial lateral thicknesses metatarsal 3

Hypothesis Test Summary

	Null Hypothesis	Test	Sig.	Decision
1	The median of differences between HomM3Lth and HomM3Mth equals 0.	Related-Samples Wilcoxon Signed Rank Test	.026	Reject the null hypothesis.

Asymptotic significances are displayed. The significance level is .05.

H. sapiens plantar dorsal thicknesses metatarsal 4

Hypothesis Test Summary

	Null Hypothesis	Test	Sig.	Decision
1	The median of differences between HomM4Pth and HomM4Dth equals 0.	Related-Samples Wilcoxon Signed Rank Test	.717	Retain the null hypothesis.

Asymptotic significances are displayed. The significance level is .05.

H. sapiens plantar medial thicknesses metatarsal 4

Hypothesis Test Summary

	Null Hypothesis	Test	Sig.	Decision
1	The median of differences between HomM4Pth and HomM4Mth equals 0.	Related-Samples Wilcoxon Signed Rank Test	.224	Retain the null hypothesis.

Asymptotic significances are displayed. The significance level is .05.

H. sapiens plantar lateral thicknesses metatarsal 4

Hypothesis Test Summary

	Null Hypothesis	Test	Sig.	Decision
1	The median of differences between HomM4Pth and HomM4Lth equals 0.	Related-Samples Wilcoxon Signed Rank Test	.296	Retain the null hypothesis.

Asymptotic significances are displayed. The significance level is .05.

H. sapiens dorsal medial thicknesses metatarsal 4

Hypothesis Test Summary

	Null Hypothesis	Test	Sig.	Decision
1	The median of differences between HomM4Dth and HomM4Mth equals 0.	Related-Samples Wilcoxon Signed Rank Test	.016	Reject the null hypothesis.

Asymptotic significances are displayed. The significance level is .05.

H. sapiens dorsal lateral thicknesses metatarsal 4

Hypothesis Test Summary

	Null Hypothesis	Test	Sig.	Decision
1	The median of differences between HomM4Dth and HomM4Lth equals 0.	Related-Samples Wilcoxon Signed Rank Test	.009	Reject the null hypothesis.

Asymptotic significances are displayed. The significance level is .05.

H. sapiens medial lateral thicknesses metatarsal 4

Hypothesis Test Summary

	Null Hypothesis	Test	Sig.	Decision
1	The median of differences between HomM4Mth and HomM4Lth equals 0.	Related-Samples Wilcoxon Signed Rank Test	.627	Retain the null hypothesis.

Asymptotic significances are displayed. The significance level is .05.

H. sapiens plantar dorsal thicknesses metatarsal 5

Hypothesis Test Summary

	Null Hypothesis	Test	Sig.	Decision
1	The median of differences between HomM5Pth and HomM5Dth equals 0.	Related-Samples Wilcoxon Signed Rank Test	.512	Retain the null hypothesis.

Asymptotic significances are displayed. The significance level is .05.

H. sapiens plantar medial thicknesses metatarsal 5

Hypothesis Test Summary

	Null Hypothesis	Test	Sig.	Decision
1	The median of differences between HomM5Pth and HomM5Mth equals 0.	Related-Samples Wilcoxon Signed Rank Test	.003	Reject the null hypothesis.

Asymptotic significances are displayed. The significance level is .05.

H. sapiens plantar lateral thicknesses metatarsal 5

Hypothesis Test Summary

	Null Hypothesis	Test	Sig.	Decision
1	The median of differences between HomM5Pth and HomM5Lth equals 0.	Related-Samples Wilcoxon Signed Rank Test	.016	Reject the null hypothesis.

Asymptotic significances are displayed. The significance level is .05.

H. sapiens dorsal medial thicknesses metatarsal 5

Hypothesis Test Summary

	Null Hypothesis	Test	Sig.	Decision
1	The median of differences between HomM5Dth and HomM5Mth equals 0.	Related-Samples Wilcoxon Signed Rank Test	.007	Reject the null hypothesis.

Asymptotic significances are displayed. The significance level is .05.

H. sapiens dorsal lateral thicknesses metatarsal 5

Hypothesis Test Summary

	Null Hypothesis	Test	Sig.	Decision
1	The median of differences between HomM5Dth and HomM5Lth equals 0.	Related-Samples Wilcoxon Signed Rank Test	.011	Reject the null hypothesis.

Asymptotic significances are displayed. The significance level is .05.

H. sapiens medial lateral thicknesses metatarsal 5

Hypothesis Test Summary

	Null Hypothesis	Test	Sig.	Decision
1	The median of differences between HomM5Lth and HomM5Mth equals 0.	Related-Samples Wilcoxon Signed Rank Test	.474	Retain the null hypothesis.

Asymptotic significances are displayed. The significance level is .05.

5.2.3. P. t. schweinfurthii maximum thickness comparisons

P. t. schweinfurthii plantar dorsal thicknesses metatarsal 1

Hypothesis Test Summary

	Null Hypothesis	Test	Sig.	Decision
1	The median of differences between SchwM1Pth and SchwM1Dth equals 0.	Related-Samples Wilcoxon Signed Rank Test	.002	Reject the null hypothesis.

Asymptotic significances are displayed. The significance level is .05.

P. t. schweinfurthii plantar medial thicknesses metatarsal 1

Hypothesis Test Summary

	Null Hypothesis	Test	Sig.	Decision
1	The median of differences between SchwM1Pth and SchwM1Mth equals 0.	Related-Samples Wilcoxon Signed Rank Test	.047	Reject the null hypothesis.

Asymptotic significances are displayed. The significance level is .05.

P. t. schweinfurthii plantar lateral thicknesses metatarsal 1

Hypothesis Test Summary

	Null Hypothesis	Test	Sig.	Decision
1	The median of differences between SchwM1Pth and SchwM1Lth equals 0.	Related-Samples Wilcoxon Signed Rank Test	.264	Retain the null hypothesis.

Asymptotic significances are displayed. The significance level is .05.

P. t. schweinfurthii dorsal medial thicknesses metatarsal 1

Hypothesis Test Summary

	Null Hypothesis	Test	Sig.	Decision
1	The median of differences between SchwM1Dth and SchwM1Mth equals 0.	Related-Samples Wilcoxon Signed Rank Test	.028	Reject the null hypothesis.

Asymptotic significances are displayed. The significance level is .05.

P. t. schweinfurthii dorsal lateral thicknesses metatarsal 1

Hypothesis Test Summary

	Null Hypothesis	Test	Sig.	Decision
1	The median of differences between SchwM1Dth and SchwM1Lth equals 0.	Related-Samples Wilcoxon Signed Rank Test	.000	Reject the null hypothesis.

Asymptotic significances are displayed. The significance level is .05.

P. t. schweinfurthii medial lateral thicknesses metatarsal 1

Hypothesis Test Summary

	Null Hypothesis	Test	Sig.	Decision
1	The median of differences between SchwM1Lth and SchwM1Mth equals 0.	Related-Samples Wilcoxon Signed Rank Test	.089	Retain the null hypothesis.

Asymptotic significances are displayed. The significance level is .05.

P. t. schweinfurthii plantar dorsal thicknesses metatarsal 2

Hypothesis Test Summary

	Null Hypothesis	Test	Sig.	Decision
1	The median of differences between SchwM2Pth and SchwM2Dth equals 0.	Related-Samples Wilcoxon Signed Rank Test	.102	Retain the null hypothesis.

Asymptotic significances are displayed. The significance level is .05.

P. t. schweinfurthii plantar medial thicknesses metatarsal 2

Hypothesis Test Summary

	Null Hypothesis	Test	Sig.	Decision
1	The median of differences between SchwM2Pth and SchwM2Mth equals 0.	Related-Samples Wilcoxon Signed Rank Test	.445	Retain the null hypothesis.

Asymptotic significances are displayed. The significance level is .05.

P. t. schweinfurthii plantar lateral thicknesses metatarsal 2

Hypothesis Test Summary

	Null Hypothesis	Test	Sig.	Decision
1	The median of differences between SchwM2Pth and SchwM2Lth equals 0.	Related-Samples Wilcoxon Signed Rank Test	.313	Retain the null hypothesis.

Asymptotic significances are displayed. The significance level is .05.

P. t. schweinfurthii dorsal medial thicknesses metatarsal 2

Hypothesis Test Summary

	Null Hypothesis	Test	Sig.	Decision
1	The median of differences between SchwM2Dth and SchwM2Mth equals 0.	Related-Samples Wilcoxon Signed Rank Test	.671	Retain the null hypothesis.

Asymptotic significances are displayed. The significance level is .05.

P. t. schweinfurthii dorsal lateral thicknesses metatarsal 2

Hypothesis Test Summary

	Null Hypothesis	Test	Sig.	Decision
1	The median of differences between SchwM2Dth and SchwM2Lth equals 0.	Related-Samples Wilcoxon Signed Rank Test	.006	Reject the null hypothesis.

Asymptotic significances are displayed. The significance level is .05.

P. t. schweinfurthii medial lateral thicknesses metatarsal 2

Hypothesis Test Summary

	Null Hypothesis	Test	Sig.	Decision
1	The median of differences between SchwM2Lth and SchwM2Mth equals 0.	Related-Samples Wilcoxon Signed Rank Test	.033	Reject the null hypothesis.

Asymptotic significances are displayed. The significance level is .05.

P. t. schweinfurthii plantar dorsal thicknesses metatarsal 3

Hypothesis Test Summary

	Null Hypothesis	Test	Sig.	Decision
1	The median of differences between SchwM3Pth and SchwM3Dth equals 0.	Related-Samples Wilcoxon Signed Rank Test	.001	Reject the null hypothesis.

Asymptotic significances are displayed. The significance level is .05.

P. t. schweinfurthii plantar medial thicknesses metatarsal 3

Hypothesis Test Summary

	Null Hypothesis	Test	Sig.	Decision
1	The median of differences between SchwM3Pth and SchwM3Mth equals 0.	Related-Samples Wilcoxon Signed Rank Test	.075	Retain the null hypothesis.

Asymptotic significances are displayed. The significance level is .05.

P. t. schweinfurthii plantar lateral thicknesses metatarsal 3

Hypothesis Test Summary

	Null Hypothesis	Test	Sig.	Decision
1	The median of differences between SchwM3Pth and SchwM3Lth equals 0.	Related-Samples Wilcoxon Signed Rank Test	.003	Reject the null hypothesis.

Asymptotic significances are displayed. The significance level is .05.

P. t. schweinfurthii dorsal medial thicknesses metatarsal 3

Hypothesis Test Summary

	Null Hypothesis	Test	Sig.	Decision
1	The median of differences between SchwM3Dth and SchwM3Mth equals 0.	Related-Samples Wilcoxon Signed Rank Test	.056	Retain the null hypothesis.

Asymptotic significances are displayed. The significance level is .05.

P. t. schweinfurthii dorsal lateral thicknesses metatarsal 3

Hypothesis Test Summary

	Null Hypothesis	Test	Sig.	Decision
1	The median of differences between SchwM3Dth and SchwM3Lth equals 0.	Related-Samples Wilcoxon Signed Rank Test	.213	Retain the null hypothesis.

Asymptotic significances are displayed. The significance level is .05.

P. t. schweinfurthii medial lateral thicknesses metatarsal 3

Hypothesis Test Summary

	Null Hypothesis	Test	Sig.	Decision
1	The median of differences between SchwM3Lth and SchwM3Mth equals 0.	Related-Samples Wilcoxon Signed Rank Test	.619	Retain the null hypothesis.

Asymptotic significances are displayed. The significance level is .05.

P. t. schweinfurthii plantar dorsal thicknesses metatarsal 4

Hypothesis Test Summary

	Null Hypothesis	Test	Sig.	Decision
1	The median of differences between SchwM4Pth and SchwM4Dth equals 0.	Related-Samples Wilcoxon Signed Rank Test	.000	Reject the null hypothesis.

Asymptotic significances are displayed. The significance level is .05.

P. t. schweinfurthii plantar medial thicknesses metatarsal 4

Hypothesis Test Summary

	Null Hypothesis	Test	Sig.	Decision
1	The median of differences between SchwM4Pth and SchwM4Mth equals 0.	Related-Samples Wilcoxon Signed Rank Test	.000	Reject the null hypothesis.

Asymptotic significances are displayed. The significance level is .05.

P. t. schweinfurthii plantar lateral thicknesses metatarsal 4

Hypothesis Test Summary

	Null Hypothesis	Test	Sig.	Decision
1	The median of differences between SchwM4Pth and SchwM4Lth equals 0.	Related-Samples Wilcoxon Signed Rank Test	.000	Reject the null hypothesis.

Asymptotic significances are displayed. The significance level is .05.

P. t. schweinfurthii dorsal medial thicknesses metatarsal 4

Hypothesis Test Summary

	Null Hypothesis	Test	Sig.	Decision
1	The median of differences between SchwM4Dth and SchwM4Mth equals 0.	Related-Samples Wilcoxon Signed Rank Test	.022	Reject the null hypothesis.

Asymptotic significances are displayed. The significance level is .05.

P. t. schweinfurthii dorsal lateral thicknesses metatarsal 4

Hypothesis Test Summary

	Null Hypothesis	Test	Sig.	Decision
1	The median of differences between SchwM4Dth and SchwM4Lth equals 0.	Related-Samples Wilcoxon Signed Rank Test	.002	Reject the null hypothesis.

Asymptotic significances are displayed. The significance level is .05.

P. t. schweinfurthii medial lateral thicknesses metatarsal 4

Hypothesis Test Summary

	Null Hypothesis	Test	Sig.	Decision
1	The median of differences between SchwM4Lth and SchwM4Mth equals 0.	Related-Samples Wilcoxon Signed Rank Test	.109	Retain the null hypothesis.

Asymptotic significances are displayed. The significance level is .05.

P. t. schweinfurthii plantardorsal thicknesses metatarsal 5

Hypothesis Test Summary

	Null Hypothesis	Test	Sig.	Decision
1	The median of differences between SchwM5Pth and SchwM5Dth equals 0.	Related-Samples Wilcoxon Signed Rank Test	.000	Reject the null hypothesis.

Asymptotic significances are displayed. The significance level is .05.

P. t. schweinfurthii plantar medial thicknesses metatarsal 5

Hypothesis Test Summary

	Null Hypothesis	Test	Sig.	Decision
1	The median of differences between SchwM5Pth and SchwM5Mth equals 0.	Related-Samples Wilcoxon Signed Rank Test	.000	Reject the null hypothesis.

Asymptotic significances are displayed. The significance level is .05.

P. t. schweinfurthii plantar lateral thicknesses metatarsal 5

Hypothesis Test Summary

	Null Hypothesis	Test	Sig.	Decision
1	The median of differences between SchwM5Pth and SchwM5Lth equals 0.	Related-Samples Wilcoxon Signed Rank Test	.000	Reject the null hypothesis.

Asymptotic significances are displayed. The significance level is .05.

P. t. schweinfurthii dorsal medial thicknesses metatarsal 5

Hypothesis Test Summary

	Null Hypothesis	Test	Sig.	Decision
1	The median of differences between SchwM5Dth and SchwM5Mth equals 0.	Related-Samples Wilcoxon Signed Rank Test	.227	Retain the null hypothesis.

Asymptotic significances are displayed. The significance level is .05.

P. t. schweinfurthii dorsal lateral thicknesses metatarsal 5

Hypothesis Test Summary

	Null Hypothesis	Test	Sig.	Decision
1	The median of differences between SchwM5Dth and SchwM5Lth equals 0.	Related-Samples Wilcoxon Signed Rank Test	.002	Reject the null hypothesis.

Asymptotic significances are displayed. The significance level is .05.

P. t. schweinfurthii medial lateral thicknesses metatarsal 5

Hypothesis Test Summary

	Null Hypothesis	Test	Sig.	Decision
1	The median of differences between SchwM5Mth and SchwM5Lth equals 0.	Related-Samples Wilcoxon Signed Rank Test	.011	Reject the null hypothesis.

Asymptotic significances are displayed. The significance level is .05.

5.2.5P-values for Kruskal-Wallis one-way ANOVA between positions of maximum thickness at all cortices between all species.

Interspecific comparison between positions of maximum plantar thickness in metatarsal 1

Hypothesis Test Summary

	Null Hypothesis	Test	Sig.	Decision
1	The distribution of PnHmSchMT1PTh is the same across categories of Grouping3.	Independent-Samples Kruskal-Wallis Test	.093	Retain the null hypothesis.

Asymptotic significances are displayed. The significance level is .05.

Interspecific comparison between positions of maximum plantar thickness in metatarsal 2

Hypothesis Test Summary

	Null Hypothesis	Test	Sig.	Decision
1	The distribution of PnHmSchMT2PTh is the same across categories of Grouping3.	Independent-Samples Kruskal-Wallis Test	.199	Retain the null hypothesis.

Asymptotic significances are displayed. The significance level is .05.

Interspecific comparison between positions of maximum plantar thickness in metatarsal 3

Hypothesis Test Summary

	Null Hypothesis	Test	Sig.	Decision
1	The distribution of PnHmSchMT3PTh is the same across categories of Grouping3.	Independent-Samples Kruskal-Wallis Test	.225	Retain the null hypothesis.

Asymptotic significances are displayed. The significance level is .05.

Interspecific comparison between positions of maximum plantar thickness in metatarsal 4

Hypothesis Test Summary

	Null Hypothesis	Test	Sig.	Decision
1	The distribution of PnHmSchMT4PTh is the same across categories of Grouping3.	Independent-Samples Kruskal-Wallis Test	.000	Reject the null hypothesis.

Asymptotic significances are displayed. The significance level is .05.

Interspecific comparison between positions of maximum plantar thickness in metatarsal 5

Hypothesis Test Summary

	Null Hypothesis	Test	Sig.	Decision
1	The distribution of PnHmSchMT5PTh is the same across categories of Grouping3.	Independent-Samples Kruskal-Wallis Test	.001	Reject the null hypothesis.

Asymptotic significances are displayed. The significance level is .05.

Interspecific comparison between positions of maximum dorsal thickness in metatarsal 1

Hypothesis Test Summary

	Null Hypothesis	Test	Sig.	Decision
1	The distribution of PnHmSchMT1DTh is the same across categories of Grouping3.	Independent-Samples Kruskal-Wallis Test	.038	Reject the null hypothesis.

Asymptotic significances are displayed. The significance level is .05.

Interspecific comparison between positions of maximum dorsal thickness in metatarsal 2

Hypothesis Test Summary

	Null Hypothesis	Test	Sig.	Decision
1	The distribution of PnHmSchMT2DTh is the same across categories of Grouping3.	Independent-Samples Kruskal-Wallis Test	.008	Reject the null hypothesis.

Asymptotic significances are displayed. The significance level is .05.

Interspecific comparison between positions of maximum dorsal thickness in metatarsal 3

Hypothesis Test Summary

	Null Hypothesis	Test	Sig.	Decision
1	The distribution of PnHmSchMT3DTh is the same across categories of Grouping3.	Independent-Samples Kruskal-Wallis Test	.000	Reject the null hypothesis.

Asymptotic significances are displayed. The significance level is .05.

Interspecific comparison between positions of maximum dorsal thickness in metatarsal 4

Hypothesis Test Summary

	Null Hypothesis	Test	Sig.	Decision
1	The distribution of PnHmSchMT4DTh is the same across categories of Grouping3.	Independent-Samples Kruskal-Wallis Test	.258	Retain the null hypothesis.

Asymptotic significances are displayed. The significance level is .05.

Interspecific comparison between positions of maximum plantar thickness in metatarsal 5

Hypothesis Test Summary

	Null Hypothesis	Test	Sig.	Decision
1	The distribution of PnHmSchMT5DTh is the same across categories of Grouping3.	Independent-Samples Kruskal-Wallis Test	.910	Retain the null hypothesis.

Asymptotic significances are displayed. The significance level is .05.

Interspecific comparison between positions of maximum medial thickness in metatarsal 1

Hypothesis Test Summary

	Null Hypothesis	Test	Sig.	Decision
1	The distribution of PnHmSchMT1MTh is the same across categories of Grouping3.	Independent-Samples Kruskal-Wallis Test	.003	Reject the null hypothesis.

Asymptotic significances are displayed. The significance level is .05.

Interspecific comparison between positions of maximum medial thickness in metatarsal 2

Hypothesis Test Summary

	Null Hypothesis	Test	Sig.	Decision
1	The distribution of PnHmSchMT2MTh is the same across categories of Grouping3.	Independent-Samples Kruskal-Wallis Test	.038	Reject the null hypothesis.

Asymptotic significances are displayed. The significance level is .05.

Interspecific comparison between positions of maximum medial thickness in metatarsal 3

Hypothesis Test Summary

	Null Hypothesis	Test	Sig.	Decision
1	The distribution of PnHmSchMT3MTh is the same across categories of Grouping3.	Independent-Samples Kruskal-Wallis Test	.392	Retain the null hypothesis.

Asymptotic significances are displayed. The significance level is .05.

Interspecific comparison between positions of maximum medial thickness in metatarsal 4

Hypothesis Test Summary

	Null Hypothesis	Test	Sig.	Decision
1	The distribution of PnHmSchMT4MTh is the same across categories of Grouping3.	Independent-Samples Kruskal-Wallis Test	.225	Retain the null hypothesis.

Asymptotic significances are displayed. The significance level is .05.

Interspecific comparison between positions of maximum medial thickness in metatarsal 5

Hypothesis Test Summary

	Null Hypothesis	Test	Sig.	Decision
1	The distribution of PnHmSchMT5MTh is the same across categories of Grouping3.	Independent-Samples Kruskal-Wallis Test	.011	Reject the null hypothesis.

Asymptotic significances are displayed. The significance level is .05.

Interspecific comparison between positions of maximum lateral thickness in metatarsal 1

Hypothesis Test Summary

	Null Hypothesis	Test	Sig.	Decision
1	The distribution of PnHmSchMT1LTh is the same across categories of Grouping3.	Independent-Samples Kruskal-Wallis Test	.005	Reject the null hypothesis.

Asymptotic significances are displayed. The significance level is .05.

Interspecific comparison between positions of maximum lateral thickness in metatarsal 2

Hypothesis Test Summary

	Null Hypothesis	Test	Sig.	Decision
1	The distribution of PnHmSchMT2LTh is the same across categories of Grouping3.	Independent-Samples Kruskal-Wallis Test	.353	Retain the null hypothesis.

Asymptotic significances are displayed. The significance level is .05.

Interspecific comparison between positions of maximum lateral thickness in metatarsal 3

Hypothesis Test Summary

	Null Hypothesis	Test	Sig.	Decision
1	The distribution of PnHmSchMT3LTh is the same across categories of Grouping3.	Independent-Samples Kruskal-Wallis Test	.823	Retain the null hypothesis.

Asymptotic significances are displayed. The significance level is .05.

Interspecific comparison between positions of maximum lateral thickness in metatarsal 4

Hypothesis Test Summary

	Null Hypothesis	Test	Sig.	Decision
1	The distribution of PnHmSchMT4LTh is the same across categories of Grouping3.	Independent-Samples Kruskal-Wallis Test	.381	Retain the null hypothesis.

Asymptotic significances are displayed. The significance level is .05.

Interspecific comparison between positions of maximum lateral thickness in metatarsal 5

Hypothesis Test Summary

	Null Hypothesis	Test	Sig.	Decision
1	The distribution of PnHmSchMT5LTh is the same across categories of Grouping3.	Independent-Samples Kruskal-Wallis Test	.234	Retain the null hypothesis.

Asymptotic significances are displayed. The significance level is .05.

5.2.6 P-values for Kruskal-Wallis one-way ANOVA between positions of maximum geometry change in all species by metatarsal.

Interspecific comparison between positions of maximum change in geometry on the plantar surface in metatarsal 1

Hypothesis Test Summary

	Null Hypothesis	Test	Sig.	Decision
1	The distribution of PnHmSchMT1MC is the same across categories of Grouping3.	Independent-Samples Kruskal-Wallis Test	.007	Reject the null hypothesis.

Asymptotic significances are displayed. The significance level is .05.

Interspecific comparison between positions of maximum change in geometry on the plantar surface in metatarsal 2

Hypothesis Test Summary

	Null Hypothesis	Test	Sig.	Decision
1	The distribution of PnHmSchMT2MC is the same across categories of Grouping3.	Independent-Samples Kruskal-Wallis Test	.082	Retain the null hypothesis.

Asymptotic significances are displayed. The significance level is .05.

4

Interspecific comparison between positions of maximum change in geometry on the plantar surface in metatarsal 3

Hypothesis Test Summary

	Null Hypothesis	Test	Sig.	Decision
1	The distribution of PnHmSchMT3MC is the same across categories of Grouping3.	Independent-Samples Kruskal-Wallis Test	.112	Retain the null hypothesis.

Asymptotic significances are displayed. The significance level is .05.

Interspecific comparison between positions of maximum change in geometry on the plantar surface in metatarsal 4

Hypothesis Test Summary

	Null Hypothesis	Test	Sig.	Decision
1	The distribution of PnHmSchMT4MC is the same across categories of Grouping3.	Independent-Samples Kruskal-Wallis Test	.001	Reject the null hypothesis.

Asymptotic significances are displayed. The significance level is .05.

Interspecific comparison between positions of maximum change in geometry on the plantar surface in metatarsal 1

Hypothesis Test Summary

	Null Hypothesis	Test	Sig.	Decision
1	The distribution of PnHmSchMT5MC is the same across categories of Grouping3.	Independent-Samples Kruskal-Wallis Test	.906	Retain the null hypothesis.

Asymptotic significances are displayed. The significance level is .05.

5.2.7 P-values for Kruskal-Wallis one-way ANOVA between positions of maximum geometry change in P. paniscus and P. t. schweinfurthii by metatarsal.

Interspecific comparison in two species of *Pan*between positions of maximum change in geometry on the plantar surface in metatarsal 1

Hypothesis Test Summary

	Null Hypothesis	Test	Sig.	Decision
1	The distribution of PpPtsMCMT1 is the same across categories of Grouping2.	Independent-Samples Mann-Whitney U Test	.553	Retain the null hypothesis.

Asymptotic significances are displayed. The significance level is .05.

Interspecific comparison in two species of *Pan* between positions of maximum change in geometry on the plantar surface in metatarsal 2

Hypothesis Test Summary

	Null Hypothesis	Test	Sig.	Decision
1	The distribution of PpPtsMCMT2 is the same across categories of Grouping2.	Independent-Samples Mann-Whitney U Test	.017	Reject the null hypothesis.

Asymptotic significances are displayed. The significance level is .05.

Interspecific comparison in two species of *Pan* between positions of maximum change in geometry on the plantar surface in metatarsal 3

Hypothesis Test Summary

	Null Hypothesis	Test	Sig.	Decision
1	The distribution of PpPtsMCMT3 is the same across categories of Grouping2.	Independent-Samples Mann-Whitney U Test	1.000	Retain the null hypothesis.

Asymptotic significances are displayed. The significance level is .05.

Interspecific comparison in two species of *Pan* between positions of maximum change in geometry on the plantar surface in metatarsal 4

Hypothesis Test Summary

	Null Hypothesis	Test	Sig.	Decision
1	The distribution of PpPtsMCMT4 is the same across categories of Grouping2.	Independent-Samples Mann-Whitney U Test	.003	Reject the null hypothesis.

Asymptotic significances are displayed. The significance level is .05.

Interspecific comparison in two species of *Pan* between positions of maximum change in geometry on the plantar surface in metatarsal 5

Hypothesis Test Summary

	Null Hypothesis	Test	Sig.	Decision
1	The distribution of PpPtsMCMT5 is the same across categories of Grouping2.	Independent-Samples Mann-Whitney U Test	.839	Retain the null hypothesis.

Asymptotic significances are displayed. The significance level is .05.

5.2.6. Interspecific comparisons in change in geometry by metatarsal

P. paniscus: H. sapiens: P. t. schweinfurthii metatarsal 1

Hypothesis Test Summary

	Null Hypothesis	Test	Sig.	Decision
1	The distribution of PnHmSchMT1MC is the same across categories of Grouping3.	Independent-Samples Kruskal-Wallis Test	.007	Reject the null hypothesis.

Asymptotic significances are displayed. The significance level is .05.

P. paniscus: H. sapiens: P. t. schweinfurthii metatarsal 2

Hypothesis Test Summary

	Null Hypothesis	Test	Sig.	Decision
1	The distribution of PnHmSchMT2MC is the same across categories of Grouping3.	Independent-Samples Kruskal-Wallis Test	.082	Retain the null hypothesis.

Asymptotic significances are displayed. The significance level is .05.

P. paniscus: H. sapiens: P. t. schweinfurthii metatarsal 3

Hypothesis Test Summary

	Null Hypothesis	Test	Sig.	Decision
1	The distribution of PnHmSchMT3MC is the same across categories of Grouping3.	Independent-Samples Kruskal-Wallis Test	.112	Retain the null hypothesis.

Asymptotic significances are displayed. The significance level is .05.

P. paniscus: H. sapiens: P. t. schweinfurthii metatarsal 4

Hypothesis Test Summary

	Null Hypothesis	Test	Sig.	Decision
1	The distribution of PnHmSchMT4MC is the same across categories of Grouping3.	Independent-Samples Kruskal-Wallis Test	.001	Reject the null hypothesis.

Asymptotic significances are displayed. The significance level is .05.

P. paniscus: H. sapiens: P. t. schweinfurthii metatarsal 5

Hypothesis Test Summary

	Null Hypothesis	Test	Sig.	Decision
1	The distribution of PnHmSchMT5MC is the same across categories of Grouping3.	Independent-Samples Kruskal-Wallis Test	.906	Retain the null hypothesis.

Asymptotic significances are displayed. The significance level is .05.

5.2.7. Interspecific comparisons in change in geometry in Pan by metatarsal

P. paniscus: P. t. schweinfurthii metatarsal 1

Hypothesis Test Summary

	Null Hypothesis	Test	Sig.	Decision
1	The distribution of PpPtsMCMT1 is the same across categories of Grouping2.	Independent-Samples Mann-Whitney U Test	.553	Retain the null hypothesis.

Asymptotic significances are displayed. The significance level is .05.

P. paniscus: P. t. schweinfurthii metatarsal 2

Hypothesis Test Summary

	Null Hypothesis	Test	Sig.	Decision
1	The distribution of PpPtsMCMT2 is the same across categories of Grouping2.	Independent-Samples Mann-Whitney U Test	.017	Reject the null hypothesis.

Asymptotic significances are displayed. The significance level is .05.

P. paniscus: P. t. schweinfurthii metatarsal 3

Hypothesis Test Summary

	Null Hypothesis	Test	Sig.	Decision
1	The distribution of PpPtsMCMT3 is the same across categories of Grouping2.	Independent-Samples Mann-Whitney U Test	1.000	Retain the null hypothesis.

Asymptotic significances are displayed. The significance level is .05.

P. paniscus: P. t. schweinfurthii metatarsal 4

Hypothesis Test Summary

	Null Hypothesis	Test	Sig.	Decision
1	The distribution of PpPtsMCMT4 is the same across categories of Grouping2.	Independent-Samples Mann-Whitney U Test	.003	Reject the null hypothesis.

Asymptotic significances are displayed. The significance level is .05.

P. paniscus: P. t. schweinfurthii metatarsal 5

Hypothesis Test Summary

	Null Hypothesis	Test	Sig.	Decision
1	The distribution of PpPtsMCMT5 is the same across categories of Grouping2.	Independent-Samples Mann-Whitney U Test	.839	Retain the null hypothesis.

Asymptotic significances are displayed. The significance level is .05.

5.2.8 Intraspecific comparisons in maximum position of thickness and change in geometry by metatarsal

P. paniscus maximum plantar thickness comparison with maximum change in geometry in metatarsal 1

Hypothesis Test Summary

	Null Hypothesis	Test	Sig.	Decision
1	The median of differences between PanM1MaxC and PanM1Pth equals 0.	Related-Samples Wilcoxon Signed Rank Test	.649	Retain the null hypothesis.

Asymptotic significances are displayed. The significance level is .05.

P. paniscus maximum dorsal thickness comparison with maximum change in geometry in metatarsal 1

Hypothesis Test Summary

	Null Hypothesis	Test	Sig.	Decision
1	The median of differences between PanM1MaxC and PanM1Dth equals 0.	Related-Samples Wilcoxon Signed Rank Test	.010	Reject the null hypothesis.

Asymptotic significances are displayed. The significance level is .05.

P. paniscus maximum medial thickness comparison with maximum change in geometry in metatarsal 1

Hypothesis Test Summary

	Null Hypothesis	Test	Sig.	Decision
1	The median of differences between PanM1MaxC and PanM1Mth equals 0.	Related-Samples Wilcoxon Signed Rank Test	.587	Retain the null hypothesis.

Asymptotic significances are displayed. The significance level is .05.

P. paniscus maximum lateral thickness comparison with maximum change in geometry in metatarsal 1

Hypothesis Test Summary

	Null Hypothesis	Test	Sig.	Decision
1	The median of differences between PanM1MaxC and PanM1Lth equals 0.	Related-Samples Wilcoxon Signed Rank Test	.108	Retain the null hypothesis.

Asymptotic significances are displayed. The significance level is .05.

P. paniscus maximum plantar thickness comparison with maximum change in geometry in metatarsal 2

Hypothesis Test Summary

	Null Hypothesis	Test	Sig.	Decision
1	The median of differences between PanM2MaxC and PanM2Pth equals 0.	Related-Samples Wilcoxon Signed Rank Test	.733	Retain the null hypothesis.

Asymptotic significances are displayed. The significance level is .05.

P. paniscus maximum dorsal thickness comparison with maximum change in geometry in metatarsal 2

Hypothesis Test Summary

	Null Hypothesis	Test	Sig.	Decision
1	The median of differences between PanM2MaxC and PanM2Dth equals 0.	Related-Samples Wilcoxon Signed Rank Test	.001	Reject the null hypothesis.

Asymptotic significances are displayed. The significance level is .05.

P. paniscus maximum medial thickness comparison with maximum change in geometry in metatarsal 2

Hypothesis Test Summary

	Null Hypothesis	Test	Sig.	Decision
1	The median of differences between PanM2MaxC and PanM2Mth equals 0.	Related-Samples Wilcoxon Signed Rank Test	.001	Reject the null hypothesis.

Asymptotic significances are displayed. The significance level is .05.

P. paniscus maximum lateral thickness comparison with maximum change in geometry in metatarsal 2

Hypothesis Test Summary

	Null Hypothesis	Test	Sig.	Decision
1	The median of differences between PanM2MaxC and PanM2Lth equals 0.	Related-Samples Wilcoxon Signed Rank Test	.002	Reject the null hypothesis.

Asymptotic significances are displayed. The significance level is .05.

P. paniscus maximum plantar thickness comparison with maximum change in geometry in metatarsal 3

Hypothesis Test Summary

	Null Hypothesis	Test	Sig.	Decision
1	The median of differences between PanM3MaxC and PANm3Pth equals 0.	Related-Samples Wilcoxon Signed Rank Test	.053	Retain the null hypothesis.

Asymptotic significances are displayed. The significance level is .05.

P. paniscus maximum dorsal thickness comparison with maximum change in geometry in metatarsal 3

Hypothesis Test Summary

	Null Hypothesis	Test	Sig.	Decision
1	The median of differences between PanM3MaxC and PanM3Dth equals 0.	Related-Samples Wilcoxon Signed Rank Test	.001	Reject the null hypothesis.

Asymptotic significances are displayed. The significance level is .05.

P. paniscus maximum medial thickness comparison with maximum change in geometry in metatarsal 3

Hypothesis Test Summary

	Null Hypothesis	Test	Sig.	Decision
1	The median of differences between PanM3MaxC and PanM3Mth equals 0.	Related-Samples Wilcoxon Signed Rank Test	.063	Retain the null hypothesis.

Asymptotic significances are displayed. The significance level is .05.

P. paniscus maximum lateral thickness comparison with maximum change in geometry in metatarsal 3

Hypothesis Test Summary

	Null Hypothesis	Test	Sig.	Decision
1	The median of differences between PanM3MaxC and PanM3Lth equals 0.	Related-Samples Wilcoxon Signed Rank Test	.032	Reject the null hypothesis.

Asymptotic significances are displayed. The significance level is .05.

P. paniscus maximum plantar thickness comparison with maximum change in geometry in metatarsal 4

Hypothesis Test Summary

	Null Hypothesis	Test	Sig.	Decision
1	The median of differences between PanM4MaxC and PanM4Pth equals 0.	Related-Samples Wilcoxon Signed Rank Test	.009	Reject the null hypothesis.

Asymptotic significances are displayed. The significance level is .05.

P. paniscus maximum dorsal thickness comparison with maximum change in geometry in metatarsal 4

Hypothesis Test Summary

	Null Hypothesis	Test	Sig.	Decision
1	The median of differences between PanM4MaxC and PanM4Dth equals 0.	Related-Samples Wilcoxon Signed Rank Test	.050	Reject the null hypothesis.

Asymptotic significances are displayed. The significance level is .05.

P. paniscus maximum medial thickness comparison with maximum change in geometry in metatarsal 4

Hypothesis Test Summary

	Null Hypothesis	Test	Sig.	Decision
1	The median of differences between PanM4MaxC and PanM4Mth equals 0.	Related-Samples Wilcoxon Signed Rank Test	.001	Reject the null hypothesis.

Asymptotic significances are displayed. The significance level is .05.

P. paniscus maximum lateral thickness comparison with maximum change in geometry in metatarsal 4

Hypothesis Test Summary

	Null Hypothesis	Test	Sig.	Decision
1	The median of differences between PanM4MaxC and PanM4Lth equals 0.	Related-Samples Wilcoxon Signed Rank Test	.025	Reject the null hypothesis.

Asymptotic significances are displayed. The significance level is .05.

P. paniscus maximum plantar thickness comparison with maximum change in geometry in metatarsal 5

Hypothesis Test Summary

	Null Hypothesis	Test	Sig.	Decision
1	The median of differences between PanM5MaxC and PanM5Pth equals 0.	Related-Samples Wilcoxon Signed Rank Test	.232	Retain the null hypothesis.

Asymptotic significances are displayed. The significance level is .05.

P. paniscus maximum dorsal thickness comparison with maximum change in geometry in metatarsal 5

Hypothesis Test Summary

	Null Hypothesis	Test	Sig.	Decision
1	The median of differences between PanM5MaxC and PanM5Dth equals 0.	Related-Samples Wilcoxon Signed Rank Test	.267	Retain the null hypothesis.

Asymptotic significances are displayed. The significance level is .05.

P. paniscus maximum medial thickness comparison with maximum change in geometry in metatarsal 5

Hypothesis Test Summary

	Null Hypothesis	Test	Sig.	Decision
1	The median of differences between PanM5MaxC and PanM5Dth equals 0.	Related-Samples Wilcoxon Signed Rank Test	.267	Retain the null hypothesis.

Asymptotic significances are displayed. The significance level is .05.

P. paniscus maximum lateral thickness comparison with maximum change in geometry in metatarsal 5

Hypothesis Test Summary

	Null Hypothesis	Test	Sig.	Decision
1	The median of differences between PanM5MaxC and PanM5Mth equals 0.	Related-Samples Wilcoxon Signed Rank Test	.105	Retain the null hypothesis.

Asymptotic significances are displayed. The significance level is .05.

5.2.9H. sapiens maximum thicknessescompared with maximum change in geometry by metatarsal

H. sapiens maximum plantar thickness comparison with maximum change in geometry in metatarsal 1

Hypothesis Test Summary

	Null Hypothesis	Test	Sig.	Decision
1	The median of differences between HomM1MaxC and HomM1Pth equals 0.	Related-Samples Wilcoxon Signed Rank Test	.883	Retain the null hypothesis.

Asymptotic significances are displayed. The significance level is .05.

H. sapiens maximum dorsal thickness comparison with maximum change in geometry in metatarsal 1

Hypothesis Test Summary

	Null Hypothesis	Test	Sig.	Decision
1	The median of differences between HomM1MaxC and HomM1Dth equals 0.	Related-Samples Wilcoxon Signed Rank Test	.125	Retain the null hypothesis.

Asymptotic significances are displayed. The significance level is .05.

H. sapiens maximum medial thickness comparison with maximum change in geometry in metatarsal 1

Hypothesis Test Summary

	Null Hypothesis	Test	Sig.	Decision
1	The median of differences between HomM1MaxC and HomM1Mth equals 0.	Related-Samples Wilcoxon Signed Rank Test	.005	Reject the null hypothesis.

Asymptotic significances are displayed. The significance level is .05.

H. sapiens maximum lateral thickness comparison with maximum change in geometry in metatarsal 1

Hypothesis Test Summary

	Null Hypothesis	Test	Sig.	Decision
1	The median of differences between HomM1MaxC and HomM1Lth equals 0.	Related-Samples Wilcoxon Signed Rank Test	.000	Reject the null hypothesis.

Asymptotic significances are displayed. The significance level is .05.

H. sapiens maximum plantar thickness comparison with maximum change in geometry in metatarsal 2

Hypothesis Test Summary

	Null Hypothesis	Test	Sig.	Decision
1	The median of differences between HomM2MaxC and HomM2Pth equals 0.	Related-Samples Wilcoxon Signed Rank Test	.014	Reject the null hypothesis.

Asymptotic significances are displayed. The significance level is .05.

H. sapiens maximum dorsal thickness comparison with maximum change in geometry in metatarsal 2

Hypothesis Test Summary

	Null Hypothesis	Test	Sig.	Decision
1	The median of differences between HomM2MaxC and HomM2Dth equals 0.	Related-Samples Wilcoxon Signed Rank Test	.002	Reject the null hypothesis.

Asymptotic significances are displayed. The significance level is .05.

H. sapiens maximum medial thickness comparison with maximum change in geometry in metatarsal 2

Hypothesis Test Summary

	Null Hypothesis	Test	Sig.	Decision
1	The median of differences between HomM2MaxC and HomM2Mth equals 0.	Related-Samples Wilcoxon Signed Rank Test	.001	Reject the null hypothesis.

Asymptotic significances are displayed. The significance level is .05.

H. sapiens maximum lateral thickness comparison with maximum change in geometry in metatarsal 2

Hypothesis Test Summary

	Null Hypothesis	Test	Sig.	Decision
1	The median of differences between HomM2MaxC and HomM2Lth equals 0.	Related-Samples Wilcoxon Signed Rank Test	.001	Reject the null hypothesis.

Asymptotic significances are displayed. The significance level is .05.

H. sapiens maximum plantar thickness comparison with maximum change in geometry in metatarsal 3

Hypothesis Test Summary

	Null Hypothesis	Test	Sig.	Decision
1	The median of differences between HomM3MaxC and HomM3Pth equals 0.	Related-Samples Wilcoxon Signed Rank Test	.184	Retain the null hypothesis.

Asymptotic significances are displayed. The significance level is .05.

H. sapiens maximum dorsal thickness comparison with maximum change in geometry in metatarsal 3

Hypothesis Test Summary

	Null Hypothesis	Test	Sig.	Decision
1	The median of differences between HomM3MaxC and HomM3Dth equals 0.	Related-Samples Wilcoxon Signed Rank Test	.000	Reject the null hypothesis.

Asymptotic significances are displayed. The significance level is .05.

H. sapiens maximum medial thickness comparison with maximum change in geometry in metatarsal 3

Hypothesis Test Summary

	Null Hypothesis	Test	Sig.	Decision
1	The median of differences between HomM3MaxC and HomM3Mth equals 0.	Related-Samples Wilcoxon Signed Rank Test	.002	Reject the null hypothesis.

Asymptotic significances are displayed. The significance level is .05.

H. sapiens maximum lateral thickness comparison with maximum change in geometry in metatarsal 3

Hypothesis Test Summary

	Null Hypothesis	Test	Sig.	Decision
1	The median of differences between HomM3MaxC and HomM3Lth equals 0.	Related-Samples Wilcoxon Signed Rank Test	.000	Reject the null hypothesis.

Asymptotic significances are displayed. The significance level is .05.

H. sapiens maximum plantar thickness comparison with maximum change in geometry in metatarsal 4

Hypothesis Test Summary

	Null Hypothesis	Test	Sig.	Decision
1	The median of differences between HomM4MaxC and HomM4Pth equals 0.	Related-Samples Wilcoxon Signed Rank Test	.002	Reject the null hypothesis.

Asymptotic significances are displayed. The significance level is .05.

H. sapiens maximum dorsal thickness comparison with maximum change in geometry in metatarsal 4

Hypothesis Test Summary

	Null Hypothesis	Test	Sig.	Decision
1	The median of differences between HomM4MaxC and HomM4Dth equals 0.	Related-Samples Wilcoxon Signed Rank Test	.000	Reject the null hypothesis.

Asymptotic significances are displayed. The significance level is .05.

H. sapiens maximum medial thickness comparison with maximum change in geometry in metatarsal 4

Hypothesis Test Summary

	Null Hypothesis	Test	Sig.	Decision
1	The median of differences between HomM4MaxC and HomM4Mth equals 0.	Related-Samples Wilcoxon Signed Rank Test	.000	Reject the null hypothesis.

Asymptotic significances are displayed. The significance level is .05.

H. sapiens maximum lateral thickness comparison with maximum change in geometry in metatarsal 4

Hypothesis Test Summary

	Null Hypothesis	Test	Sig.	Decision
1	The median of differences between HomM4MaxC and HomM4Lth equals 0.	Related-Samples Wilcoxon Signed Rank Test	.000	Reject the null hypothesis.

Asymptotic significances are displayed. The significance level is .05.

H. sapiens maximum plantar thickness comparison with maximum change in geometry in metatarsal 5

Hypothesis Test Summary

	Null Hypothesis	Test	Sig.	Decision
1	The median of differences between HomM5MaxC and HomM5Pth equals 0.	Related-Samples Wilcoxon Signed Rank Test	.001	Reject the null hypothesis.

Asymptotic significances are displayed. The significance level is .05.

H. sapiens maximum dorsal thickness comparison with maximum change in geometry in metatarsal 5

Hypothesis Test Summary

	Null Hypothesis	Test	Sig.	Decision
1	The median of differences between HomM5MaxC and HomM5Dth equals 0.	Related-Samples Wilcoxon Signed Rank Test	.004	Reject the null hypothesis.

Asymptotic significances are displayed. The significance level is .05.

H. sapiens maximum medial thickness comparison with maximum change in geometry in metatarsal 5

Hypothesis Test Summary

	Null Hypothesis	Test	Sig.	Decision
1	The median of differences between HomM5MaxC and HomM5Mth equals 0.	Related-Samples Wilcoxon Signed Rank Test	.000	Reject the null hypothesis.

Asymptotic significances are displayed. The significance level is .05.

H. sapiens maximum lateral thickness comparison with maximum change in geometry in metatarsal 5

Hypothesis Test Summary

	Null Hypothesis	Test	Sig.	Decision
1	The median of differences between HomM5MaxC and HomM5Lth equals 0.	Related-Samples Wilcoxon Signed Rank Test	.000	Reject the null hypothesis.

Asymptotic significances are displayed. The significance level is .05.

5.2.10 P. t. schweinfurthii maximum thicknesses compared with maximum change in geometry by metatarsal

P. t. schweinfurthii maximum plantar thickness comparison with maximum change in geometry in metatarsal 1

Hypothesis Test Summary

	Null Hypothesis	Test	Sig.	Decision
1	The median of differences between SchwM1MaxC and SchwM1Pth equals 0.	Related-Samples Wilcoxon Signed Rank Test	.003	Reject the null hypothesis.

Asymptotic significances are displayed. The significance level is .05.

P. t. schweinfurthii maximum dorsal thickness comparison with maximum change in geometry in metatarsal 1

Hypothesis Test Summary

	Null Hypothesis	Test	Sig.	Decision
1	The median of differences between SchwM1MaxC and SchwM1Dth equals 0.	Related-Samples Wilcoxon Signed Rank Test	.667	Retain the null hypothesis.

Asymptotic significances are displayed. The significance level is .05.

P. t. schweinfurthii maximum medial thickness comparison with maximum change in geometry in metatarsal 1

Hypothesis Test Summary

	Null Hypothesis	Test	Sig.	Decision
1	The median of differences between SchwM1MaxC and SchwM1Mth equals 0.	Related-Samples Wilcoxon Signed Rank Test	.060	Retain the null hypothesis.

Asymptotic significances are displayed. The significance level is .05.

P. t. schweinfurthii maximum lateral thickness comparison with maximum change in geometry in metatarsal 1

Hypothesis Test Summary

	Null Hypothesis	Test	Sig.	Decision
1	The median of differences between SchwM1MaxC and SchwM1Lth equals 0.	Related-Samples Wilcoxon Signed Rank Test	.001	Reject the null hypothesis.

Asymptotic significances are displayed. The significance level is .05.

P. t. schweinfurthii maximum plantar thickness comparison with maximum change in geometry in metatarsal 2

Hypothesis Test Summary

	Null Hypothesis	Test	Sig.	Decision
1	The median of differences between SchwM2MaxC and SchwM2Pth equals 0.	Related-Samples Wilcoxon Signed Rank Test	.066	Retain the null hypothesis.

Asymptotic significances are displayed. The significance level is .05.

P. t. schweinfurthii maximum dorsal thickness comparison with maximum change in geometry in metatarsal 2

Hypothesis Test Summary

	Null Hypothesis	Test	Sig.	Decision
1	The median of differences between SchwM2MaxC and SchwM2Dth equals 0.	Related-Samples Wilcoxon Signed Rank Test	.000	Reject the null hypothesis.

Asymptotic significances are displayed. The significance level is .05.

P. t. schweinfurthii maximum medial thickness comparison with maximum change in geometry in metatarsal 2

Hypothesis Test Summary

	Null Hypothesis	Test	Sig.	Decision
1	The median of differences between SchwM2MaxC and SchwM2Mth equals 0.	Related-Samples Wilcoxon Signed Rank Test	.000	Reject the null hypothesis.

Asymptotic significances are displayed. The significance level is .05.

P. t. schweinfurthii maximum lateral thickness comparison with maximum change in geometry in metatarsal 2

Hypothesis Test Summary

	Null Hypothesis	Test	Sig.	Decision
1	The median of differences between SchwM2MaxC and SchwM2Lth equals 0.	Related-Samples Wilcoxon Signed Rank Test	.016	Reject the null hypothesis.

Asymptotic significances are displayed. The significance level is .05.

P. t. schweinfurthii maximum plantar thickness comparison with maximum change in geometry in metatarsal 3

Hypothesis Test Summary

	Null Hypothesis	Test	Sig.	Decision
1	The median of differences between SchwM3MaxC and SchwM3Pth equals 0.	Related-Samples Wilcoxon Signed Rank Test	.745	Retain the null hypothesis.

Asymptotic significances are displayed. The significance level is .05.

P. t. schweinfurthii maximum dorsal thickness comparison with maximum change in geometry in metatarsal 3

Hypothesis Test Summary

	Null Hypothesis	Test	Sig.	Decision
1	The median of differences between SchwM3MaxC and SchwM3Dth equals 0.	Related-Samples Wilcoxon Signed Rank Test	.000	Reject the null hypothesis.

Asymptotic significances are displayed. The significance level is .05.

P. t. schweinfurthii maximum medial thickness comparison with maximum change in geometry in metatarsal 3

Hypothesis Test Summary

	Null Hypothesis	Test	Sig.	Decision
1	The median of differences between SchwM3MaxC and SchwM3Mth equals 0.	Related-Samples Wilcoxon Signed Rank Test	.022	Reject the null hypothesis.

Asymptotic significances are displayed. The significance level is .05.

P. t. schweinfurthii maximum lateral thickness comparison with maximum change in geometry in metatarsal 3

Hypothesis Test Summary

	Null Hypothesis	Test	Sig.	Decision
1	The median of differences between SchwM3MaxC and SchwM3Lth equals 0.	Related-Samples Wilcoxon Signed Rank Test	.001	Reject the null hypothesis.

Asymptotic significances are displayed. The significance level is .05.

P. t. schweinfurthii maximum plantar thickness comparison with maximum change in geometry in metatarsal 4

Hypothesis Test Summary

	Null Hypothesis	Test	Sig.	Decision
1	The median of differences between SchwM4MaxC and SchwM4Pth equals 0.	Related-Samples Wilcoxon Signed Rank Test	.000	Reject the null hypothesis.

Asymptotic significances are displayed. The significance level is .05.

P. t. schweinfurthii maximum dorsal thickness comparison with maximum change in geometry in metatarsal 4

Hypothesis Test Summary

	Null Hypothesis	Test	Sig.	Decision
1	The median of differences between SchwM4MaxC and SchwM4Dth equals 0.	Related-Samples Wilcoxon Signed Rank Test	.558	Retain the null hypothesis.

Asymptotic significances are displayed. The significance level is .05.

P. t. schweinfurthii maximum medial thickness comparison with maximum change in geometry in metatarsal 4

Hypothesis Test Summary

	Null Hypothesis	Test	Sig.	Decision
1	The median of differences between SchwM4MaxC and SchwM4Mth equals 0.	Related-Samples Wilcoxon Signed Rank Test	.001	Reject the null hypothesis.

Asymptotic significances are displayed. The significance level is .05.

P. t. schweinfurthii maximum lateral thickness comparison with maximum change in geometry in metatarsal 4

Hypothesis Test Summary

	Null Hypothesis	Test	Sig.	Decision
1	The median of differences between SchwM4MaxC and SchwM4Lth equals 0.	Related-Samples Wilcoxon Signed Rank Test	.001	Reject the null hypothesis.

Asymptotic significances are displayed. The significance level is .05.

P. t. schweinfurthii maximum plantar thickness comparison with maximum change in geometry in metatarsal 5

Hypothesis Test Summary

	Null Hypothesis	Test	Sig.	Decision
1	The median of differences between SchwM5MaxC and SchwM5Pth equals 0.	Related-Samples Wilcoxon Signed Rank Test	.454	Retain the null hypothesis.

Asymptotic significances are displayed. The significance level is .05.

P. t. schweinfurthii maximum dorsal thickness comparison with maximum change in geometry in metatarsal 5

Hypothesis Test Summary

	Null Hypothesis	Test	Sig.	Decision
1	The median of differences between SchwM5MaxC and SchwM5Dth equals 0.	Related-Samples Wilcoxon Signed Rank Test	.002	Reject the null hypothesis.

Asymptotic significances are displayed. The significance level is .05.

P. t. schweinfurthii maximum medial thickness comparison with maximum change in geometry in metatarsal 5

Hypothesis Test Summary

	Null Hypothesis	Test	Sig.	Decision
1	The median of differences between SchwM5MaxC and SchwM5Mth equals 0.	Related-Samples Wilcoxon Signed Rank Test	.000	Reject the null hypothesis.

Asymptotic significances are displayed. The significance level is .05.

P. t. schweinfurthii maximum lateral thickness comparison with maximum change in geometry in metatarsal 5

Hypothesis Test Summary

	Null Hypothesis	Test	Sig.	Decision
1	The median of differences between SchwM5MaxC and SchwM5Lth equals 0.	Related-Samples Wilcoxon Signed Rank Test	.000	Reject the null hypothesis.

Asymptotic significances are displayed. The significance level is .05.